DESIGN AND CONSTRUCTION OF A COMPUTERIZED DIE SWELL APPARATUS

by

© Mazen Kamil Samara

A Thesis Submitted to the Faculty of Graduate Studies and Research in Partial Fulfillment of the Requirements for the Degree of Master of Engineering

Department of Chemical Engineering
McGill University
Montreal, Canada

August 1985

ABSTRACT

Extrudate swell is an important phenomenon exhibited by most polymer melts. As a material property, it could be of significant theoretical value in understanding the rheological behaviour of these melts. Furthermore, extrudate swell is an important factor in the design and operation of plastics processing equipment. Various techniques for the measurement of extrudate swell are reviewed and discussed.

An apparatus has been designed and constructed to measure the extrudate swell of polymer melts, with the aid of a thermostating chamber and a photodiode array. Both digital and analog outputs may be obtained, and the digital output may be analyzed directly with the help of a microcomputer.

The apparatus has been used to measure the extrudate swell behaviour of five wire coating low density polyethylene resins at different shear rates. Also the extrudate swell of a short glass-fiber filled polypropylene melt and of a thermotropic liquid crystal polymer resin has been evaluated.

RESUME

Le gonflement du jonc à la sortie d'une filière est un phénomène important manifesté par la plupart des polymères fondus. Comme propriété du matériel, il peut avoir une valeur théorique significative dans la compréhension du comportement de ces liquides. De plus, le gonflement du jonc joue un rôle important dans la conception et le fonctionnement des procédés de mise en forme des polymères. Plusieurs techniques pour la mesure du gonflement du jonc sont présentées et discutées.

Un appareil a été conçu et construit pour mesurer le gonflement du jonc des polymères fondus, à l'aide d'un bain isotherme et d'une rangée de diodes photoélectriques. Des données digitales et analogues peuvent être obtenues, les données digitales pouvant être directement analysées par micro-ordinateur.

L'appareil a été utilisé pour mesurer le comportment, à différents taux de cisaillement, du gonflement du jonc de cinq résines de polyéthylène basse densité, utilisées principalement pour l'isolation des cables. Finalement, l'évaluation du gonflement du jonc d'un polypropylène fondu, renforcé de courtes fibres de verre, ainsi que d'un polymère thermotropique de cristaux liquides a été faite.

ACKNOWLEDGEMENTS

I would like to express my sincere gratitude to my research supervisor, Professor and Chairman Musa R. Kamal, for his advice and guidance throughout the course of this work. I am grateful to Dr. L. Utracki and Professor J.M. Dealy for their helpful comments and suggestions. I would like to thank Dr. C.K. Jen for designing the first version of the Signal Converter and for his constant help with suggestions and equipment. I would also like to thank Dr. P. Cielo for his valuable advice concerning the optical system.

I am greatly thankful to Mr. R. Kinsella for designing the Camera Module and to Mr. W. Thong for designing the Data Logger. I wish to thank Messrs. A. Kallos, T. Mutel and T. Samurkas for their helpful comments and discussions.

I wish to thank Mr. H. Alexander for constructing the Thermostating Chamber, Mr. A. Krish and Mr. J. Dumont for their assistance with equipment and instrumentation problems.

I wish to thank my colleagues E. Chu, A. Haber, J. Giacomin and all the members of the fifth floor for their advice and assistance with various aspects of the project.

I wish to thank Northern Telecom Canada Limited for providing the polyethylene resins, the Canadian National Research Council for providing some of the equipment and technical assistance, and the Department of Chemical Engineering at

McGill University. Financial support from the Natural Sciences and Engineering Research Council of Canada, and the Ministère de l'Education du Gouvernement du Québec is also acknowledged.

I would like to thank Miss Pat Fong for her excellent typing of this thesis.

Last, but certainly not least, I would like to thank my family for their unlimited love, support and encouragement.

TO MY BELOVED PARENTS

TABLE OF CONTENTS

Page

LIST OF FIGURES

LIST OF TABLES

CHAPTER 1

INTRODUCTION

Rheological properties of molten polymers are of practical interest to those sectors of the plastics industry in which materials are processed in the molten state. This includes resin manufacturers and compounders, machinery manufacturers, and plastics processors. The uses to which rheological data are put include the evaluation of experimental resins, the selection of a resin for a particular process, quality and process control, screening of experimental resins, and process modeling.

Polymer melts usually exhibit viscoelastic behaviour; therefore, it is important to evaluate both the viscous and the elastic aspects of polymer melt flow and their effects in polymer processing systems. Viscous properties have been studied, characterized and specified for many years by flow tests such as melt index and viscosity vs. shear rate curves. Generally, elastic properties have received less attention, although it is well recognized now that elastic properties play an important role.

The elastic nature of polymer melts is manifested in extrusion processes by the phenomenon of extrudate swell, in which the extrudate cross-section is greater than that of the

die opening. Extrudate swell depends upon fundamental properties of the polymer, such as the molecular weight and its distribution, and on the flow conditions, such as the shear rate, shear stress, L/D ratio and melt temperature. The effect plays a significant role in important manufacturing techniques such as extrusion, injection molding and fiber spinning, and is, therefore, an extremely important engineering problem.

Although numerous studies on extrudate swell exist, the models proposed do not provide a clear picture as to the relative importance of the various rheological parameters. There is still disagreement regarding the molecular structure effects for many polymers. The contributions of molecular, rheological and geometrical effects to extrudate swell are not well understood, and the field still lacks a comprehensive theory. At the present time, one can conclude only that a properly executed extrudate swell experiment yields an empirically defined material function that may be of use in classifying and comparing materials in specific applications.

Since the unconstrained recoil of the extrudate depends on the time allowed for recovery and other phenomena, like sagging of the extrudate under its own weight and its possible cooling, the technique and conditions involved in the determination of extrudate swell limit the reliability and scope of the experimental results. To a great extent, this explains the wide discrepancy among the results obtained by different

researchers concerning the effect of different factors on extrudate swell.

A survey of the existing techniques shows that two methods are mainly employed to measure capillary swell of polymer melts. In the first method, the polymer melt is extruded directly into air or into a hot oven, after which the material is allowed to solidify by cooling and the diameter of the solid extrudate is measured. A variation of this method is to anneal the extrudate, before measurement of the relaxed diameter with a micrometer. In the second method, the melt is extruded into an oil filled thermostating chamber, where the swelling is usually followed by means of a photographic technique. Although the second method eliminates many of the inadequacies of the first, it still has many limitations. A detailed account of existing capillary swell measurement techniques is provided in Chapter 2 of this thesis.

In order to obtain a better understanding of the extrudate swell phenomenon, there is need for a dependable, non-contact, automated measurement technique that would yield accurate information regarding extrudate swell and its dependence on design and process conditions. The study of extrudate swell would be facilitated significantly by automatically and continuously processing and analyzing the data.

The main objective of the present study is to develop an automatic apparatus to measure capillary extrudate swell of

polymer melts. The specific objectives of the work described in this thesis are outlined below:

(1) To design and construct a thermostating chamber to provide conditions under which the swelling would occur at a constant temperature, close to the extrusion temperature, and in the absence of gravitational sagging and interfacial effects.

(2) To design and construct a diameter detection system to provide a precise non-contact measurement of extrudate swell of polymer melts. An analog output from the system would drive a chart recorder and digital output would be passed to a microcomputer.

(3) To interface the diameter detection system to the microcomputer and to develop the necessary software to process the data.

(4) To test the developed apparatus and to work out a reliable experimental procedure to measure the swell. This would include an evaluation of the measurement error as well as definition of the limitations and constraints of the developed apparatus.

In order to test the developed apparatus and to obtain representative measurements, the following investigations have been carried out:

(1) The extrudate swell behaviour of five wire coating low density polyethylene (LDPE) resins was studied at different shear rates. The rheological charac-

teristics of these resins were studied earlier by Al-Bastaki (1). His results regarding extrudate swell are compared with data obtained using the new apparatus.

(2) The extrudate swell of a short glass-fiber filled polypropylene melt was also investigated.

(3) The extrudate swell behaviour of a thermotropic liquid crystal polymer (LCP) resin was also evaluated..

CHAPTER 2

TECHNICAL BACKGROUND

2.1 Extrudate Swell

2.1.1 Capillary Extrudate Swell

At the exit of a capillary, slit or die of any shape, an emerging stream of polymeric liquid normally undergoes a significant change in cross-sectional area from that of the channel in which it has been flowing. Several terms are used to describe this phenomenon, such as "die swell", "jet swell", "extrudate expansion" and "post-extrusion swell". In recent years, however, the term "extrudate swell" has become the accepted nomenclature. If the channel is noncircular, then the extrudate also undergoes a change of shape. Attention in this study will be restricted to the case of extrusion from a capillary die and, therefore, to the problem of capillary extrudate swell. In this case, the extrudate swell ratio (B) is defined as the ratio of the diameter of the extrudate, D_e, to that of the die, D_c:

$$B = D_e/D_c \qquad (2.1)$$

Extrudate swell can occur even in the case of Newtonian liquids at low Reynolds numbers (2), but the effects are more

pronounced in the case of viscoelastic liquids. Polymeric melts exhibit viscoelasticity and fading memory. Thus, they are characterized by the ability to snap back, when the external deforming forces are removed. Polymeric melts exhibit approximately the same D_e/D_c values at low shear rates as exhibited by Newtonian fluids, but swell to 2-4 times the die diameter at high shear rates (3).

From a structural point of view, it is believed that extrudate swell occurs as a result of disorientation of the molecules that have been oriented within the capillary by the shear and/or elongational flow fields. From the rheological point of view, on the other hand, it is believed that extrudate swell occurs as a result of the recovery of the elastic deformation imposed in the die. The swelling of viscoelastic fluids is connected to a sudden recovery of stored elastic energy and a subsequent continuation of relaxation at a slower rate.

Extrudate swell is a very complex phenomenon, which depends upon fundamental properties of the polymer such as the molecular weight, molecular weight distribution and chain branching, as well as on the flow conditions such as the shear rate, shear stress, geometry and dimensions of the die (L/D ratio) and melt temperature. It also depends on the elapsed time after exiting the die.

2.1.2 The Origin of Extrudate Swell

Extrudate swell is not limited to viscoelastic fluids. It is established now that Newtonian jets swell by about 13% at very low Reynolds numbers (2). This is apparently due to streamline adjustments, as the liquid emerges from an opening into air and acquires a free surface (3). The swelling of viscoelastic fluids is connected to a sudden recovery of stored elastic energy and subsequent stress relaxation. Different extrudate swell mechanisms, which have been proposed, will be presented in this section.

According to Chapoy et al. (4), two aspects dominate the efforts to elucidate the mechanism which is responsible for producing the swell. The first considers the swell to result only from the partial recovery of tensile strains imposed at the die entrance, which relax during die passage. The dissipation of these strains, during the period of travel through the capillary, can be estimated by using a Maxwell model with one or more relaxation times. This aspect is no doubt important for short dies (small length to diameter ratio), which may often be the case for commercial processing equipment, or for materials having long relaxation times.

The second aspect considers the swell to result only from recoverable elastic shear strains imposed during die passage. The swell can be related to the recoverable elastic strain via Hook's law, using J_e, the equilibrium elastic compliance and the steady state shear stress, σ_{12}. This aspect pre-supposes

steady state conditions: (a) entrance strains have relaxed during capillary passage, and (b) flow is fully developed, with respect to both shear and normal stresses. For a given shear rate, this aspect is clearly independent of the residence time in the capillary.

Maxwell and Nguyen (5) and others (6-9) emphasized that elasticity of the melt is the cause of the extrudate swell. As the melt passes through the die, it is sheared according to the velocity gradient across the diameter of the die. In the region of high velocity gradient, this shearing orients molecular segments in the direction of the flow. The molecules are thus forced into a higher energy state and a less probable configuration. As the extrudate leaves the die, the shearing stress disappears and the molecules are free to return to their preferred, random-coiled configuration - the lower energy state. A unit volume of oriented melt inside the die will become shorter in length and greater in width, when the shear stress is removed as the melt exits the die, thus producing the extrudate swell. The rate and amount of swell will be dependent on the elastic recovery from the sheared configuration to the random-coiled configuration. The amount of recoiling determines the amount of extrudate swell, and the rate of recoiling determines the rate of extrudate swell.

Leblanc (9) supported the suggestion that extrudate swell results from disorientation of macromolecules previously aligned within the die. The observation that extrudate swell

increases with weight average molecular weight and polydispersity supports this hypothesis, since the orientation along flow lines increases with macromolecular chain size.

Cotten (10, 11) used a laser beam to follow the swelling of a filled rubber extrudate. He found that almost half of the ultimate swelling occurred in less than 0.2 seconds, and this was followed by a much slower relaxation, which took 4-5 minutes to reach approximately 95% of the ultimate swell. He suggested that two distinct relaxation mechanisms contribute to the observable swell of the extrudate, and both of these originate from the deformation imposed in the extensional flow region at the die entrance. The initial, very fast recovery represents solid-like elastic recoil of the quasi-network. The much slower relaxation that follows could be the result of disorientation of molecular chains that were aligned in the direction of flow. An increase in die length reduces the magnitude of the very fast (instantaneous) swell. Cotten attributed this to the relaxation of the quasi-network, possibly due to slippage of chain entanglements. However, an increase in die length has almost no effect on the magnitude of the subsequent slow swell (relaxation) region. This interpretation is at variance with the more common view relating die swell (at least partially) to the normal forces generated by the shear flow within the capillary.

Vlachopoulos (3), in an extensive review of extrudate swell, suggested four combined mechanisms to be responsible

for extrudate swell: Newtonian swell, sudden elastic recovery, stress relaxation and inelastic recovery. While the first three mechanisms are widely accepted among researchers, the inelastic recovery theory was proposed only recently by Tanner (12), who assumed that swell is due to an increase in the resistance to deformation of elongated filaments near the extrudate surface. He considered the extrudate as consisting of two layers: an outer layer of thickness equal to 0.05-0.1 diameters, which is in tension, and an inner layer which is in compression.

2.2 Factors Affecting Extrudate Swell

Extrudate swell is a complex phenomenon which is affected by many factors. Among others, it depends on the wall shear rate or shear stress in the die, the die geometry, the extrusion temperature and the elapsed time after exiting the die. It also depends on the molecular structure of the polymer and on the filler content in the melt. The effects of these factors are discussed in this section.

2.2.1 Shear Rate and Shear Stress

One would expect extrudate swell to increase with shear rate, since, as suggested above, swell is largely the manifestation of the recovery by the material of strains imposed during extrusion. Indeed this has been observed (6, 9, 13-19) with both thermoplastics and rubber compounds.

2.2.2 Temperature

There is no general agreement in the literature regarding the dependency of extrudate swell on the capillary (or extrusion) temperature. A number of studies (15, 20-23) have found that extrudate swell decreases with temperature increase, if plotted as a function of shear rate. However, some of these studies (15, 21, 22) have found that plotting extrudate swell against shear stress (wall shear stress in the die, $\sigma_w = D\Delta P/4L$) eliminates the temperature dependence. According to Graessley et al. (15), the collapse of data at different temperatures to a single curve suggests that extrudate swell is primarily a function of shear stress.

On the other hand, it was reported that extrudate swell increased with temperature at constant shear stress for polypropylene-polyethylene blends (24) and for PVC (25). In the case of PVC, this anomalous behaviour was interpreted by the melting of particulate structures of the polymer in the investigated temperature range.

Leblanc (9) suggested that, at constant extrusion rate, the swell should decrease as temperature rises, since, at constant shear rate, the viscosity decreases with increasing temperature, and, consequently, the elastic strain related to flow resistance within the die also decreases. In addition, the relaxation rate of viscoelastic materials increases with temperature and, therefore, a large percentage of the elastic

strains will decay within the die itself as temperature increases.

2.2.3 Length to Diameter (L/D) Ratio

It is well-known (3, 8, 14, 20, 23) that the swelling ratio decreases as L/D increases, approaching a constant level at large values of L/D. Polyethylene usually requires long capillaries ($L/D > 20$) to reach the asymptotic swelling ratio (21, 14), while polystyrenes exhibit a relatively constant ratio at $L/D > 12$. An extensive review of the effect of L/D on extrudate swell is available (13).

The dependence of swell ratio on L/D may be explained by considering that the elastic strain at the entrance of the die is larger than the equilibrium strain associated with flow within the die. Depending on the length of the die, the extent of molecular relaxation determines the value of die swell at the exit. If the die is sufficiently long, only a steady equilibrium value remains. This constant value is a material characteristic, depending only upon the shear rate and the temperature.

2.2.4 Filler Effect

Because of the technological and commercial importance of fillers, many studies exist regarding the effects of fillers on viscoelastic properties, including extrudate swell (8, 11, 26-30). Fillers used commonly are carbon black, glass beads, calcium carbonate, calcium silicate, titanium oxide, etc.

(26). It is now well-established that the addition of fillers reduces the amount of extrudate swell (11, 26, 29). As the filler concentration increases, the swelling ratio decreases.

2.2.5 Molecular Structure

Extrudate swell is influenced by molecular structure parameters such as molecular weight (MW), molecular weight distribution (MWD), and the frequency of long chain branching (LCB). For polystyrene, most authors agree (15, 16, 21) that extrudate swell increases with weight average molecular weight (M_w) and polydispersity. For high density polyethylene, the same trend has been observed (31), although Mendelson and Finger (33) and Shroff and Shida (32) have reported the converse. Rheological studies with low density polyethylenes have shown that, among other factors, the frequency of LCB is of great importance. While Mendelson and Finger (34) have reported that extrudate swell decreases as LCB increases, most recent investigations (35, 36) suggest that the opposite is true, that is, extrudate swell increases, for the same conditions, as LCB increases.

While the true molecular origin of elastic properties of polymer melts is not yet clearly understood, it is generally accepted that higher molecular weights are associated with higher levels of stored elastic energy at a given shear rate. Consequently, it is reasonable to expect that extrudate swell will increase as the molecular weight is increased.

2.3 Methods of Predicting Extrudate Swell

2.3.1 Models Based on the Theory of Rubber Elasticity

Several theories, based on elastic solid analysis, have been proposed in the literature to predict extrudate swell. These theories generally incorporate the observation that extrudate swell is related to the recoverable shear strain, S_R, defined as:

$$S_R = \tau_{12} J_e \qquad (2.2)$$

where J_e is the steady state shear compliance and τ_{12} is the shear stress. Since this equation applies to the region of linear viscoelastic behaviour, it cannot be relied upon except at low shear rates. However, it is often observed that Equation (2.2) continues to fit experimental data, even at higher shear rates (37). It has been shown (38) that S_R can be calculated from normal stress measurements in the limiting low shear rate region, where the viscosity is Newtonian and the first normal stress difference, N_1, is proportional to $\dot{\gamma}^2$. For this particular case:

$$S_R = N_1/2\tau_{12} \qquad (2.3)$$

The various relationships proposed to relate recoverable shear strain and extrudate swell ratio, B, were reviewed by Vlachopoulos *et al.* (3, 17), Utracki *et al.* (39) and by

Vinogradov et al. (40). A summary of some of the important relationships is given in Table 2.1.

Utracki et al. (39) extrapolated the experimental first normal stress difference versus shear rate data to higher shear rates and thus determined the recoverable shear strain values on the basis of Equation (2.3). Comparison of the experimental extrudate swell values to those predicted by the various relationships revealed that the experimental results agreed best with the relationship proposed by Tanner (Equation (2.13)).

In order to account for Newtonian swell, Equation (2.13) is often rearranged and the term 0.1 is added. The following equation is thus obtained:

$$B = (1 + S_R^2/2)^{1/6} + 0.1 \qquad (2.14)$$

The theories discussed above neglect velocity and stress field rearrangements at the die exit. The work carried out by Whipple and Hill (48) showed that pronounced non-linearities in the velocity profile can exist at the die exit and that what happens experimentally is grossly different from what is assumed to occur in elastic-like fluid theories.

In general, experimental studies indicate that the proposed relationships between extrudate swell and recoverable shear strain are useful to some extent. However, they suffer from limitations associated with some of the assumptions em-

TABLE 2.1

Proposed Relationships Between Capillary Extrudate Swell and Recoverable Shear Strain

Reference	Proposed Relationship*	
Spencer and Dillon (41)	$S_R = B^2 - B^{-2}$	(2.4)
Nakajima and Shida (42)	$S_R = B^2 - B^{-4}$	(2.5)
Bagley and Duffey (6)	$S_R^2 = B^4 - B^{-2}$	(2.6)
Bagley and Duffey (6)	$S_R^2 = B^4 + 2B^{-2} - 3$	(2.7)
Vlachopoulos et al. (16)	$S_w^2 = 3(B^4 + 2B^{-2} - 3)$	(2.8)
Mendelson et al. (43)	$S^2 = 6B^2 \ln B$	(2.9)
Rigbi (44)	$S_w = 4(B - 1)$	(2.10)
Spencer (45)	$S_w = (B - 1)/0.1555$	(2.11)
Cogswell (46)	$B^2 = (2 S_w/3)(1 + S_w^{-2})^{3/2} - S_w^{-2}$	(2.12)
Tanner (47)	$S_w^2 = 2(B^6 - 1)$	(2.13)

* S_w is the recoverable shear strain at the wall, i.e. $S_w = J_e \tau_{12,w}$.

ployed. One problem that is associated with these theories is that recovery (swell) is assumed to be instantaneous, whereas, in reality, recovery is time-dependent, and only some part of it takes place instantaneously. Another problem is that these relationships are generally derived based on the assumption of linear viscoelasticity, although the practical applications are always outside this range. An additional complication arises in connection with the attempt to relate analytically viscometric material functions to non-viscometric flow (37). Even if the proposed relationships were assumed to hold, their utility would still be limited, due to the unavailability of direct experimental techniques to measure the first normal stress difference values in the high shear rate range encountered in actual processes.

2.3.2 Models Based on Numerical Methods

As mentioned earlier, even Newtonian fluids exhibit extrudate swell. The value of capillary extrudate swell for Newtonian fluids varies from 1.13 at low shear rates to 0.87 at high shear rates (2). Polymer melts exhibit the same low shear rate swell value in the Newtonian plateau region (49). Theories on extrudate swell based on elastic solid analysis cannot explain this behaviour. In recent years, studies were carried out to predict extrudate swell of Newtonian and viscoelastic fluids by employing the finite element methods to solve the relevant transport equations.

Tanner (50) and Nickell *et al.* (51) used a finite element program to solve the dynamic and continuity equations for a Newtonian fluid in the neighborhood of the capillary exit. They determined the shape of the emerging free surface by applying the boundary conditions specifying that the normal stress, the shear stress and the normal velocity are zero at the surface. They predicted a swell ratio of 1.13, in agreement with experimental observations. Finite element and finite difference analyses of Newtonian swell were also made by Allan (52) and by Ryan and Dutta (53).

The swell value of 0.87, valid at high Reynolds numbers, can be predicted by using a simple combination of mass and momentum balances (2). Thus, the Newtonian flow problem is well understood, and the theory is in good agreement with the data at both low and high Reynolds numbers.

The numerical calculation of die swell for a viscoelastic fluid has been considered more recently by several authors (54-62). Only limited success has been achieved at the present time, since the calculations extend over a very limited range of elastic forces. Several different die geometries were studied; capillary, slit, straight annular, converging and diverging annular dies.

Crochet and Keunings (56-58) carried out their numerical analysis for creeping flow of Newtonian, Power Law and Maxwell fluids. Results could be obtained up to $\lambda\dot{\gamma}_w = 0.75$, where λ is the relaxation time and $\dot{\gamma}_w$ is the shear rate at the wall.

The dimensionless number, $\lambda\dot{\gamma}_w$, is known as the Deborah Number and it gives a measure of elasticity. In a subsequent paper by the same authors (59), the Oldroyd three-constant model was used. This model introduces a retardation time and reduces to the Maxwell fluid for viscometric flows. It was observed that the addition of a retardation time has a considerable impact upon the quality of the finite element calculation of die swell and that higher elasticity (values of $\lambda\dot{\gamma}_w = 4$) could be accommodated. Capillary and slit die swell values were calculated and compared with Tanner's (47) elastic solid theory predictions. Good agreement was obtained. Capillary extrudate swell predictions were also in agreement with experimental data reported by Racin and Bogue (21).

Reddy and Tanner (60) studied the swelling of a sheet of fluid modelled by the second order fluid equation. Finite element computer methods were utilized. No comparison with experimental data was given.

Coleman (55) calculated slit die swell for a Maxwell fluid using a finite element method, different from that used by Crochet and Keunings (56-58). He was able to obtain convergence up to $\lambda\dot{\gamma}_w = 1.25$, which is higher than the maximum value reached by the latter (56), using the same constitutive equation. Similar swell values were obtained in these two studies.

Recently, Mitsoulis (62) performed extrudate swell calculations, using a finite element technique which involves an

upwinding scheme. He was able to obtain convergence for higher elasticity levels ($\lambda\dot{\gamma}_w = 4.5$), by employing an empirical constitutive equation.

The outstanding problem in the numerical simulation of viscoleastic flows concerns the upper limit on the dimensionless elasticity parameter (Deborah Number), above which the numerical algorithms fail to converge. The limit is relatively low, so low in fact that many of the important experimental results fall outside the range of numerical simulation. In the case of extrudate swell simulation, the presence of the free surface makes the problem even more complex. Detailed reviews of numerical simulations of extrudate swell were given by Vlachopoulos (3) and more recently by Tanner (63).

All of the models discussed above assume isothermal conditions. However, in the actual case, due to the generation of heat by viscous dissipation, the viscosity of the melt is reduced and the flow patterns are more complex than in the isothermal case.

Phouc and Tanner (61) investigated the flow during extrusion of a Newtonian fluid, with a temperature-dependent viscosity. A finite element method was used, and it was found that extrudate expansion up to 70% of the die diameter was obtained due to temperature effects.

In summary, it can be concluded that no satisfactory theory has been developed so far which can predict swell from

basic rheological properties, especially at high shear rates or Deborah Numbers.

2.4 Capillary Extrudate Swell Measurement Techniques

The development of dependable relationships between extrudate swell, B, and S_R has been hampered by inaccuracies in the experimental techniques employed to measure the parameter B. Since the unconstrained recoil of the extrudate is dependent on the time allowed for recovery and other phenomena, like sagging of the extrudate under its own weight and its possible cooling, the technique and conditions involved in the determination of extrudate swell affected the reliability and scope of the experimental results. Thus, it is not surprising that a survey of the existing techniques for determining the extrudate swell of polymer melts indicates that there are many discrepancies among the experimental data reported. The principal experimental methods for measurement of capillary swell are described below.

One of the commonly employed techniques is to cool the extrudate, in cold water or ambient air, after emerging from the capillary and to measure the diameter of the solidified extrudate employing a micrometer (16-18). The diameter of the extrudate is approximately obtained by means of a density correction which is based on the assumption of isotropic shrinkage.

$$D_e = D_s(\rho_s/\rho_e)^{1/3} \qquad (2.15)$$

where D and ρ are the diameter and the density of the extrudate, respectively. Subscripts e and s refer to the extrudate melt in the die and the solidified extrudate, respectively. However, in many cases, the complete recovery of the extrudate requires a substantial amount of time (in the order of minutes). Therefore, it is possible that the extrudate solidifies faster than the elastic stresses can relax, thus "freezing" the stresses into the solidified strand. As a result, the extrudate does not achieve its equilibrium degree of expansion. Furthermore, interfacial effects in water cooling and gravitational sagging in air cooling could affect the extrudate diameter. It is important that the density correction should be applied cautiously. This is particularly relevant in the case of semi-crystalline polymers, where the solid density is known to depend on crystallization kinetics. Thus, it is evident that the extrudate swell obtained using this method is susceptible to significant errors.

A number of techniques have been developed to allow the extrudate to recover completely by annealing in an oven for a long duration of time at a temperature lower than the extrusion temperature (15, 19, 42). Han (13) and Racin and Bogue (21) extruded the polymer directly into an oven kept at the extrusion temperature and took photographs of the extrudate to determine the swell. Although Racin and Bogue found sag to be

an unimportant source of error in their studies, it is generally believed that gravitational sagging reduces the extrudate diameter.

White and Roman (64) compared capillary swell values for HDPE, obtained using the following four different techniques:

(1) The frozen extrudate diameter was measured using a micrometer.

(2) Direct photographs of the extrudate were taken as it emerged from the capillary.

(3) The solidified extrudates were annealed in hot silicone oil at temperatures above the melting temperature until they reached constant diameter. The extrudates were then removed and measured with a micrometer.

(4) The melt was extruded into a bath of silicone oil at the same temperature as the extrusion temperature. Photographs of the extrudate in the bath were taken between 5-10 minutes after the extrudate emerged from the capillary.

The above methods gave substantially different results. The first two methods yield extrudates with frozen-in residual stresses, while the last two involve completely recovered samples. The third method does not remove the effect of sag and tends to be associated with the flattening of the extrudate on one side, due to the procedure used in annealing. Swell was found to increase in the order of listing, i.e. the

lowest swell value was obtained with the frozen extrudate and highest value was obtained with the fourth method. This conclusion agrees with the results obtained by Han (13), which indicate that swell of frozen extrudates is significantly lower than that obtained when the extrudate was held at the extrusion temperature for a period of time, in order to permit complete relaxation.

A more elaborate procedure, which allows measurement of swell as a function of time, over long periods in the absence of sag, is to extrude the polymer into a bath containing a relatively low viscosity oil at a temperature higher than the melting temperature of the polymer. The density of the oil should be equal to or slightly lower than that of the melt. This technique was developed by Utracki et al. (39), and it was used extensively at McGill University (1, 65-68). They extruded the melt into a series of oil-filled test tubes at a sequence of wall shear rates. After waiting a sufficient length of time for the equilibrium swell to be attained, photographs of the diameter of the still molten extrudate samples were taken through a side window in the thermostating bath containing the test tubes. The melt diameter was then determined by comparison of the melt images to that of a standard.

By taking a series of photos of a single extrudate at different times, this technique has been used to study the time dependency of swell (1, 65-68). This technique repre-

sents a distinct improvement in comparison with other techniques. However, the procedures of taking photographs and subsequent development of films are cumbersome and time-consuming.

When extrudate swell measurement is considered, thermoplastics and elastomers exhibit fundamentally different types of behaviour. The former, in the melt state within the die, give extrudates which solidify rapidly after leaving the die and, therefore, must be annealed at a suitable temperature to allow for the equilibrium swelling value to be reached. Consequently, all techniques developed for assessing the extrudate swell of thermoplastics must involve some relaxation period before the measurement. With elastomers, the glass transition temperature, T_g, is so low that macromolecular motions still occur at room temperature, allowing the extrudate to relax after leaving the die and to reach the equilibrium value of swelling within a reasonable time and without further annealing. Consequently, fast and automatic measuring techniques are easier to develop for the extrudate swell of rubber.

The weighing method (9), which is the most commonly used technique with elastomers and rubber compounds, consists of weighing a given extrudate length and calculating the extrudate swelling according to

$$B = \left[(W/L\rho S_o)^{1/2} - 1 \right] \times 100 \qquad (2.16)$$

where B is the swelling (in %), L is the extrudate length (in cm), W is its weight (in g), ρ is the density of the material (in g/cm^3) and S_o is the die cross-sectional area (in cm^2). A standard procedure has been recommended in conjunction with this method for the assessment of extrusion characteristics of rubber, according to which it is recommended to allow the extrudate to relax for at least 30 minutes before cutting the length L (9).

Pliskin (30) has described an instrument that can be used for the rapid measurement of extrudate swell. This device was designed for in-plant quality control of elastomers and consists of a piston-driven capillary extruder together with a pair of photocells mounted to permit the precise measurement of the time, t, required for the extrudate to travel a distance L. The velocity of the extrudate is (L/t) and the swell ratio is:

$$\frac{D_{(TS)}}{D_o} = \left[\frac{V}{(L/t)}\right]^{1/2} = \left(\frac{Vt}{L}\right)^{1/2} \qquad (2.16)$$

where V is the average velocity of flow in the die and TS is the temperature of the solidified extrudate. A modification of this device was described by Tokita (69).

When Pliskin's method is used for determining B, the time is usually too short to allow the equilibrium swell to be attained.

Another device, which makes a direct determination of swelling during extrusion, is the Monsanto Automatic Die Swell Detector (37, 70-72). The basic components of this device are shown in Figure 2.1. A laser beam (25 microns in diameter) is projected through a rotating prism, so that it passes across the extrudate. A receiver senses the time during which the sweeping beam is interrupted by the extrudate. A vertical scanning mechanism can be used to determine the shape of the extrudate and thus the short-term time-dependency of the swell. According to the commercial specifications, extrudate diameters between 0.25 and 5.0 mm can be measured, and the vertical scanning distance is 308 mm. Cotten (11, 29) and Leblanc (73) used this technique to measure extrudate swell of filled rubbers as a function of time. From the available description, the details of the measurement procedure are not clear. Additional information could not be obtained from the manufacturer. Our experience, as will be shown later in this work, suggests that this technique cannot be used with unpigmented molten polymers, where the light passes through the central part of the extrudate.

The C.W. Brabender (74) Die Swell Tester was designed for continuous on-line measurement of extrudate swell. The unit employs an opto-electronic measuring system to continuously provide contact free measurement of the extrudate diameter. Infra-red light is scattered as it impinges on the measured object (the extrudate in this case), and, then, the intensity

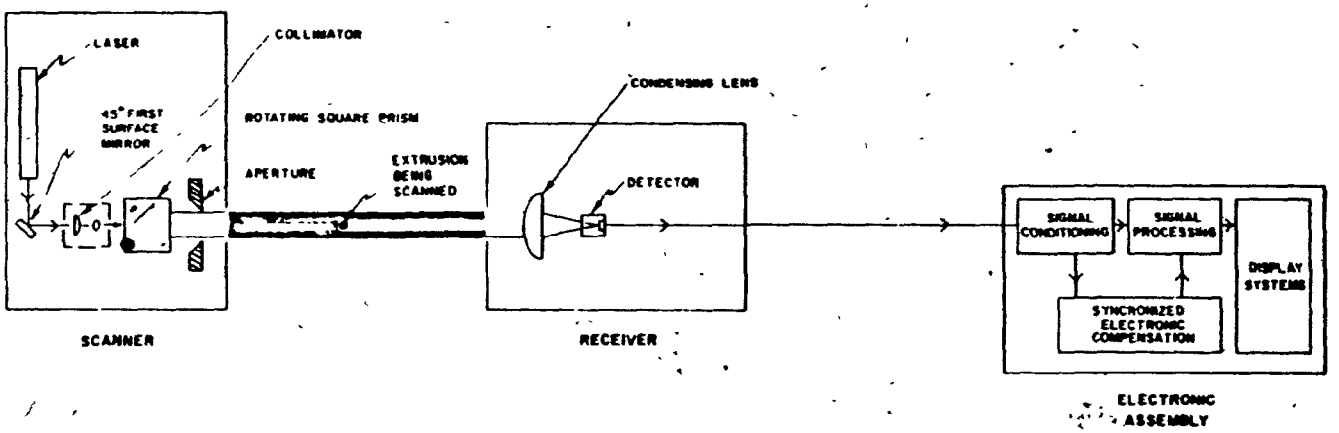

FIGURE 2.1. The Monsanto Automatic Die Swell Detector

is compared with the intensity of a reference beam. The diameter or the thickness of the object is calculated and displayed using electronic circuitry. This device would be hard to use in conjunction with a thermostating chamber. Therefore, it would be more applicable to the measurement of transient swell in rubber.

Figure 2.2 shows the basic elements of a Digital Dimension Meter, developed by Zimmer Ohg and marketed by the Optikon Corporation (75). This device can be used for on-line monitoring of the outside diameter of opaque and transparent tubes, rods and fibers. Collimated light, from a halogen lamp, back-lights the measured object, projecting its image onto a quantization plane, through a magnifying lens. The quantization plane, probably a photodiode array, is scanned once every 1 mS and the number of obstructed photodiodes is counted. This corresponds to the diameter of the measured object. In the case of transparent objects, the array is scanned from the outside towards the center. In this way, the transparent zone in the middle is ignored. This device gives an instantaneous digital readout and a corresponding analog signal. The device does not have any facility for digital storage of the data. No published data are available to confirm the suitability of this device for extrudate swell measurement.

A photodiode array and collimated light source constitute the basic components of a measurement device developed by

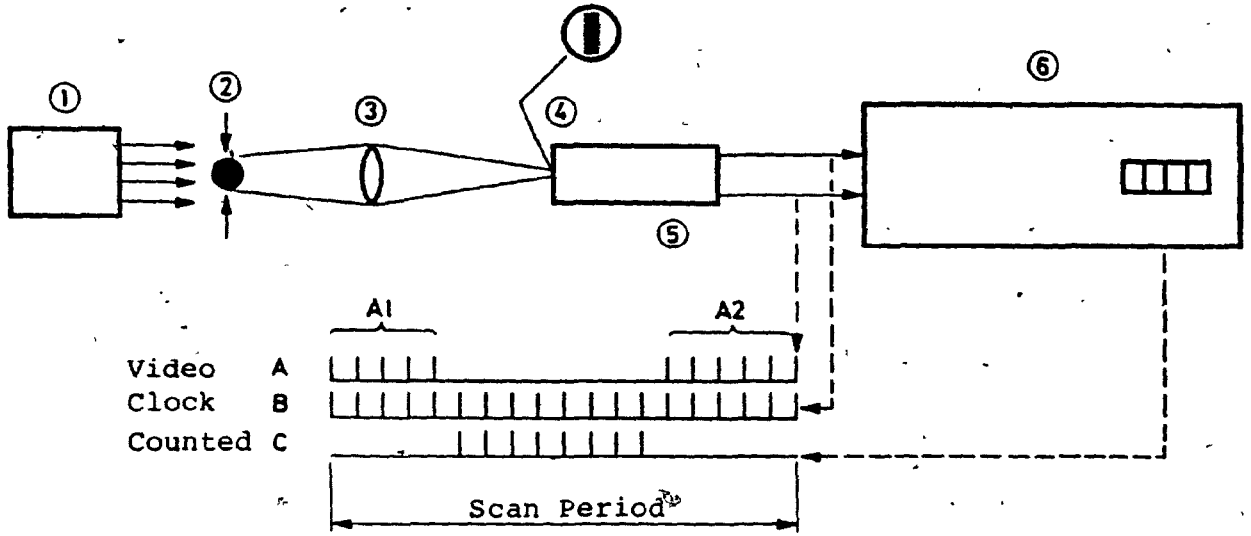

1. Light Source
2. Specimen
3. Lens
4. Quantization Plane
5. Optical Head
6. Signal Controller

FIGURE 2.2. The Digital Dimension Meter

Metrelic Sarl in France (76). It was successfully used by Magnin (77) to measure the diameter of thin fibers (50-200 μm). Utilizing the diffraction phenomenon, he counted the fringes of the interference pattern to define the diameter. A similar device has been used by Agassant (78) for extrudate swell measurement. The extrudate was scanned vertically, just below the tip of the die. The data were acquired on a chart recorder. The measurements were performed nonisothermally. This explains the fact that the problems associated with the transparent melt, as will be shown later, were not encountered. Since the work has not been published yet, no details can be given here.

2.5 Diameter Detection Systems

For the accurate measurement of the diameter of soft, delicate, hot or moving objects, non-contacting sensors must be used. Devices of this type include optical sensors, sonic sensors and capacitive gauging sensors, which make use of the dielectric properties of the object.

Optical sensors have advantages emanating from the nature of light itself. The principal advantages are:

(a) They do not require direct mechanical contact between the sensor and the object to be measured.

(b) The response time is limited only by the photodetector and associated electronics (extremely fast).

(c) Light variations are directly converted to electrical signals.

Among the many types of optical sensors, solid state image scanners are gaining popularity, both for research and industrial applications. A brief discussion of the operating characteristics of optical sensors will be presented in this section. More detailed information can be found elsewhere (79-84).

2.5.1 Solid State Image Scanners

The principle of operation of solid state image scanners is based on the generation of a pattern of charge carriers in silicon crystals, when these crystals are illuminated. These silicon crystals are known as photodiodes.

2.5.1.1 Silicon as a Photodetector

Pure silicon, at a temperature of absolute zero, in darkness, is an insulator, since the electrons which form part of the atomic structure are securely attached to individual atoms in the crystal. If energy is imparted to the crystal, some electrons enter a state in which they are free to move through the crystal as though it were a metal. The electrons leave holes in the crystal lattice. These holes can also move through the crystal and behave as positive charges. Heat could result from these electron-hole pairs (dark current). Also, light can be generated, if the protons are sufficiently

energetic, that is, if the wavelength is less than 1.1 μm, corresponding to the near infra-red and visible regions of the spectrum. Thus, in order to measure the light intensity incident on the silicon, one measures the concentration of electron-hole pairs. This is most readily done with an electric field, by measuring the current which passes between the electrodes forming the field. The photodiode is a structure giving an electric field localized within the surface of the silicon crystal.

2.5.1.2 Photodiode Arrays

Solid state photodiode array devices are available in two basic designs: a self-scanned photodiode array (SSPD), and a charge-coupled photodiode array (CCPD). Both devices are integrated solid state structures comprising: (i) a linear or two-dimensional array of sensing elements, in which incident light is absorbed and converted into electrical charge, (ii) an array of one-to-one correspondence storage elements, on which charge is integrated and stored, and (iii) a sampling circuit for generating a sequential readout of the charge stored in individual elements.

The major differences between the SSPD and the CCPD devices are the sampling or readout technique and the associated circuitry. The SSPD employs digital shift register scanning, which entails a multiplexed sequential sampling of the photodiode charge storage. The CCPD employs charge-coupled shift

registers, which entails simultaneous sampling of the photodiode charge followed by sequential readout.

Photodiode sensing elements are utilized by both the SSPD and the CCPD. The charge-coupled shift register device (CCPD) provides superior low fixed pattern and readout noise. For this reason, CCPD was used in this study. Hereafter in this discussion, the CCPD device will be referred to simply as "photodiode array".

Photodiode arrays are functionally similar to Vidicon (TV) tubes, but they offer the added advantages of great geometric accuracy, broader spectral range, higher scan rates, smaller size, low voltage and power requirements, plus solid state ruggedness and reliability (85).

For one-dimensional measurements, such as the width of plates, diameters of rods and fibers, level, and thickness, etc., a linear photodiode array is normally used.

The principle of the technique is outlined below. An image of the object to be measured is formed on the array, in silhouette or in reflected light, and the number of elements obscured or illuminated is counted electronically by the sequence of operations indicated in Figure 2.3. The video signal from every element is proportional to the incident light intensity. These signals are compared with a preset threshold value and, consequently, a pattern of black and white (illuminated or obscured) elements is achieved. Since the element spacing and the optical magnification are known, the dimension

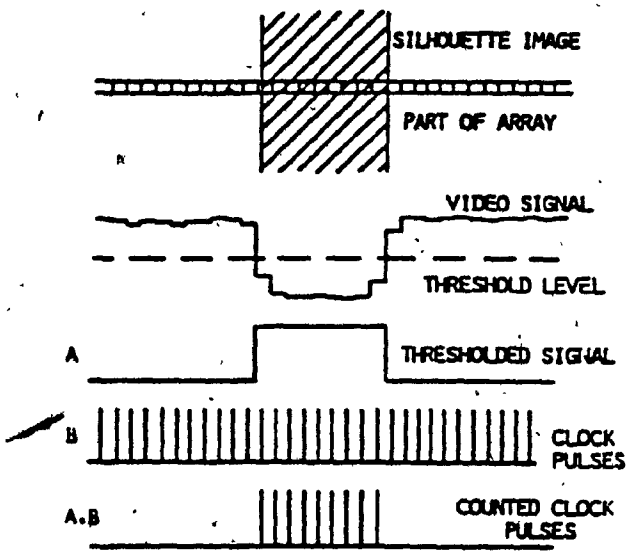

FIGURE 2.3. Basic Principle of Dimension Measurement Using a Solid-State Array

of the object in the direction of the array axis can be calculated. The edges in the image will not necessarily be spacially synchronized with the element spacing, so one element in the vicinity of each image edge will give a signal level part way between black and white. This causes a one-element uncertainty in the position of each edge, as defined by the thresholding operation. Also, optical edges may not be perfectly sharp, and this may cause additional uncertainty in the measurement. Therefore, the measurement accuracy is not absolute, and it is determined by the optical magnification and the number of elements which can be disposed across the width of the image. Accuracy depends also on the spacing between the elements. Smaller elements (and, therefore, smaller center-to-center spacing) and larger magnification of the object being measured, would reduce the error in the measurement.

Linear, matrix and circular arrays are available, offering a wide choice of both resolution and sensitivity. Linear arrays, with a number of elements ranging from 64 to 4096, and matrices, in the 256 x 256 size range, are now commercially available (86, 87). Matrix arrays, as large as 1024 x 1024, have been reported (86).

Linear photodiode arrays have been widely used in high precision non-contact measurements of objects, shape recognition and sorting, and defect detection. A wide range of examples of their usage has been reported (88-92).

2.5.2 Illumination Sources

Some of the common illumination sources are tungesten, quartz halogen, fluorescent, mercury and xenon lamps or lasers. The common ways to arrange these sources include front-line or -spot and back-line or -spot illumination, as well as collimated back lighting. Front-line illumination is used normally with a linear solid state image sensor, when the details of the object are to be obtained. Back-line illumination is used, when only the edges of the object are to be located. Back illumination normally gives better contrast. When back-spot illumination is used, only one photodiode is needed, but, in this case, the light source must be scanned along the dimension of the object to be measured. This technique is employed in the Monsanto Die Swell Detector (71, 72) described earlier.

While the light intensity required for the image sensor is well-defined, only a small percentage of the light actually reaches the sensor. Therefore, in choosing a suitable light source, such factors as "f" number and magnification of the lens and the surface of the object (light or dark, diffuse or specular) must be considered. More detailed information may be found elsewhere (93, 94).

White light contains many frequencies (colors) and intensities, and it comes from many directions. It is described as incoherent light. Beams of incoherent light spread out after a short distance, becoming wider and less intense with in-

creasing distance. Even if a beam of white light is filtered so that it is monochromatic, it will still be incoherent, as its waves are not in phase with one another. On the other hand, laser beam is monochromatic and coherent. This allows it to maintain a high level of brightness (95, 96).

CHAPTER 3

APPARATUS AND EXPERIMENTAL PROCEDURE

3.1 Apparatus

The main objective of this study was to develop an apparatus which automatically and accurately measures capillary extrudate swell. Such an apparatus was designed, constructed and tested.

3.1.1 The Extrusion System

An Instron Universal Testing Instrument (Floor Model, TT-CM-L) was used in conjunction with an Instron Capillary Rheometer (Type MCR, Instron Co., Canton, MA, U.S.A.) to extrude the polymer. Figure 3.1 shows a schematic diagram of the major components of the Instron capillary rheometer system. The barrel consists of a hardened stainless steel cylinder, with an accurately ground 9.525 mm inside diameter, mounted on a special support assembly underneath the moving crosshead of the Instron tester. A hardened plunger, which is also accurately ground to fit the inside of the barrel, is driven by the moving crosshead of the machine. The crosshead can be driven at speeds in the range of 0.5-50 cm/min. The force on the sample is detected by a strain gauge load cell (Type CFM). The force on the sample is detected by a strain

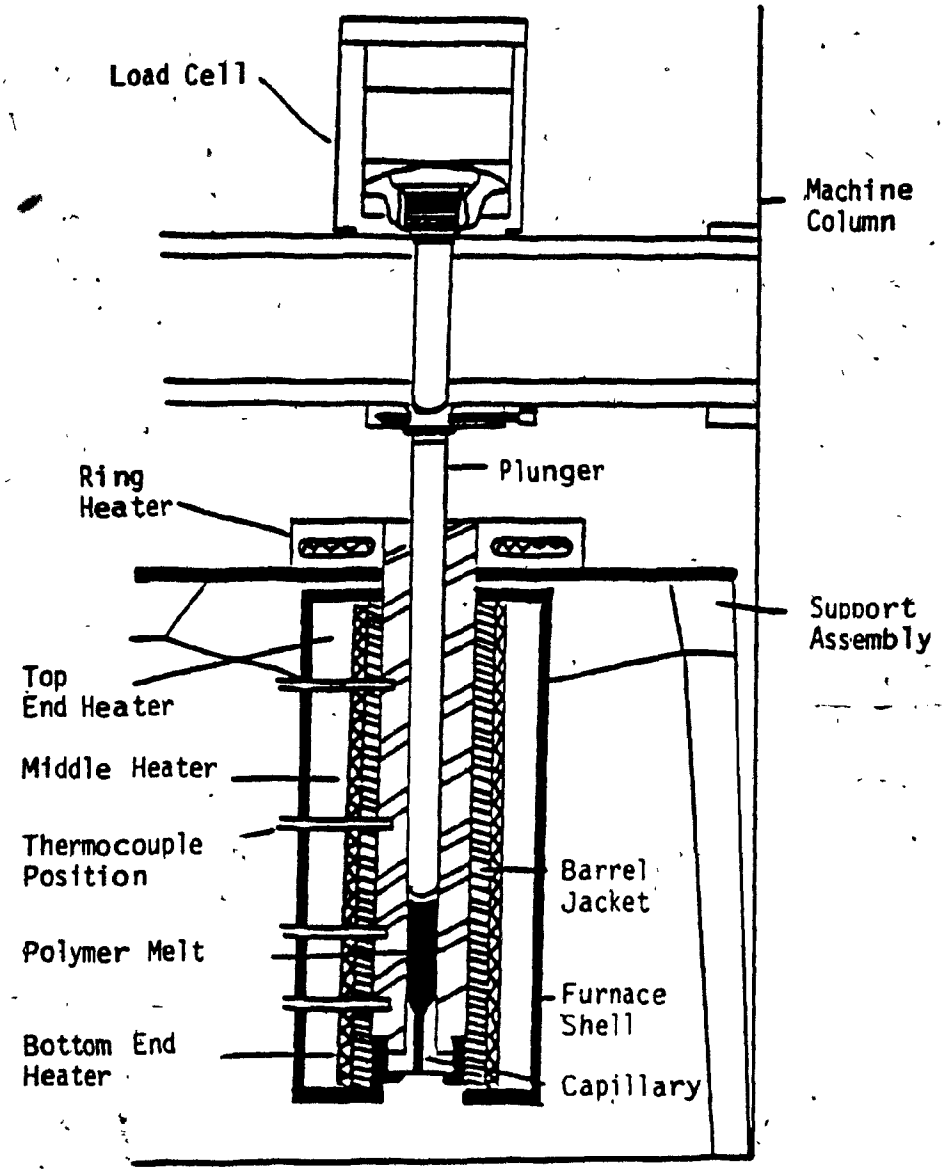

FIGURE 3.1. Schematic of Instron Capillary Rheometer

gauge load cell mounted on a ball-and-socket in the support assembly so that the system is self-aligning. The capillary is inserted in the bottom of the barrel and is held in place with a clamping nut. The barrel and the capillary are heated using a 3-zone heating system in the extrusion barrel. Temperature control is provided with a Speedomax H current adjusting type controller, and the system is capable of maintaining the temperature within ±0.5°C of the set point. Further information regarding the Instron capillary rheometer can be found elsewhere (97).

The capillary used in this study had a diameter of 1.32 mm (0.052 in.), an L/D ratio of 40, and an entrance angle of 90°.

3.1.2 The Overall System

A general scheme of the overall measuring system is shown in Figure 3.2. The resin is extruded from the Instron barrel through the die and into a thermostating chamber. An expanded and collimated laser beam is used as a back-light source to cast the shadow of the polymeric extrudate onto a linear photodiode array. An achromatic lens is used to magnify this shadow. The electrical signal from the photodiode array is then processed with specially designed circuitry (signal converter). The unit which contains the array and the signal converter is designated as the Camera Module. The Data Logger, which is also called the Sample Controller, was designed

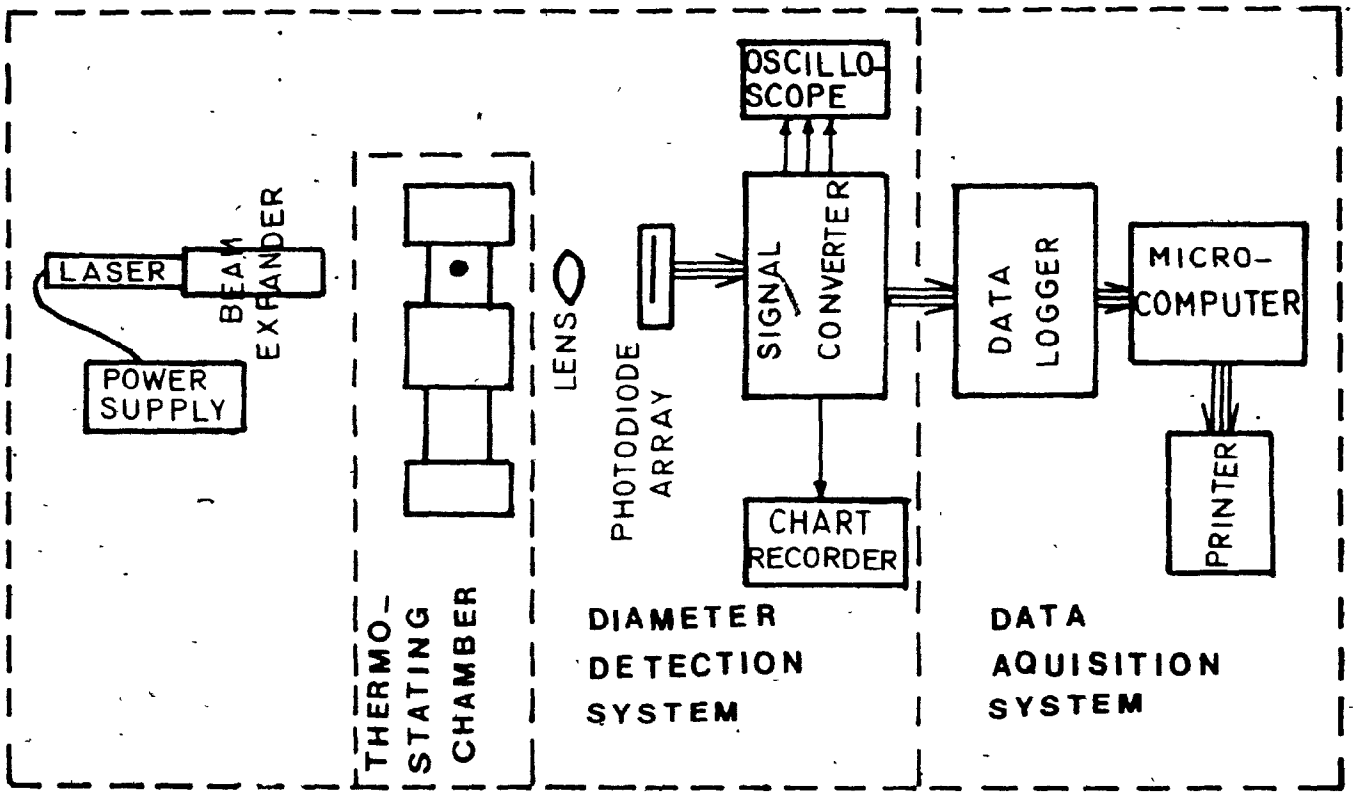

FIGURE 3.2. General Scheme of the Overall Measuring System

to enable real time acquisition of data, using a microcomputer. Photographs of the various components of the apparatus are shown in Figures 3.3, 3.4 and 3.5.

The apparatus consists of three major parts:

(1) The Thermostating Chamber

(2) The Data Detection System

(3) The Data Acquisition System

A detailed description of each of these parts is presented below.

3.1.3 The Thermostating Chamber

As mentioned earlier, two problems could arise during extrusion of the polymer directly into air for the purpose of extrudate swell measurement. Firstly, if the polymer melt is extruded into ambient air, then this could lead to premature freezing and the development of frozen-in stresses. Secondly, if the melt is extruded into a heated oven, then the extrudate would sag under its own weight. Either of these factors would lead to inaccurate extrudate swell measurement, especially with thermoplastics. The use of an appropriate oil-filled thermostating chamber eliminates both of these problems. Following the original design of Utracki et al. (39), a new thermostating chamber was designed and constructed. Many modifications were implemented to incorporate this chamber into the new apparatus.

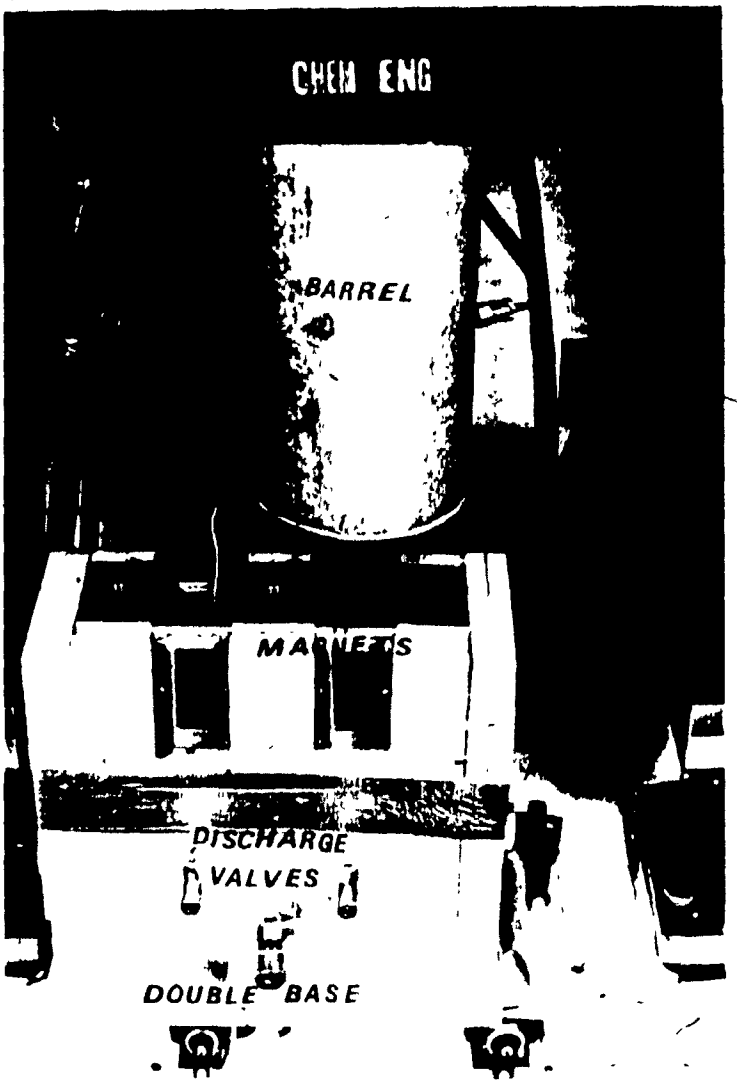

FIGURE 3.3. The Thermostating Chamber

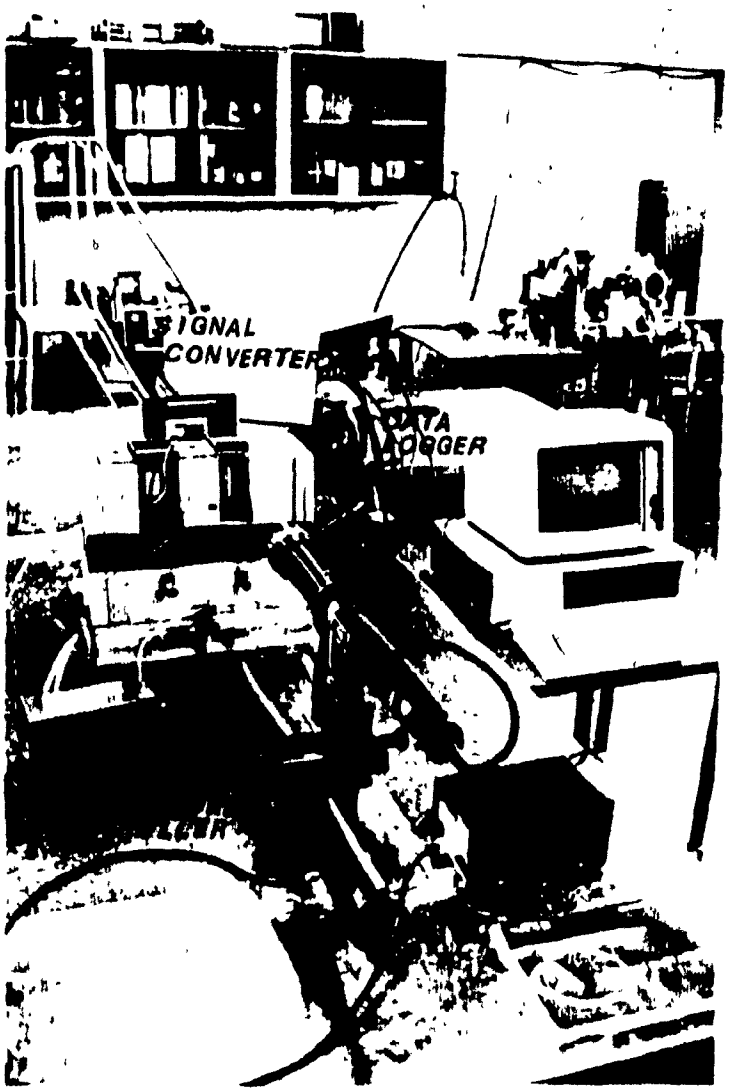

FIGURE 3.4. The Overall Measuring System

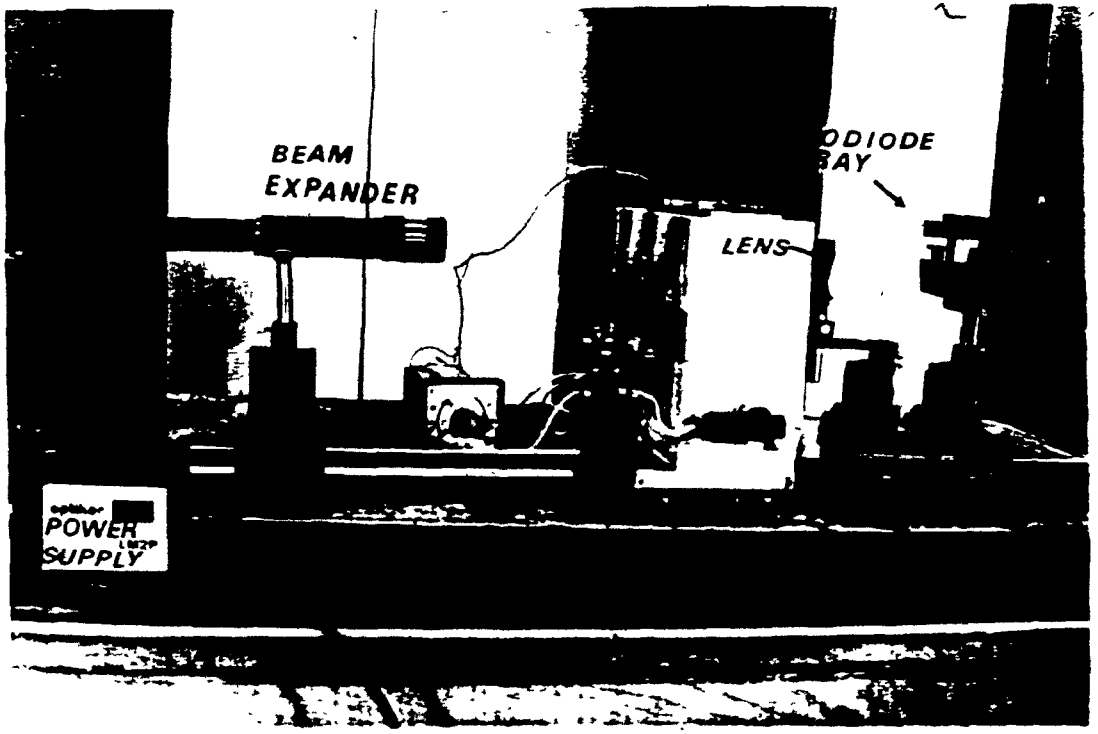

FIGURE 3.5. The Diameter Detection System

The chamber as shown in Figures 3.3 and 3.6 consists of a rectangular stainless steel container, the outer compartment, and of two rectangular stainless steel inner compartments. The inner compartments were equipped with two quartz windows each, to allow the laser beam to pass through. The windows were mounted on flanges welded to the outer sides of the compartments. Viton-O-rings were used to prevent leakage. Either of the inner compartments could be used to collect the molten extrudate during swell measurement. Normally, when one of the inner compartments was aligned with the optical measurement system, two thermocouples were immersed into the other compartment. One of the thermocouples provided feedback to the temperature controller, while the other was connected to a digital thermometer used to monitor the actual temperature.

The chamber was equipped with two plug-screw type 300 watts immersion heaters (RIO-1300, Chromalox, Rexdale, Ontario). The heaters were installed through the side walls of the outer compartment as shown in Figure 3.6. A proportional temperature controller (Model 550, Finwal, Ashland, Ma.), operating in conjunction with a type J thermocouple, was used to monitor the temperature in the inner compartments.

The chamber was fitted with a removable stainless steel cover provided with two openings to allow extrudate entry into the inner compartments. The cover was provided with metallic guides to support two magnets, which, when displaced towards

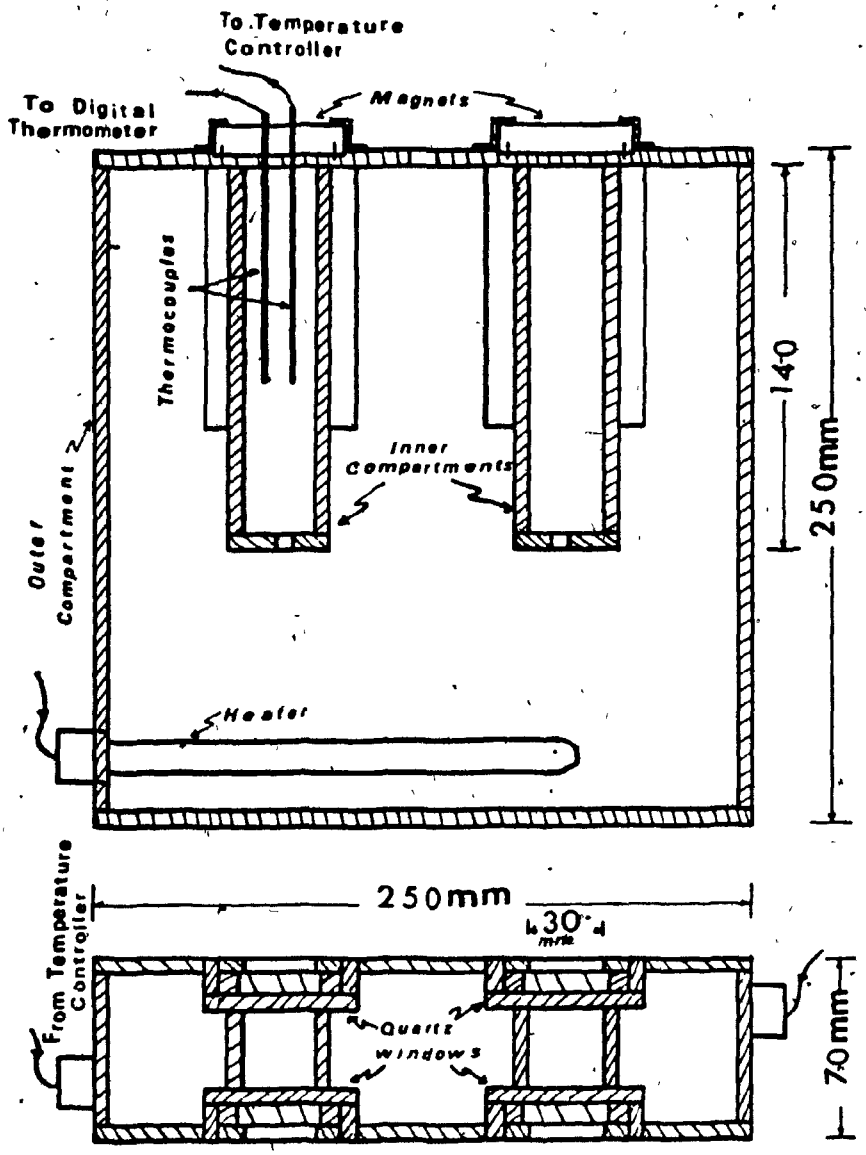

FIGURE 3.6. Top and Front Cross-Sectional Views of the Thermostating Chamber

each other, met at the center of the openings, as shown in Figure 3.3. Two pins on either side of each opening insured that the magnets held the extrudate at the center of the inner compartment during the swell experiment.

The chamber was mounted on a double base. This base, equipped with four pillow blocks, could slide on two metallic bars fixed to the base of the Instron. Such a double base arrangement made it possible to move the chamber both parallel to the optical path and perpendicular to it. This was necessary, in order to position the inner compartment under the die and for optical alignment purposes. Stoppers were provided to confine the movement of the chamber in either direction. The chamber was equipped with three discharge valves, to enable the cleaning of the compartments, if necessary.

The outer compartment was filled with 200 centistokes (cS) silicone oil (200 Fluid, Dow Corning, Toronto, Ontario). The inner compartments contained a mixture of silicone oils mainly 2 cS and 5 cS Dow Corning 200 Fluid. The oils were mixed in such proportions to obtain a density slightly lower than the melt density at the test temperature. When other oil grades were used in the inner compartments, the molten extrudate tended to float at the surface of the oil, and thus no measurement could be made.

During the early stages of testing the apparatus, double layer quartz windows were used. However, it was noticed that silicone oil vapour condensed into small droplets on the inner

sides of the two layers. Consequently, the outer quartz layers were removed. This permitted easier access to the inner quartz layers for cleaning during the experiment, if necessary. It did not result, however, in any significant increase of heat loss from the inner compartments.

As estimated, it was found that operating both heaters simultaneously made it possible to heat the thermostating chamber up to the required temperature within a reasonable period of time (≈ 50 minutes). Subsequently, heat losses could be offset by using one heater only. A 25 mm layer of Marinite was used to insulate all the metallic parts of the chamber. Several tests showed that the temperature profile in both inner compartments were identical.

An important advantage of using the chosen configuration of the outer and inner compartments was that the convection currents, in the oil of the outer compartment, do not interfere with the optical path (the path of the laser beam). Another advantage of such a configuration was that a less expensive and practically involatile 200 cS oil could be used in the outer compartment.

The following considerations had to be taken into account for choosing the dimensions of the inner compartments:

(1) The distance between the extrudate and center of the chosen magnifying lens should not exceed 62.5 mm for a magnification factor of 4. For a magnification factor of 2, this distance could extend up to 75 mm.

The formulae used to define this distance are provided in Section 3.1.4.2.

(2) The glass windows should be greater in width and in height than the expanded beam diameter (≈ 10 mm), to avoid diffraction on the edges of the windows.

(3) The compartment must not be very small, to prevent the extrudate from sticking to its walls.

(4) Large dimensions of the inner compartments could lead to significant convection currents. These currents could cause undesirable optical noise. More importantly, they could result in the displacement of the extrudate from the optical path, which would complicate the measurements.

(5) The oil used in the inner compartments is both volatile and expensive. The volatility of the 2 cS oil at 150°C is 25 percent (mass) per 24 hours. A smaller compartment would result in smaller losses of both oil and of heat.

(6) The lower halves of the inner compartments (below the quartz windows) contributed to increasing the heat-transfer area, thus reducing the time required for heat transfer from the outer oil to the inner oil. The bottom parts of the compartments also served as receptacles for collecting the cut-off parts of the extrudate.

3.1.4 The Diameter Detection System

The diameter detection system makes precise, non-contact and automatic measurements of extrudate swell. Its function is based on the analysis of the shadow cast by the extrudate, when it is back-illuminated by a collimated laser beam. The shadow is cast through a magnifying lens onto a photodiode array. Each photodiode generates a charge, which is amplified and then digitized. The digitized value is then passed to the data acquisition system for storage and analysis. A circuit is provided in the camera module to count the number of photodiodes with light below a selected threshold. The number is conveyed to the experimenter by means of seven segmented light-emitting diodes (L.E.D.'s) installed on one of the outer sides of the camera module. A corresponding analog signal can be used to drive a chart recorder.

The diameter detection system can be divided into the following components:

(i) Light source

(ii) Magnifying lens

(iii) Camera Module

(iv) Oscilloscope

(v) Chart Recorder

3.1.4.1 The Light Source

A 2 mW Helium-Neon (HeNe) gas laser (LSR-2, Optikon Corporation, Waterloo, Ontario) has been selected as a light

source (78). As mentioned in Chapter 2, due to its coherence, the laser beam maintains high intensity for long distance. The HeNe laser emits monochromatic light, at a wavelength of 632.8 microns. This wavelength lies within the range of the maximum response of the silicon-based photodiode array. This laser consists of a lasing tube and a power supply connected with a cable. Calculations have shown that a 2 mW laser is suitable for use along with the chosen photodiode array.

A laser beam expander (16X, Optikon Corporation, Waterloo, Ontario), equipped with a spatial filter (pinhole), has been used to collimate the laser beam and expand it from 0.67 mm to 10.6 mm in diameter (16 times). The beam expander is mounted on the head of the laser tube. A transverse-lateral slide, mounted on an optical bench, is used to adjust the position of this assembly in the XY and Z directions.

3.1.4.2 The Magnifying Lens

An achromatic lens, 50 mm in focal length, was used to magnify the extrudate. Magnification led to the reduction of the error in the diameter measurement. The lens was mounted on a special lens holder, and its position could be adjusted using a transverse-lateral slide.

To calculate distances of the object and the image from the lens, which correspond to certain magnification ratios, the laws for simple thin lenses were applied, namely:

$$\frac{1}{f} = \frac{1}{O} + \frac{1}{I} \qquad (3.1)$$

$$M = \frac{I}{O} \qquad (3.2)$$

where

f is the focal length of the lens in mm,

O is the distance between the object and the lens in mm (in this case, the object is the extrudate),

I is the distance between the image and the lens in mm (in this case, the image is cast on the photodiode array),

M is the magnification ratio.

For a magnification ratio of 2, the extrudate distance would be 75 mm, while the array would be 150 mm away from the lens. For a magnification ratio of 4, these distances would be 62.5 mm and 250 mm, respectively.

3.1.4.3 The Camera Module

The camera module represents the heart of the diameter detection system. It consists of a photodiode array, with its associated circuitry, and of the signal converter, which is discussed in more detail below. A block diagram of the signal converter is shown in Figure 3.7. Detailed electronic schematics are provided in Appendix A.

A Reticon linear photodiode array (RL-512G, EG & G Reticon, Sunnyvale, California, U.S.A.), amplifier and sample

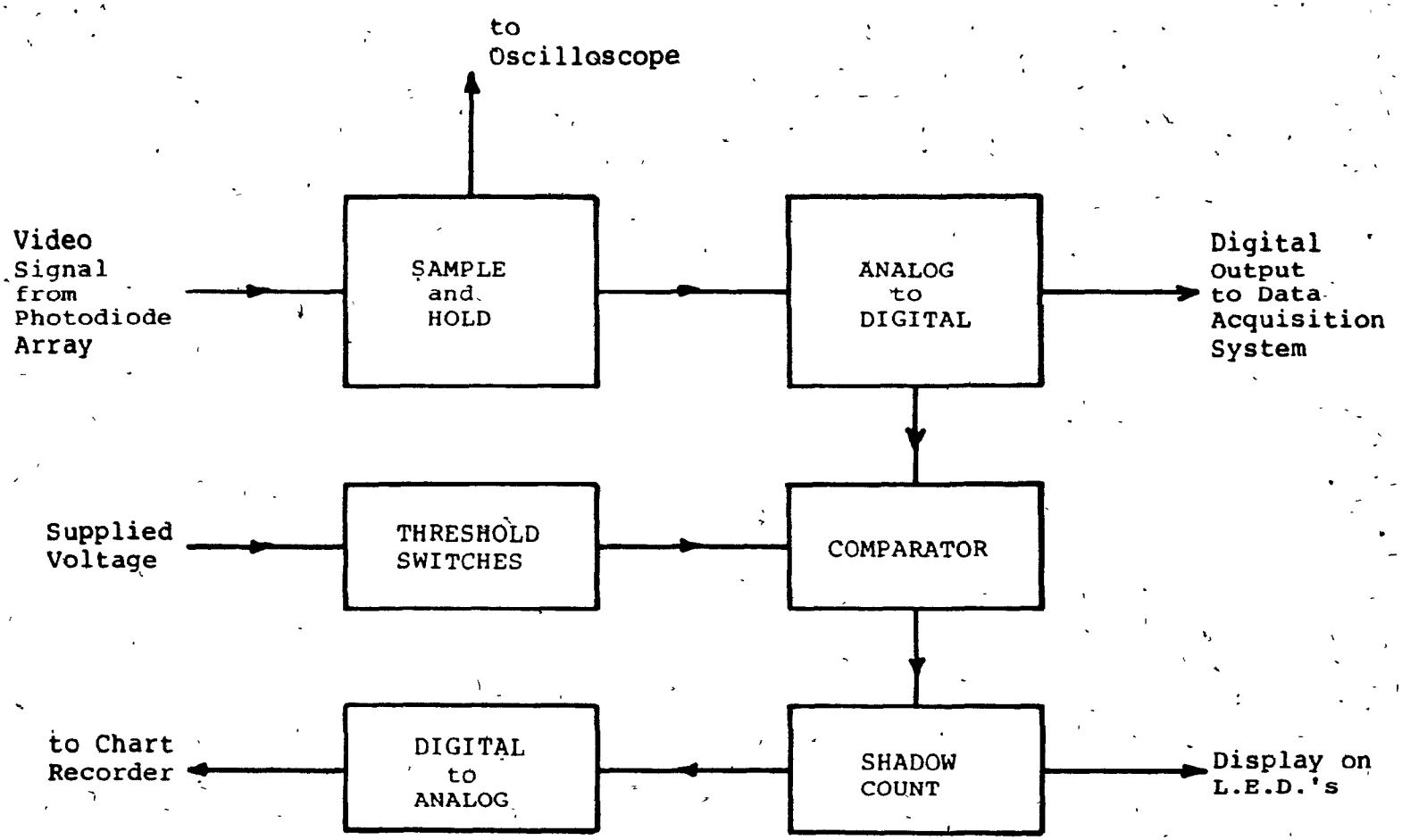

FIGURE 3.7. Block Diagram of the Signal Converter

and hold package (RC 100/105, EG & G Reticon, Sunnyvale, California, U.S.A.) has been used to perform the light sensing function (86). The "G" series array chosen provides 512 photodiodes at a spacing of 25 microns. Electronics have been provided to scan the array at a nominal rate of 4 mS per scan. The Reticon circuitry also provides a sample and hold function. This is required, because the individual photodiodes emit current, as a result of the built-up charge, for only about 300 nS, when selected. The sample and hold circuit board holds the peak value of each photodiode for the approximately 8 µS period between selection of one photodiode and the next in line. The board also provides external access for clock and blanking signal. The blanking signal is maintained low for 8 clock periods after completion of each scan of the array. This period is required for resetting the scanning circuitry.

The voltage from the sample and hold circuitry was taken from the Reticon board and then amplified into the 0-10 V range of an analog to digital converter (A/D). A high-speed amplifier was required because of the very fast rise time and settling response required. A high-speed analog to digital converter, capable of making 8-bit conversion in 1.8 µS, was used. The A/D converter and all the necesary functions, including voltage reference and clock oscillator, were contained on board one chip. An "End of Conversion" (EOC) signal was used to indicate that the digital data output was ready. It

was later used to enable a comparator for the hard-wired digital threshold circuitry. The digital output was passed through a buffer to provide the drive necessary for transmitting the data to the data logger, as well as to a digital comparator.

The digital comparator was used for counting the number of photodiodes illuminated below a certain threshold value. The threshold value was set by eight switches. These switches were positioned in the front panel of the signal converter, and, hence, they were easily accessible to the user. The comparator was enabled by a pulse of about 300 nS duration.

The comparator emits a pulse if, and only if, the photodiode value is less than the switch set value. The pulse is used as the input to two sets of counters. The first set of counters consists of three cascaded, 4-bit, binary counters. The binary output is sampled at the beginning of the blanking pulse (from the Reticon board), and the counters are cleared at the end of the blanking pulse. The output is sampled by D-latches. The outputs of the D-latches are fed into a digital-to-analog (D/A) converter. The output range is 0-10 V. The purpose of this output is to drive a chart recorder, when used.

The other set of counters consists of three cascaded BCD counter/driver chips. They can count up to 999 and directly display the result on three 7-segment L.E.D. displays. This provides a direct-view digital reading of the shadow count.

The L.E.D.'s are fixed on the front panel of the signal converter.

Two sets of counters were used, because more chips would have been required to convert the output of either set into the form required by the function of the other.

Another D/A converter was used to convert the digital value of the threshold switches to an analog level displayable on an oscilloscope. This is a very useful function. A dual-trace oscilliscope can be used to display both the voltage level per photodiode and the threshold level.

Physcially, the camera module is contained in two boxes. For simplicity, they are designated as the sensor and the signal converter.

The sensor was a small (7 x 7 x 2 cm) box made of cardboard. It contained the photodiode array with its immediate supporting circuitry. The sensor was held on a lateral-transverse slide for the adjustment of its position. This slide was placed on the same optical bench as the one holding the lens. An opening (1 x 1.5 cm) was made to expose the surface of the photodiode array. The outside surfaces of the box were painted in black to minimize any reflection of the laser beam. Ambient fluorescent light caused some fluctuations in the signal. These fluctuations were practically eliminated by using a shielding paper cylinder around the photodiode array.

The signal converter was a metallic box (30 x 30 x 20 cm) connected to the sensor by an 18-wire cable. This box con-

tained the main circuitry, as well as a triple output power supply (+5, +15 and -15 V). The power supply was connected to the main circuitry with a power cord. A switch, installed on the back panel of the box, was used to turn the power supply on and off. The 7-segment L.E.D.'s and the threshold switch set were fixed on the front panel.

Five different outputs could be derived from five coaxial plugs, installed on the front panel of the signal converter. These outputs, designated as follows, were:

(i) Video - the amplified voltage from each photodiode, which helps the alignment of the optical system and monitoring of the experiment during the measurements.

(ii) Threshold - an analog representation of the digital threshold switches.

(iii) Detected - a pulse for each photodiode counted as dark.

(iv) Trigger - a signal at the beginning of each scan; this is used to externally trigger the oscilloscope.

(v) Plot - an analog signal (0-10 V), which corresponds to the sum of the photodiodes counted as dark; a chart recorder can be driven by this signal.

The digitized signal from the photodiodes was delivered via a socket on the front panel. It was then transferred through a 14-wire cable to the data logger.

3.1.4.4 The Oscilloscope

A 20 MHz storage oscilloscope (5020ST, Kikusui, Montreal, Quebec) was used for the alignment of the optical system and the constant monitoring of this alignment. The operator must make sure that the photodiode array is fully covered by the laser beam and that the extrudate image falls within the sensing area. This is achieved by observing the video image received from the photodiodes. The oscilloscope makes it possible to identify dirt particles or other obstructions that might interfere with the accuracy of the measurement. It is also useful for establishing the threshold level, especially if a chart recorder is used for data acquisition.

3.1.4.5 The Chart Recorder

The camera module provides an analog output 0-10 V to drive a chart recorder. However, as will be explained in Section 3.2 below, this kind of output could be used only to measure the diameter (or the swell) of opaque materials, including pigmented polymers. In the common case, where light passes through the central part of the transparent extrudate, the digital values of the signals received from the photodiode

array need to be processed by the software in the microcomputer, in order to obtain the actual diameter.

3.1.5 Data Acquisition System

The data acquisition system is designed to collect, store and later analyze the results of the dynamic extrudate swell measurements. Moreover, due to the nature of the optical system employed, the use of a microcomputer for data analysis is an important factor in expediting the automatic measurement of the diameter of transparent extrudates.

When the shadow of an opaque object is cast on the photodiode array, the photodiodes which are obstructed by the object give a base (zero) level signal. On the other hand, the illuminated photodiodes give a saturation level signal. This is readily seen from the oscilloscope video signal, as shown in Figure 3.8. Correction can be made for the effect of diffraction near the edges by adjusting the threshold level, below which the photodiodes are considered dark (obstructed). Thus, by counting these photodiodes and adding them with the help of a counter, it is possible to obtain an accurate measurement of the diameter of that opaque object.

In many instances, it is desirable to measure extrudate swell for unpigmented polymers. When the temperature of an unpigmented polymer is within or above the melting range, the extrudate becomes transparent. In this case, the laser beam penetrates the central part of the extrudate, thus, fully

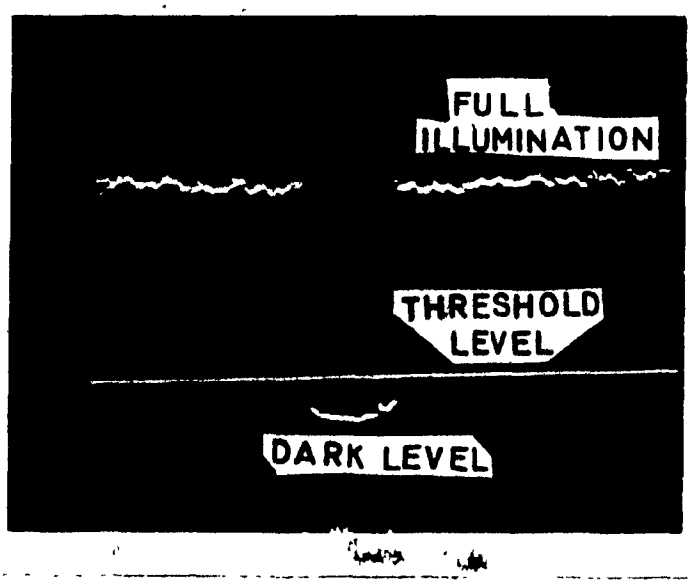

FIGURE 3.8. Illustration of the Video Signal Obtained When the Diameter of an Opaque Extrudate is Measured

illuminating the photodiodes at the center of the shadow. Due to the cylindrical shape of the extrudate, the rays falling on the edges refract towards the center. Thus, the image of the extrudate, as shown in Figure 3.9, consists of three regions: dark, white and dark again. The measured diameter corresponds to the sum of these three regions. However, the white central part of the image would be excluded, if only the photodiodes with intensity below the threshold level are counted. The number of the photodiodes counted and, consequently, the analog signal corresponding to it would not represent the actual diameter. An attempt to solve the problem using optical means is presented in Appendix B.

This problem can be solved if the digitized signals received from the photodiodes are respectively fed to a computer, where a specially prepared software package discounts the illumination of the central part of the image. This procedure permits the automatic measurement of the true diameter. Such a system was implemented in the present work.

The data acquisition system consists of three major parts:

(1) The Data Logger

(2) A Microcomputer

(3) A Printer

FIGURE 3.9. Illustration of the Video Signal Obtained When the Diameter of a Molten Extrudate is Measured

3.1.5.1 The Data Logger (Sample Controller)

The data logger is a microprocessor-controlled device, designed to sample data from the camera module. The data are subsequently transmitted to a microcomputer (IBM PC). The logger accepts the data from the camera module at 1 byte per 8 μS and then transmits it at a rate of 9600 bauds (9600 bits per second). The IBM PC can accept input at only 9600 baud (or less), including start, data and stop bits. The start and stop protocol adds a 20% overhead to the system and limits the data gathering rate of the IBM PC to 960 bits per second. This translates to 1.875 scan lines per second. A scan line here means 512 numbers, representing the digitized signals from the 512 photodiodes. The device could be set to this speed by inputting the decimal equivalent of the command byte in the logging program. The command byte is the command sent by the IBM PC to control the sampling. The device was mainly used with 34 as a command byte, which instructs it to deliver one scan line per second. For more details the reader is referred to Appendix C.

A further feature of the data logging device is its capacity to collect several consecutive line scans before transferring the data to the IBM PC. This permits the averaging of several line scans taken closely together. The device is capable of storing up to 7 consecutive samples, before transmitting the data over the serial line. The time interval

between each burst of sampling is limited to the 1.875 samples (line scans) per second.

The speed of the data logger can be increased to 19.2 K baud or 3.75 samples per second, without any modification. Higher speeds (up to 300 K baud) are possible, with some hardware modification. However, any increase in speed requires either another type of microcomputer or an addition to the IBM PC, in order to permit direct memory access (DMA) and thus faster data acquisition.

The circuitry of the data logger is contained in a metallic box, with two press buttons on the front panel. One of the buttons serves to put the logger on or off, while the other resets the contents of the buffer.

The data logger is connected by a 14-wire cable to the camera modules and by a 3-wire cable to the IBM PC.

3.1.5.2 The Microcomputer and the Software

An IBM Personal Computer (PC) equipped with two disk drives and 256 K of RAM was used in this study to collect and process the data and to transmit it to the output device, e.g. a printer.

The data logger transmits the data to the PC, where they are recorded on a floppy disk as ASCII characters. This is accomplished upon the execution of a program, especially written in BASIC. The program listing is given in Appendix D under the name LOG 5.

The program enables the operator to specify up to five sampling times, for which different numbers of line scans are to be collected. Sampling time, here, means the time elapsed between collecting one line scan and another. This time cannot be less than a minimal value of 0.53 (1/1.875) sec, but it can assume any multiple of it. The number of line scans (data points), which could be collected for one experiment, is limited only by the memory available on the floppy disk. Standard double-sided, double-density, 5-1/4" diskettes (disks) have been used. Each of these diskettes provides 360 K's of memory. Each data point occupies 512 byte or 0.5 K. Therefore, a maximum of about 700 data points (line scans) can be stored on each diskette.

In order to count the "dark" photodiodes, it is necessary to set a threshold level. On the basis of measurements carried out with calibration samples, it has been observed that a threshold level between 180 and 220 yields an invariant number (count) of the dark photodiodes. Above that level, some optical noise and slight electronic drift start to interfere with the count. The number 200 was chosen as a threshold level.

The program DECODE 6 (listed in Appendix E) converts the ASCII characters into numbers and then compares the numerical value from each photodiode with the set threshold value. Thus, using a counter, the number of the dark photodiodes is determined. The program is written in such a way as to ignore any illuminated zones in the middle of the image. It is also

designed to ignore any small particles (up to 200 microns) of dirt which would otherwise be added to the measured diameter. The final count from each line scan is multiplied by 25 (the spacing between the photodiodes) and then divided by the magnification ratio, in order to obtain the true diameter. Another counter indicates the elapsed time corresponding to the diameter measurement. Extrudate swell is obtained by dividing the measured diameter by the die diameter. The calculated extrudate swell is stored in a sequential file for further manipulation. With the help of a color-graphics card, a graphical plot of swell versus time could be shown on the screen. The sequential files with the data do not occupy much memory, and, thus, they can be stored on the disks permanently. On the other hand, the files with the ASCII characters are normally erased after decoding, due to the associated very large memory requirements.

The data, as stored in files, can be easily subjected to any mathematical manipulation.

3.1.5.3 The Printer

An Epson RX-80 printer was used to obtain printouts of the data files. It was also used in conjunction with the LOTUS 1, 2, 3 software package to obtain all the graphs included in this thesis.

3.2 Experimental and Measurement Procedure

3.2.1 System Alignment and Calibration

The thermostating chamber, with its double base, is installed on the base of the Instron. The optical bench, which holds the laser tube and the beam expander, is placed on a table in front of the Instron. The second optical bench, which holds the lens and the sensor, is placed on another table behind the Instron. The system is aligned in such a way that the laser beam is perpendicular to the surface of the quartz windows, from which it passes to the magnifying lens and onto the photodiode array.

The positions of all the components are adjustable, as described earlier. The distance between the front lens of the beam expander and the quartz window is practically unimportant. However, this distance should not be less than 20 cm, to avoid any effect of radiated heat on the front lens of the expander. The distance between the chamber and the lens and between the lens and the photodiode array are defined by the magnification ratio.

Magnification ratios of up to four are possible, using the 2 mW laser. However, for magnification ratios higher than two, the optical and electronic noise levels become more pronounced. Hence, the threshold level has to be defined accurately and carefully. Consequently, a magnification factor of two was used throughout the experimental part of this study.

The distances must be set accurately. Normally, a metallic or glass rod of a previously measured standard diameter is placed in the inner compartment and aligned with the system. The distances are then adjusted carefully, until a correct measurement result is achieved. Several other standards of different diameters are afterwards measured to ensure that the distances are observed accurately. Henceforth, the above procedure will be referred to as "calibration". In this work, the standard diameters were defined under the microscope with an accuracy of ∓ 12 μm.

In aligning the system, the first step is to check that the whole length of the photodiode array is illuminated by the laser beam. This is done by monitoring the video signal derived from the camera module, using the oscilloscope. This signal is monitored constantly, during the experiment, to ensure that the shadow of the extrudate falls on the array.

The oscilloscope is connected to the camera module by three connectors. The "Video" output is connected to its first channel, while the output designated threshold is connected to the second channel. The output "Trigger" is connected to the external trigger of the oscilloscope. The output designated "Plotter" on the camera module provides an input to a chart recorder if one is used.

3.2.2 Oil Selection

The studies made by Utracki et al. (98, 99) and similar experimental work carried out at the Chemical Engineering laboratories of McGill University were helpful in this regard. Among available oils, the 200 fluid silicone oil manufactured by Dow Corning and based on poly(dimethyl siloxane) was found to be the most appropriate, especially for polyethylene resins. This subject will be discussed in greater detail in Chapter 4 of the thesis.

To obtain a density, which matched the density of the melt at the test temperature, a mixture of 2 cS and 5 cS oils was used with all the low density polyethylenes (LDPE) and the polypropylene (PP) resins tested in this study. The exact proportion of the two components was defined experimentally. The proportion was considered satisfactory, if two conditions were met at the test temperature. Firstly, the extrudate should not float at the surface, which would have made the measurement impossible. Secondly, the extrudate should not neck down, even after thirty minutes had elapsed after the moment the experiment was started.

For all the LDPE's used, a mixture of 55% 2 cS and 45% 5 cS oils was found satisfactory.

3.2.3 Oil Heating

A temperature of 150°C was used for the oil bath, whenever a mixture of the 2 cS and 5 cS oils was used. Higher

temperatures could not be used. This limitation was imposed by the low flash points of these oils.

The inner containers were filled with the prepared mixture, leaving some space to accommodate the thermal expansion of the oil. The outer chamber was filled with the 200 cS oil. The quartz windows of the inner containers were maintained clean, using lens cleaning paper.

The thermostating chamber was brought to the required temperature, by setting the heat controller appropriately. A stable temperature was reached after about 50 minutes.

3.2.4 Melt Extrusion

The detailed procedure of operating and calibrating the Instron system can be found elsewhere (97). Some brief comments are given below.

After heating to the required temperature, the barrel (shown in Figure 3.1) is gradually filled with the resin pellets or powder. Then, the plunger is placed in the barrel. The resin requires 5-6 minutes to melt and reach the test temperature.

To release entrapped air bubbles, one must extrude some of the polymer and wait until the load returns to approximately zero. Following this, some more polymer should be extruded, until an extrudate free of air bubbles is obtained.

The chamber is moved from below the die, while the above preliminary extrusion takes place. When the extrudate is

bubble-free and the shear stress has reached a steady level, the polymer stream is cut just below the die. Immediately afterwards, the chamber is moved back under the die, and a fresh extrudate of about 7 cm is extruded downward into the chamber. Then, the extrudate is held by entrapping it between the two magnets. This can be achieved by simply pushing one of the magnets towards the other. The computer program LOG 5 is executed and thus data collection starts.

The Instron is then stopped. However, extrusion does not stop immediately. This results in the accumulation of some polymer melt on the upper surface of the magnets, especially if high shear rates are employed. It is reasonable to assume that this does not affect the results of the measurements.

3.2.5 Extrudate Swell Measurement

The measurement starts only 3-4 seconds after the swell actually starts, since some time is required before the extrudate can reach the inner compartment. For low shear rates, the time could be longer.

The program LOG 5 has to be prepared for execution in advance. The file, where the data is to be stored, should be specified, as well as the time intervals and the number of line scans (Section 3.1.5.2). After the experiment is complete, the extrudate is removed from the inner container and the barrel is cleaned for new experiments. Meanwhile, the

data is decoded using the program DECODE 6. A printout and a graph of the data can be obtained after each experiment.

3.2.6 General Remarks

A slight amount of the oil mixture was added after every experiment to compensate for evaporation. The fact, that no detectable change was observed in the oil density, appears to justify the assumption that the two components of the mixture evaporated approximately in proportion to their respective concentrations.

The laser power supply should be turned on, at least thirty minutes before starting the experiment, in order to obtain a stable output. Precautions should be taken so that neither the direct laser beam nor its reflections fall into the eyes. These precautions do not, in any way, interfere with the carrying out of the experiments.

3.3 Error Analysis, Limitations and Constraints

3.3.1 Error Analysis

Some of the important factors affecting the accuracy of the diameter measurement are listed below:

(1) The spacing between adjacent photodiodes.

(2) The magnification ratio.

(3) The accuracy of the set distances between the optical components: the extrudate, the lens and the photodiode array.

(4) The effect of diffraction of light on the edges of the measured object.

The edges of the image will not necessarily be spatially synchronized with the element spacing. So, one element in the vicinity of each image edge will give a signal level, part-way between black and white. This causes a one-element uncertainty in the position of each edge, as defined by the thresholding operation. The element-to-element spacing in the array is equal to 25 μm. Hence, an error of ∓25 μm would be intrinsic to the measurement, if the image is not magnified.

Magnification of the image would reduce this error. A magnification ratio of two, for instance, would result in a two-fold reduction of this error (down to ∓12.5 μm). One would justifiably expect that higher magnifications should decrease the error accordingly. However, higher magnification could lead to a higher error of a different nature.

The distances between the optical components should be set properly. Any inaccuracy in these distances would lead to an error. When higher magnification ratios are employed, this error increases. Such error is significant, in view of the fact that the extrudate is susceptible to some movement, though slight, in the oil.

The effect of diffraction decreases with the increase of the width of the measured object. This effect decreases substantially, when the object is magnified. If a magnifying

lens is used, diffraction becomes significant (> 5% error) only for objects 500 μm in width or less.

The accuracy of the measurement was evaluated in conjunction with eight standards (glass rods and metallic wires). The diameters of these standards, which ranged between 600 μm and 3600 μm, were measured under the microscope, with an accuracy of ∓12 μm. Afterwards, the diameters of these standards were measured again, using the apparatus with a magnification ratio of two. It was found that the difference did not exceed 12.5 μm. The measured results of measurement using the microscope and the apparatus are tabled in Appendix F.

Subsequently, the reproducibility of the measurement technique was tested. Three sets of extrudate swell experiments were performed. Each experiment was repeated five times under the same conditions. For each set, the diameters were measured and compared 12 minutes after extrusion. The difference between the maximum and minimum values within each set did not exceed 37.5 μm. The measured diameters were in the range of 2000-3000 μm. Measurement results for the three sets are listed in Appendix F.

For a magnification ratio of two, the error in diameter measurement does not exceed 37.5 μm.

The temperature in the barrel was maintained within ∓0.5°C of the set point. One would expect this to result in an error in the swell measurement. The absolute magnitude of

this error depends on the effect of temperature on extrudate swell (see Appendix B).

3.3.2 Limitations and Constraints

The proposed apparatus has the following limitations and constraints.

(1) Viton-O-rings were used for sealing the quartz glass windows. Therefore, the thermostating chamber could not be heated above 230°C, which is the maximum operating temperature for Viton.

(2) The flash point of the oils used in the chamber can impose further restriction on the maximum temperature which can be used.

(3) A maximum magnification ratio of four can be used. This limitation is imposed by the power of the laser used (2 mW).

(4) In its present configuration, the apparatus cannot be used to gauge objects wider than the expanded laser beam. The width of this beam is 10.6 mm. It is not recommended to use it for objects less than 500 μm in width, because of diffraction on the edges.

(5) No extrudate swell measurement could be recorded in the first three to four seconds. This is the time needed for the extrudate to travel through air into the viewing section of the chamber. It is also the

time needed for the operator to entrap it and start the experiment. The lost time is longer for very low shear rates. In order to solve this problem, the die barrel assembly has to be altered so as to have the tip of the die within the viewing section of the chamber. This would require an additional miniature automatic cutting and holding device.

(6) There is an upper limit imposed on the linear speed of the extrudate, and accordingly the shear rate, that could be handled with the present design. A maximum speed of 8.7 cm/sec could be handled. This corresponds to a cross-head speed of 10 cm/min for the barrel and die used in this work. At higher speeds, it was not possible to collect and hold the sample, without material accumulation at the bottom of the inner compartment. This problem could be probably solved if a more efficient automatic cutting and holding device is used.

(7) As a continuation of this project, it would be of interest to use either a stepper motor or a scanning mirror to scan part of the extrudate vertically.

(8) A maximum of 700 line scans can be collected in the course of one experiment. The maximum speed of the data acquisition system, in its present configuration, is 0.53 scan lines per second.

(9) The refractive index of the extrudate material must be different from the refractive index of the oil in the inner containers.

All the above limitations notwithstanding, the apparatus is an effective and universal tool. In addition to the measurement of extrudate swell, which was the original reason for its development, the apparatus can be used for dimensional gauging and continuous monitoring in a variety of areas of research and industry.

CHAPTER 4

REPRESENTATIVE RESULTS AND DISCUSSION

In this chapter, the results of dynamic extrudate swell measurements for some resins are presented. The primary purpose of these measurements was to test the apparatus and to illustrate its reliability. Every experiment was repeated at least once. The results were reproducible within a maximum deviation of ∓2%.

All the swelling data were corrected, using the appropriate thermal expansion coefficient (100), to account for the difference between the extrusion temperature and the temperature of the thermostating chamber. Isotropic thermal expansion was assumed. This assumption is not necessarily correct, especially with crystalline materials such as polyethylenes. However, the correction is quite small (ca. 1%). Therefore, the assumption does not contribute substantially to the measurement error.

4.1 Materials

Extrudate swell was measured for commercial wire coating polyethylene resins, supplied by Northern Telecom Canada Ltd. For reasons of confidentiality, the commercial names of the resins cannot be revealed. However, a detailed rheological

and physical-chemical characterization of the resins has been reported by Al-Bastaki (1).

The true shear rate, $\dot{\gamma}_w$, was obtained from the apparent shear rate, by using the Rabinowitsch correction. The true shear rate is presented for all measurements conducted at 190°C.

For the sake of simplicity, the same coding of resins (W1, W2, W3, W4 and W5), as used by Al-Bastaki was retained. Resins W1 and W5 were linear low density polyethylene (LLDPE), resin W4 was a linear medium density polyethylene, and resins W2 and W3 were medium density branched polyethylene. Resins W2 and W3 were blends of high and low density polyethylenes, while the remaining three resins were homopolymers.

Various properties of the resins are listed in Table 4.1, as supplied by Northern Telecom.

In addition to the polyethylene resins, an injection molding grade polypropylene resin (PRO-FAX 6501, Hercules Canada, Montreal) was tested. Moreover, a short glass fiber reinforced compound, incorporating the above polypropylene resin and 30% short glass fibers, was included in the study. The compound, which was available in the form of pellets containing fibers approximately 3 mm in length and 10 μm in diameter, was especially extruded by Fiberfill Canada, Division of Dart Industries.

TABLE 4.1

Various Properties of the Polyethylene Resins Employed in the Study

	W1	W2	W3	W4	W5
Density, gm/cm^3	0.92	0.932	0.932	0.935	0.92
Melt Index	0.7	0.21	0.2	0.4	1.6
Melting Point, ^oC	118	128	116 & 122^o	124	118
Type	Linear LDPE	Branched MDPE Blend	Branched MDPE Blend	Linear MDPE	Linear LDPE
$\bar{M}_n$	1.116×10^4	1.625×10^4	2.328×10^4	1.095×10^4	2.505×10^4
$\bar{M}_w$	9.407×10^4	1.501×10^5	9.871×10^4	2.006×10^5	1.161×10^5
$\bar{M}_z$	4.259×10^5	8.508×10^5	3.558×10^5	1.073×10^6	5.636×10^5
$\bar{M}_{z+1}$	9.494×10^5	1.955×10^6	7.752×10^5	2.685×10^6	1.449×10^6
$\bar{M}_w/\bar{M}_n$	8.429	9.236	4.240	18.320	4.635
M_v	7.189×10^4	1.098×10^5	8.029×10^4	1.267×10^5	9.144×10^4
$[\eta]$, dl/g	1.37	1.85	1.48	2.04	1.62

The last resin tested was a liquid crystal polymer (LCP) supplied by Celanese Corporation under the name LCP 2000. It is a thermotropic liquid crystal polymer based on 2,6-naphthalene dicarboxylic acid, 2,6-dihydroxynaphthalene, 6-hydroxy-2-naphthoic acid and poly(hydroxy benzoic acid). Some of its characteristics are listed below:

Density = 1.4 g/cm^3

Viscosity Average Molecular Weight, η-MW = 10,000-30,000

Melting Point, T_m = 280°C

Glass Transition Temperature, T_g = 90°C

4.2 Polyethylene Resins

The dynamic (time-dependent) extrudate swell was measured for the five polyethylene resins employed in this study at different shear rates. The upper limit of the rates used was imposed by the onset of melt fracture. All the polyethylene resins were extruded at 190°C. The oil bath temperature was 150°C.

The duration of the measurements was 12 minutes (720 sec). Al-Bastaki (1) found that this time was sufficient to achieve equilibrium extrudate swell. However, as shown in Figure 4.1, it was noticed that swell did not reach the expected equilibrium plateau. The swelling continued to increase steadily, though slowly. Figure 4.2 shows that, even after one hour after the beginning of the measurement, the swelling did not level off completely.

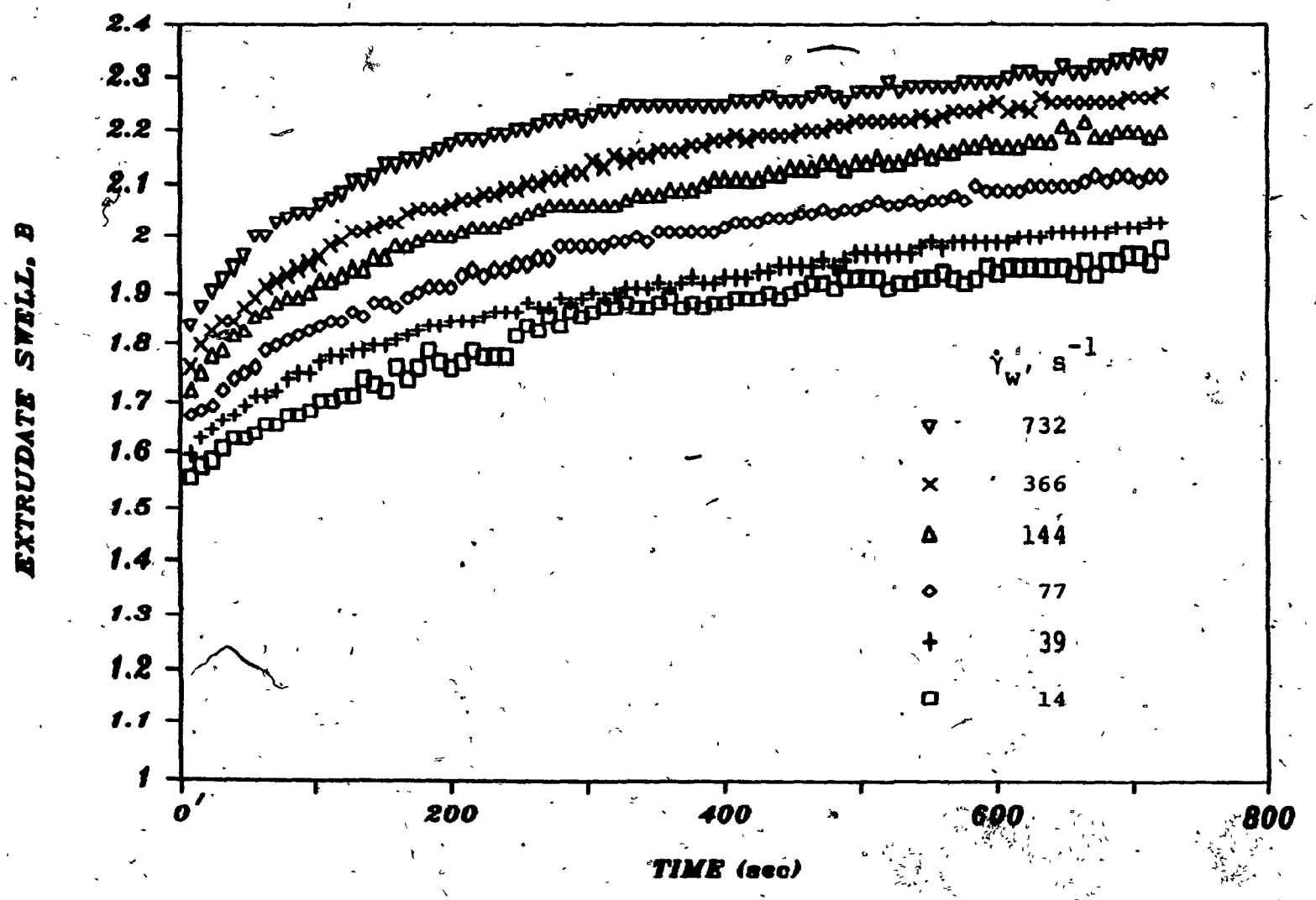

FIGURE 4.1. Time-Dependent Extrudate Swell of Resin W1, Without Correction for Oil Absorption, at Different Shear Rates, $\dot{\gamma}_w$.

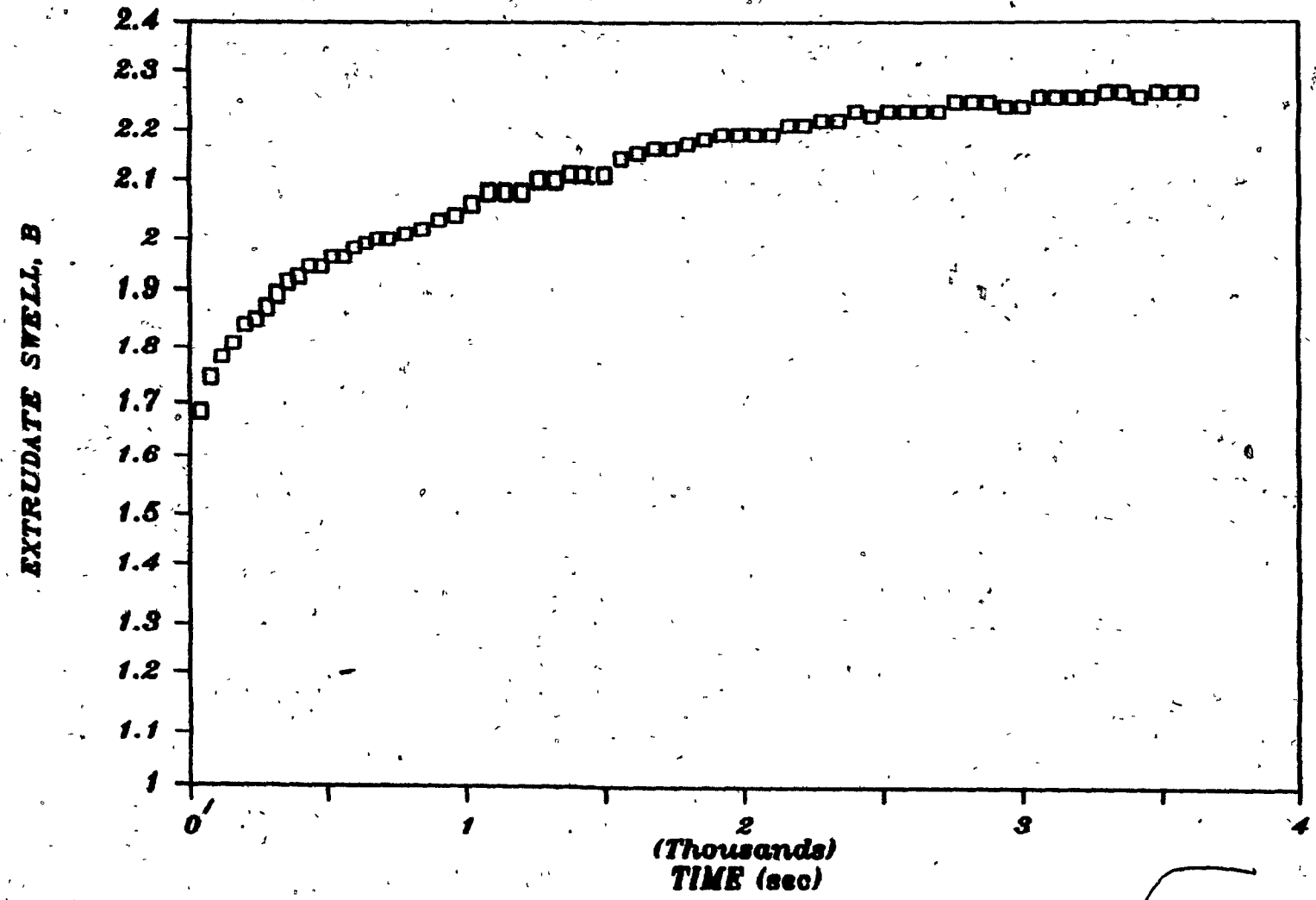

FIGURE 4.2. Time-Dependent Extrudate Swell of Resin W1; Shear Rate, $\dot{\gamma}_w$: 77 s^{-1}, Extrusion Temperature: 190°C.

Al-Bastaki (1) has shown that no significant degradation was observed during at least 16 minutes at a test temperature of 220°C. The deviation of the storage modulus, G', the loss modulus, G", and the complex viscosity, η^*, were the criteria used to evaluate degradation. This confirms that no degradation has occurred with the time scale of the measurements (16 minutes at 190°C).

It has been suggested that 40 x relaxation time is a sufficient period for elastic recovery (39). The relaxation time for the polyethylene melts is unlikely to exceed a few seconds. Therefore, it is reasonable to suspect that the persisting increase in extrudate swell after a certain period may be due to oil absorption by these polymers.

It is important to note that although the time coordinate in all extrudate swell graphs reproduced here starts at zero, the true experimental time should be 2-3 seconds longer. This is due to the fact that swelling starts at least 2-3 seconds before measurement begins, as explained in Chapter 3.

4.2.1 Oil Absorption by Polyethylenes

Utracki et al. (98, 99) have found that Dow Corning 200 fluid silicone oils do not swell polyethylene, if "medium viscosity" grades (50 cS and 100 cS) were employed. However, greater interaction between the oil and polymer occurs, when low viscosity silicone oil grades are used with polyethylene (101).

In the present study, a mixture of low viscosity grades of silicone oil (2 cS and 5 cS) had to be used in the inner compartments of the thermostating chamber, in order to provide an oil density slightly less than the polymer melt density. For polyethylene and polypropylene, the melt density is around 0.78 g/cm^3.

In order to estimate the amount of oil absorbed by the polymer, resin W1 was extruded directly into air at a wall shear rate of 77 s^{-1}. The extrudate was cut into strips of approximately equal length, about 15 cm each. The strips (extrudates) were carefully handled and weighed to the nearest 0.1 mg. The strips were then immersed into the inner containers of the thermostating chamber. The oil mixture was the same as the one used during the swell measurements. The temperature was also the same, 150°C. The extrudates were left in oil for varying times and then weighed again. In this way, the absorption of oil by the extrudate was obtained, as a function of time. The results were reproducible within ±3%. The percent weight oil absorption, based on the original weight of the extrudate strip, was calculated. It is common to use the square root of time as a parameter in the analysis of similar absorption experiments (102). The results are plotted versus time in Figure 4.3(a) and versus the square root of time in Figure 4.3(b). Figure 4.3(a) shows that an asymptotic equilibrium absorption level is approached. However, the equilibrium value, which is above 5.4%, could not be

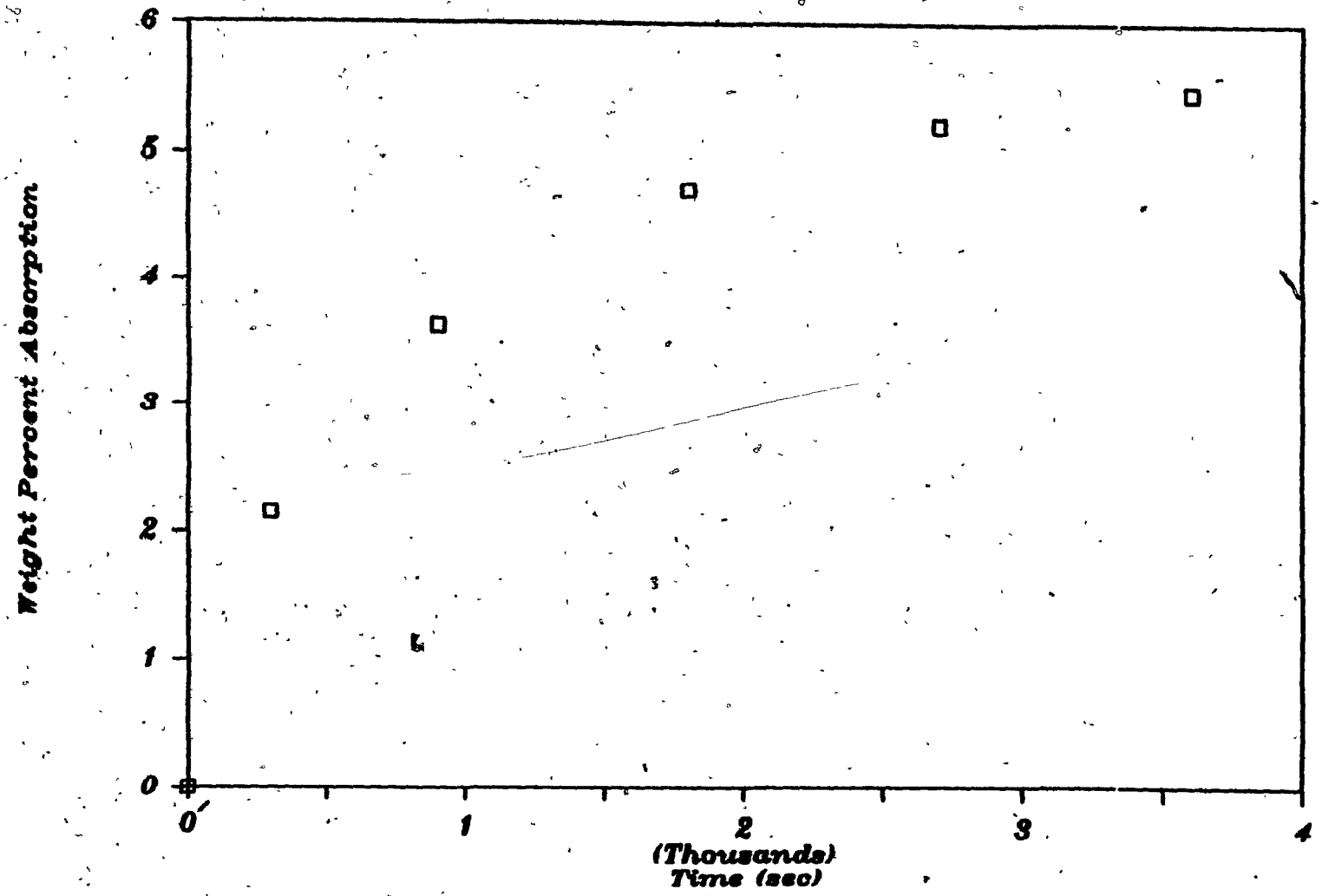

FIGURE 4.3(a). Polyethylene's (W1) Absorption of 2 cS/5 cS Mixture of Silicone Oil. Polymer's Samples Were Extruded at Shear Rate, $\dot{\gamma}_w = 77\ s^{-1}$.

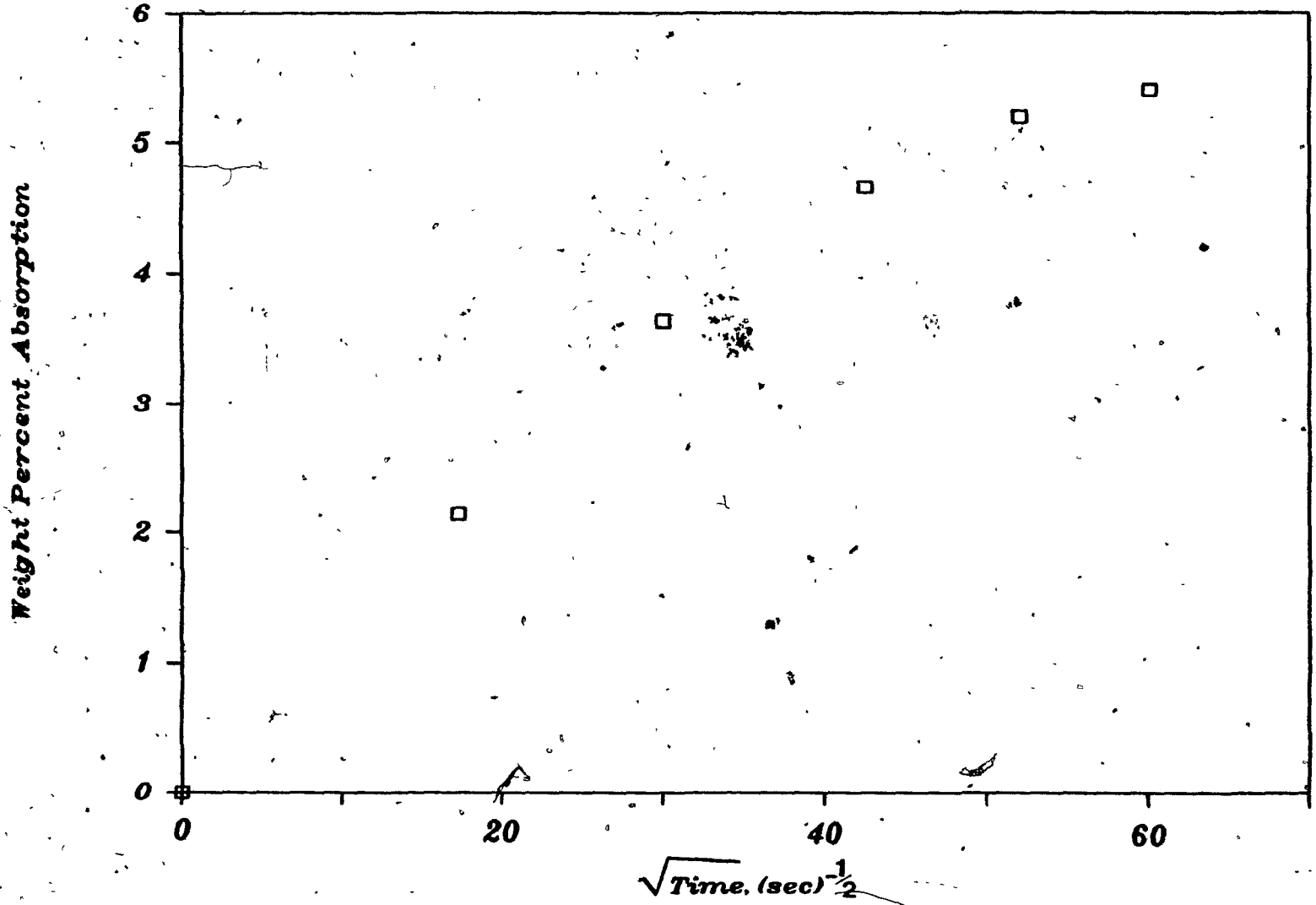

FIGURE 4.3(b). Polyethylene's (W1) Absorption of 2 cS/5 cS Mixture of Silicone Oil. Polymer's Samples Were Extruded at Shear Rate, $\dot{\gamma}_w = 77\ s^{-1}$.

reached after one hour of immersion of the polymer in oil. The plot in Figure 4.3(b) is linear in the early stages of the experiment which indicates a diffusion controlled process.

Ideally, it would be desirable to isolate the swelling due to the absorption of oil from the measured extrudate swell. The solution of this problem requires detailed knowledge and understanding of the mutual interaction between the polymer and the oil and extensive theoretical analysis. Both of these were beyond the scope of the present work. Therefore, a semi-empirical approach was used to handle the problem.

Resin W1 was extruded directly into air, again, at a wall shear rate of 77 s^{-1}. Cut extrudate strips were annealed for 20 minutes in an oven at 175°C on a bed of talc. The talc allowed the extrudate to swell and contract freely, without adhering to the surface of the container. Annealing at lower temperatures was not successful, although the melting range of the resin starts at around 120°C.

The annealed samples were placed in the heated thermostating chamber, and extrudate swell was measured at 150°C. It would be reasonable to assume that, after annealing at 175°C, all the stresses were relaxed and equilibrium extrudate swell was obtained. Consequently, any additional swell would be due to the interaction with oil. Therefore as evidence of complete annealing, it was required that the extrudate should not shorten at all after immersion in oil.

The swell was then measured using the apparatus. Curve 3 in Figure 4.4 shows the swell during the oil absorption experiment. This curve was subtracted from extrudate swell of W1 measured according to the standard procedure (Curve 1). In this way, the "estimated" or "apparent" net swell without the effect of oil was obtained (Curve 2). It can be seen that Curve 2 appears to approach a plateau, indicating that equilibrium extrudate swell is approached. All the time-dependent swell data for polyethylenes were corrected in this fashion using Curve 3. This assumes that all the polyethylene resins show the same swell as a result of interaction with oil. Also, it has been assumed that the oil absorption effect is the same at all shear rates.

Obviously, some of the above assumptions and some aspects of the experimental procedure (e.g. quenching and relaxation in talc) interfere with the accuracy of the estimates. Ideally, a more theoretical analysis would be most useful. However, it is considered that the preliminary results reported here are reasonably accurate.

From a general viewpoint, the best solution to the oil absorption problem should be based on extrusion of the melt into an inert medium that meets all the requirements indicated earlier. It is recommended that this objective should be pursued with vigor.

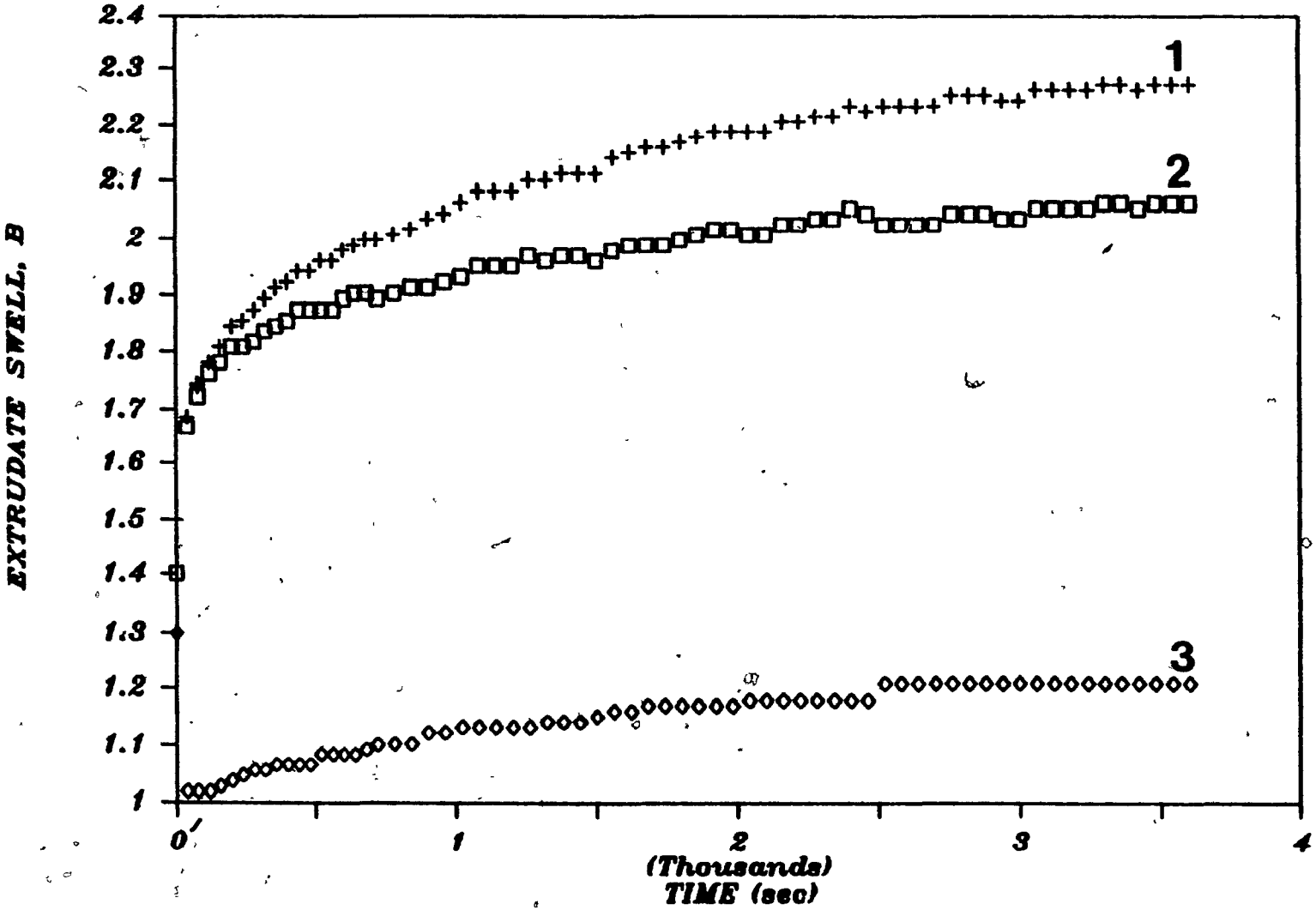

FIGURE 4.4. Effect of Oil Absorption on Extrudate Swell. Curve 1 - Swell of Resin W1 Extruded at $\dot{\gamma}_w = 77\ s^{-1}$. Curve 2 - Net Swell After Subtracting the Swell Due to the Oil. Curve 3 - Swell Due to Absorption of Oil.

4.2.2 Extrudate Swell of Polyethylene Resins

With all the polyethylene resins, a mixture of 55% (volume) 2 cS and 45% 5 cS silicone oil was used in the inner compartments of the thermostating chamber. The polyethylene resins were extruded at 190°C. The temperature of the inner compartments was maintained at 150°C. As mentioned earlier, the flash point of the mixture imposed an upper limit on this temperature.

During 720 seconds, 510 data points were obtained for each experimental measurement. For clarity, only 90 data points are shown on each graph of time-dependent extrudate swell.

The time-dependent swell of the five polyethylene resins, corrected for oil absorption, is shown in Figures 4.5 to 4.9. A comparison of Figures 4.1 to 4.5 shows the significant effect of subtracting the swell due to oil absorption to obtain the true swell for resin W1. For resins W3, W4 and W5, one can clearly see that the swell curve levels off. For W1 and W2, it is interesting to note that, at low shear rates, the swelling curve levels off completely, while, for high shear rates, it still maintains some slope though very slight.

The time-dependent swelling curves are formed by a sequence of data points. Generally, these curves should be smooth. However, the swell curves shown here show the measured values in discrete steps. This artifact is due to the nature of operation of the camera module. A photodiode

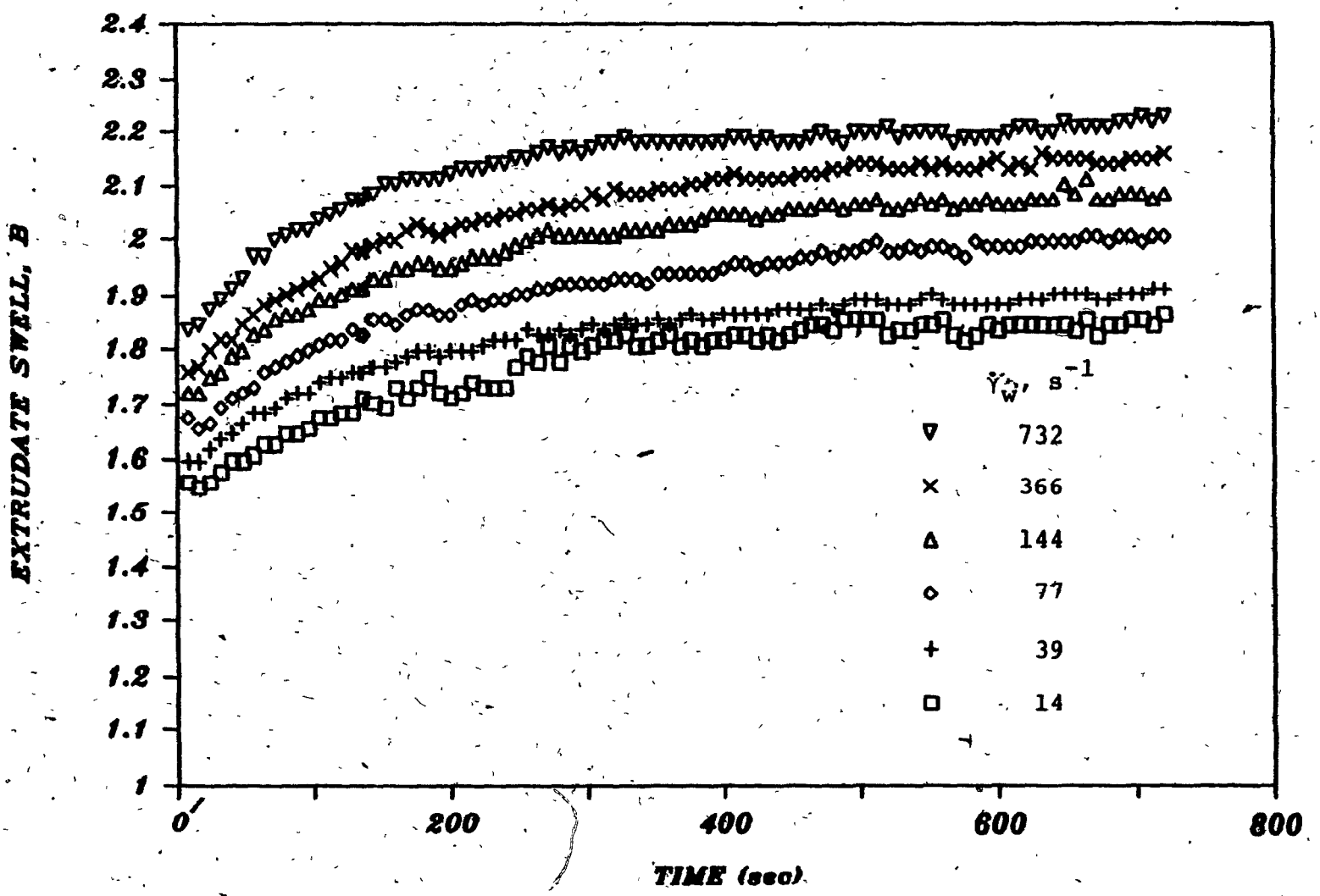

FIGURE 4.5. Extrudate Swell of Resin W1 at 190°C for Different Shear Rates, $\dot{\gamma}_w$.

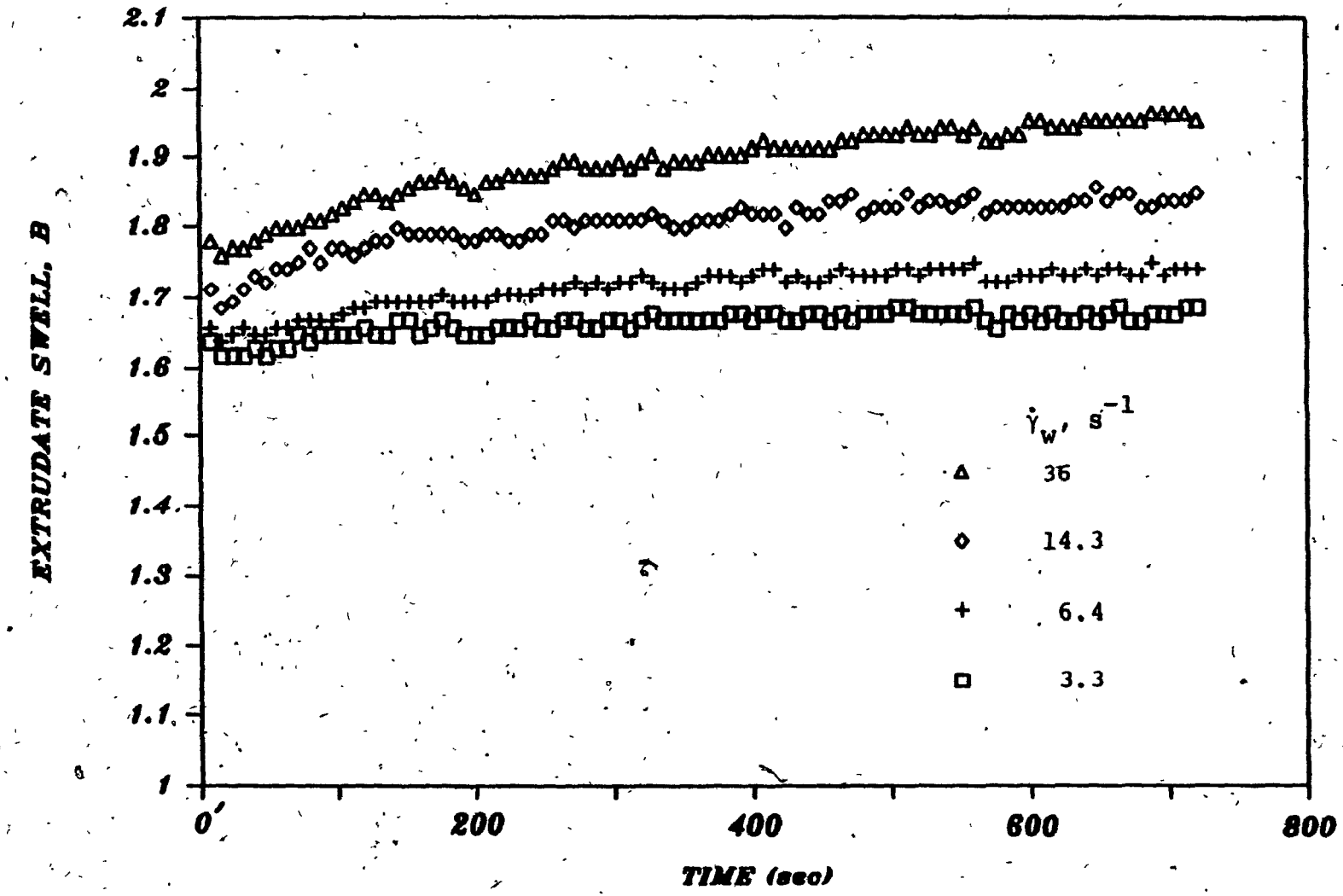

FIGURE 4.6. Extrudate Swell of Resin W2 at 190°C for Different Shear Rates, $\dot{\gamma}_w$.

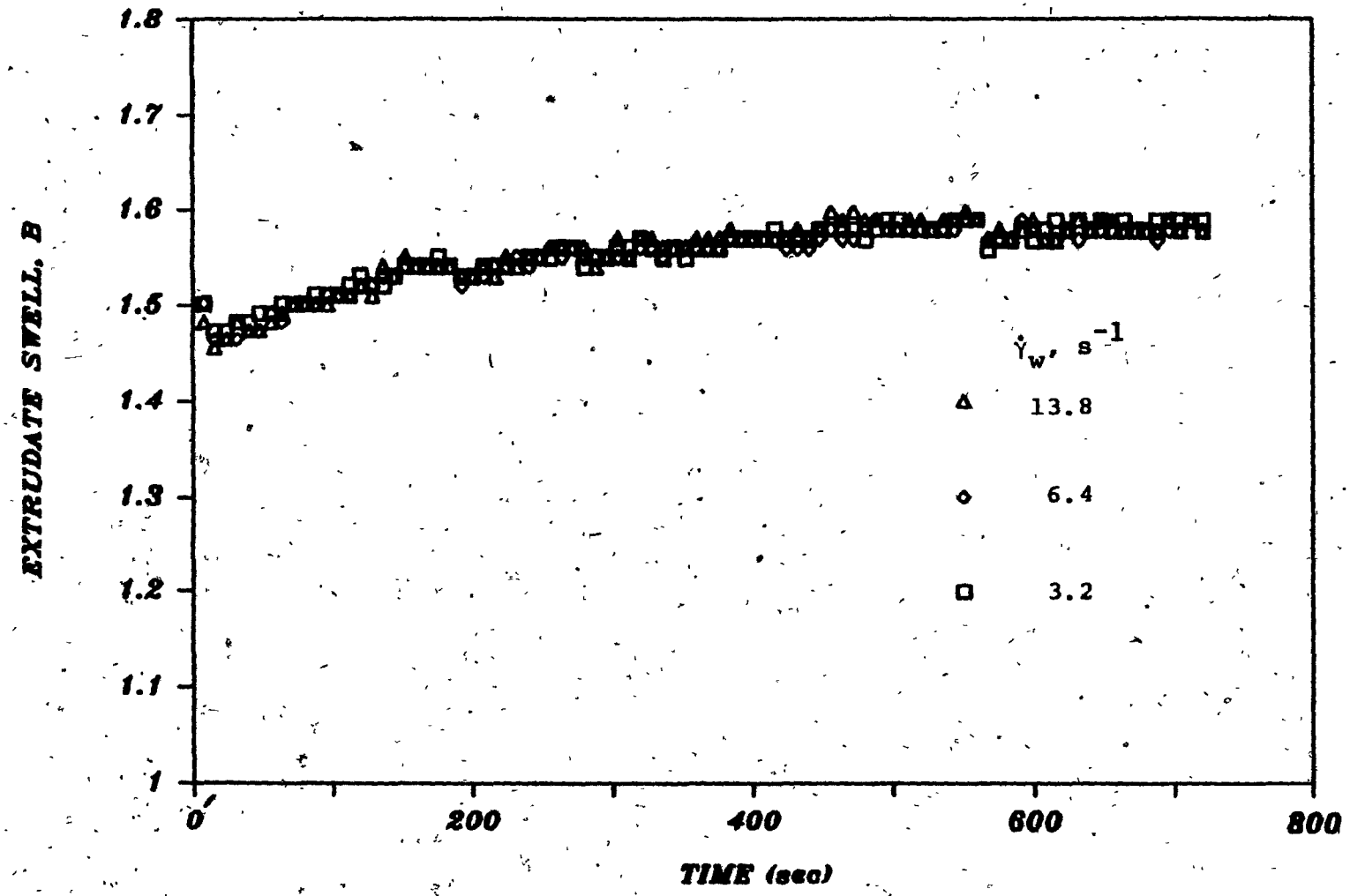

FIGURE 4.7. Extrudate Swell of Resin W3 at 190°C for Different Shear Rates, $\dot{\gamma}_w$.

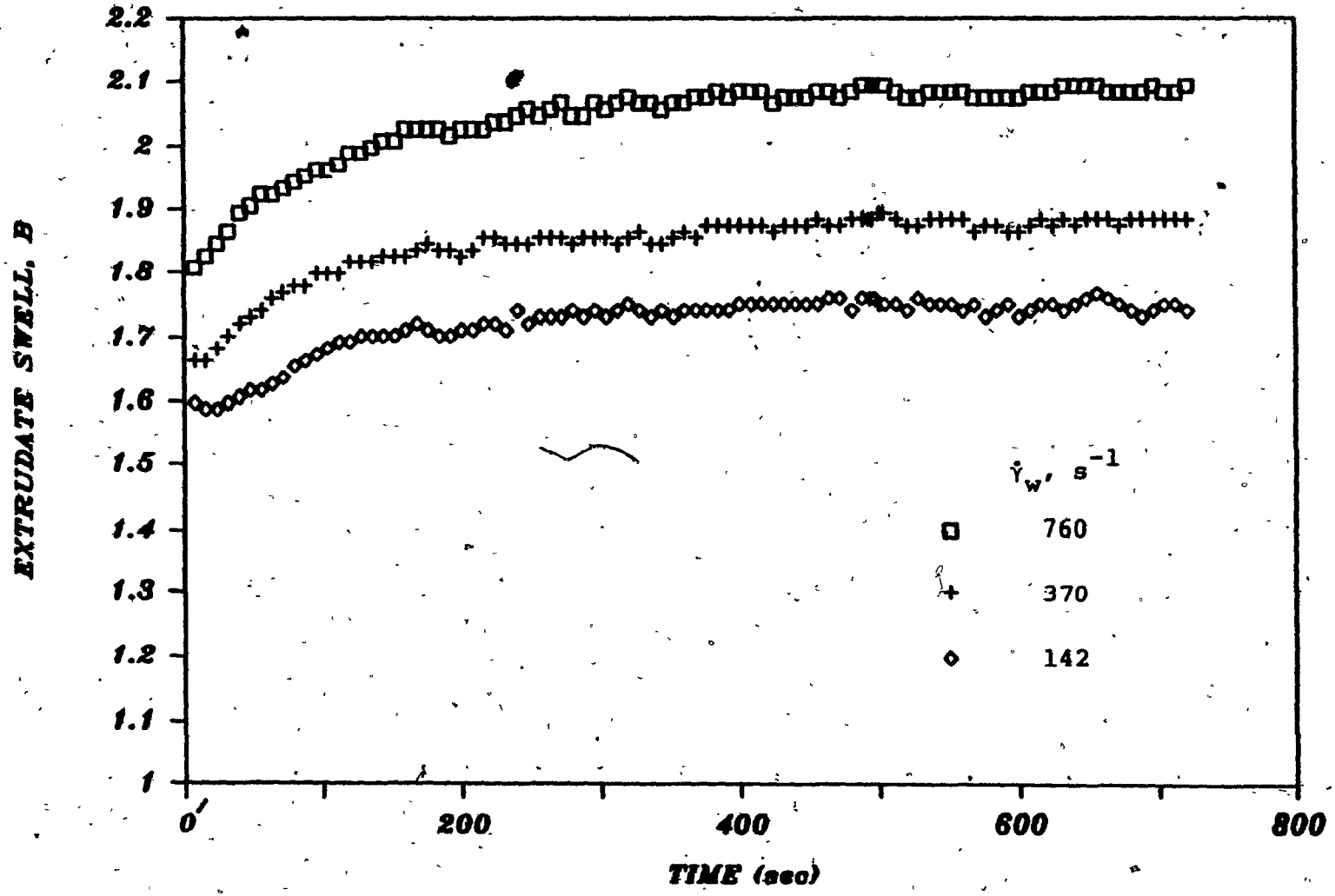

FIGURE 4.8(a). Extrudate Swell of Resin W4 at 190°C for Different Shear Rates, $\dot{\gamma}_w$.

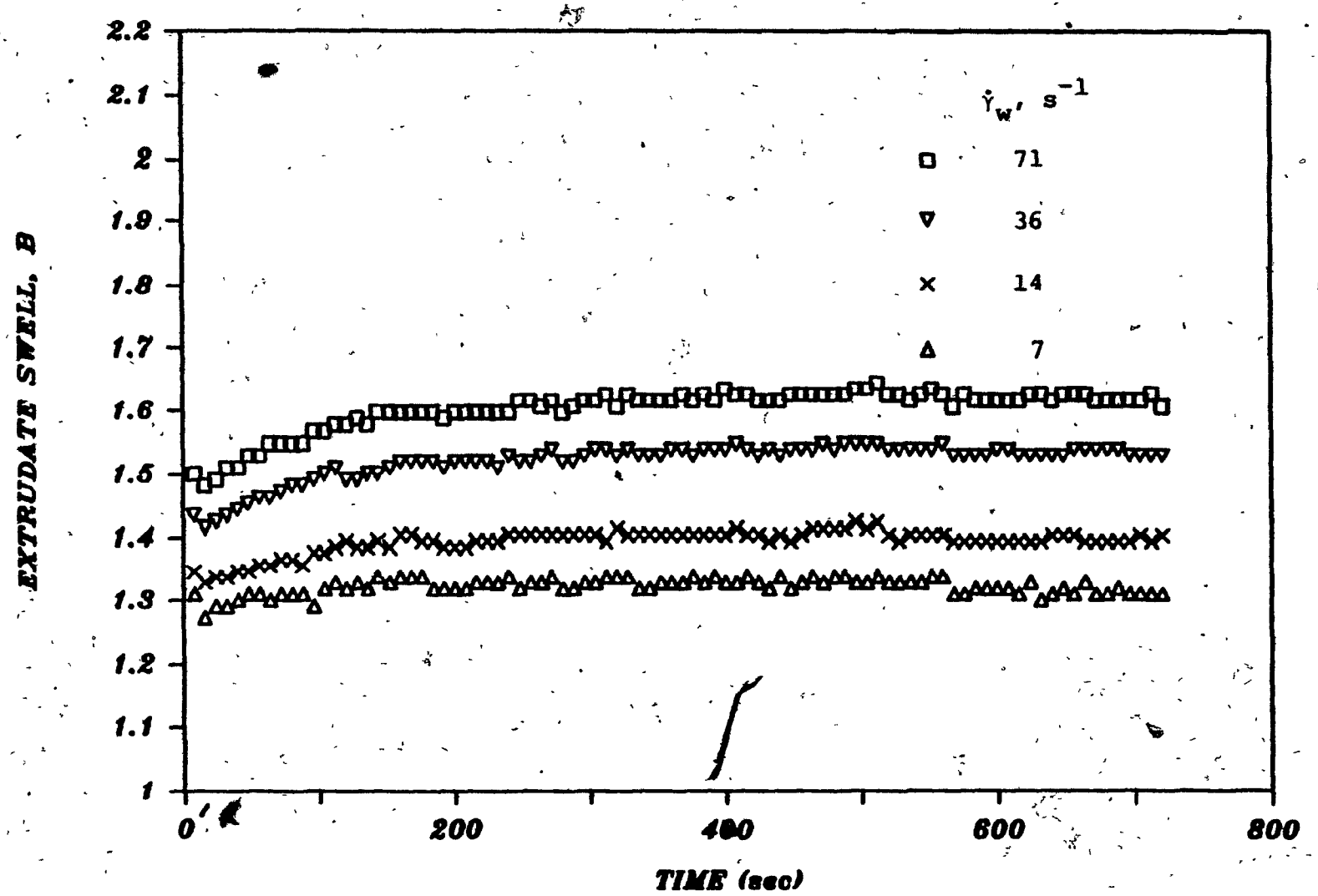

FIGURE 4.8(b). Extrudate Swell of Resin W4 at 190°C for Different Shear Rates, $\dot{\gamma}_w$.

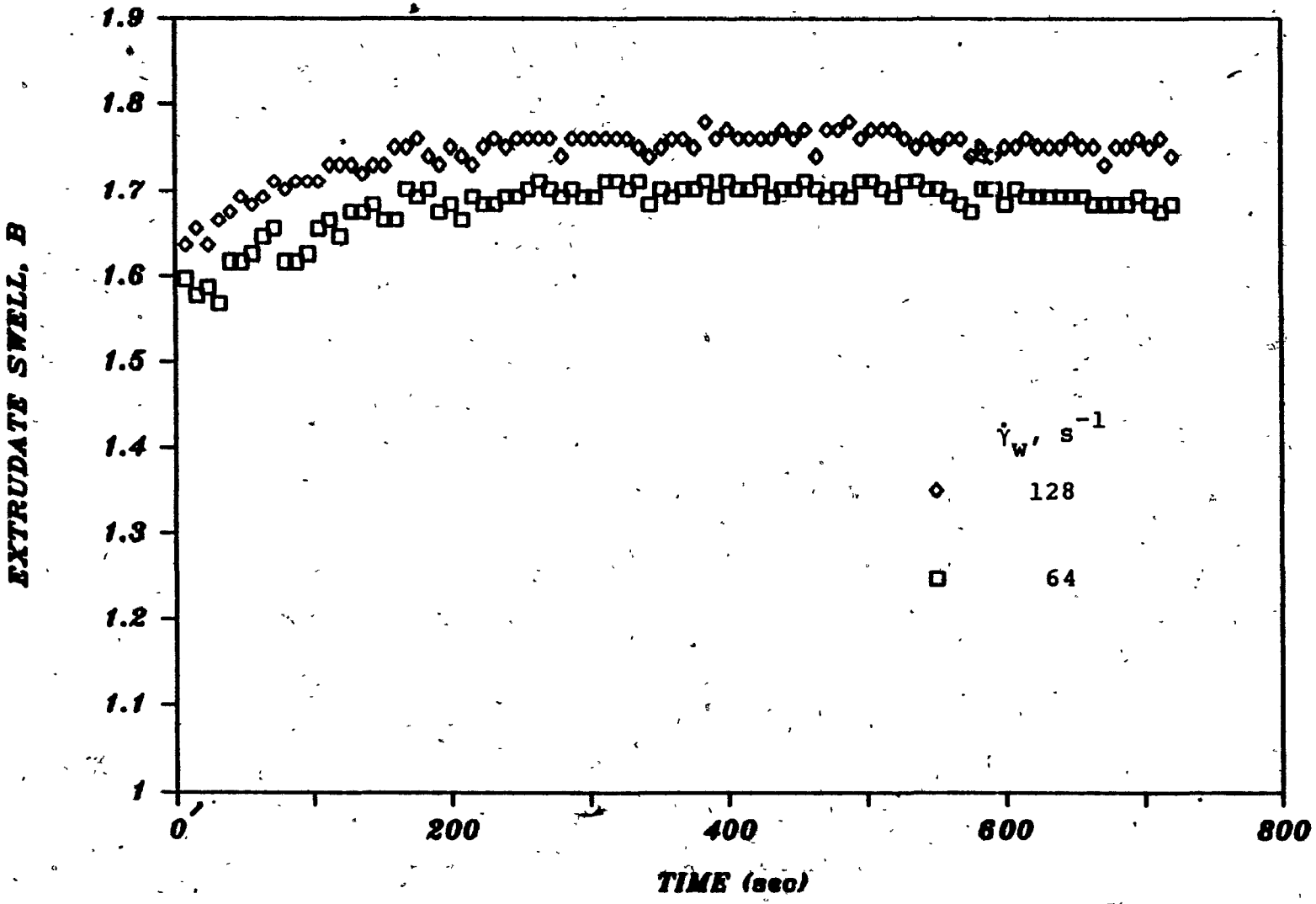

FIGURE 4.9. Extrudate Swell of Resin W5 at 190°C for Different Shear Rates, $\dot{\gamma}_w$.

changes its status from light to dark only when the signal it transmits exceeds the threshold level. If the change in diameter (swell) is very slow, then the previous value of diameter would be recorded, until the required surface area of the photodiode is obstructed, so that its status is changed to dark. The slight fluctuations in the curves may be attributed to roughness of the extrudate.

For resin W3, the swell curves at three different shear rates are identical, as shown in Figure 4.7. This indicates that extrudate swell of resin W3 is independent of shear rate in the tested range. It is important to repeat that each curve shown in Figure 4.7 has been reproduced to within 37.5 μm in diameter measurements.

It is apparent from the preceding results that about 80% of the swelling occurs almost instantaneously (in the first 2 to 3 seconds). The remaining 20% of the swelling takes place in about 5 minutes. This confirms the general belief that extrudate swell can be divided into two processes, with two different time constants. The first, which is very fast, resembles solid-like elastic recovery. The second, which is much slower, is in the range of time constants obtained in stress relaxation experiments.

Equilibrium extrudate swell, for all the resins, was approximated by the time-dependent swelling value after 720 seconds. The results, at different shear rates, are presented in Table 4.2. The dependency of the estimated equilibrium

TABLE 4.2

Extrudate Swell Values for Polyethylene Resins at Different Shear Rates After 720 Seconds

W1		W2		W3		W4		W5	
Shear Rate $\dot{\gamma}_w$, s^{-1}	Swell B	Shear Rate $\dot{\gamma}_w$, s^{-1}	Swell B	Shear Rate $\dot{\gamma}_w$, s^{-1}	Swell B	Shear Rate $\dot{\gamma}_w$, s^{-1}	Swell B	Shear Rate $\dot{\gamma}_w$, s^{-1}	Swell B
14	1.86	3.3	1.68	3.2	1.58	7	1.31	64	1.70
39	1.91	6.4	1.74	6.4	1.58	14	1.40	128	1.76
77	2.01	14.3	1.84	13.8	1.58	36	1.53		
144	2.09	36	1.96			71	1.62		
366	2.15					142	1.75		
732	2.22					370	1.88		
						760	2.09		

swell values on shear rate, for the five polyethylene resins, is shown in Figures 4.10 to 4.12. Equilibrium extrudate swell increases with shear rate for all the resins, except W3. Comparison shows that W1 swells the most, followed by W4.

Comparisons between time-dependent data obtained using the present apparatus and data obtained by Al-Bastaki (1) for the same resins and under the same conditions is shown in Figures 4.13-4.17. Al-Bastaki used a photographic technique to record extrudate swell. It is evident from the comparison that data obtained with the present method appear to exhibit a more systematic and reasonable trend.

Equilibrium extrudate swell data obtained using the two techniques are compared in Figures 4.18 to 4.22. In general, the present data appear to be more consistent and reasonable. Furthermore, the swell results obtained by Al-Bastaki (1) are much higher than those obtained in this study. The discrepancy can be partially attributed to the fact that Al-Bastaki did not account for that part of the swell due to the absorption of oil by the extrudates. Also, measurements made using the photographic technique are sensitive to errors resulting from poor calibration or if the extrudate is tilted or bent. Data obtained using the present apparatus are less sensitive to these effects.

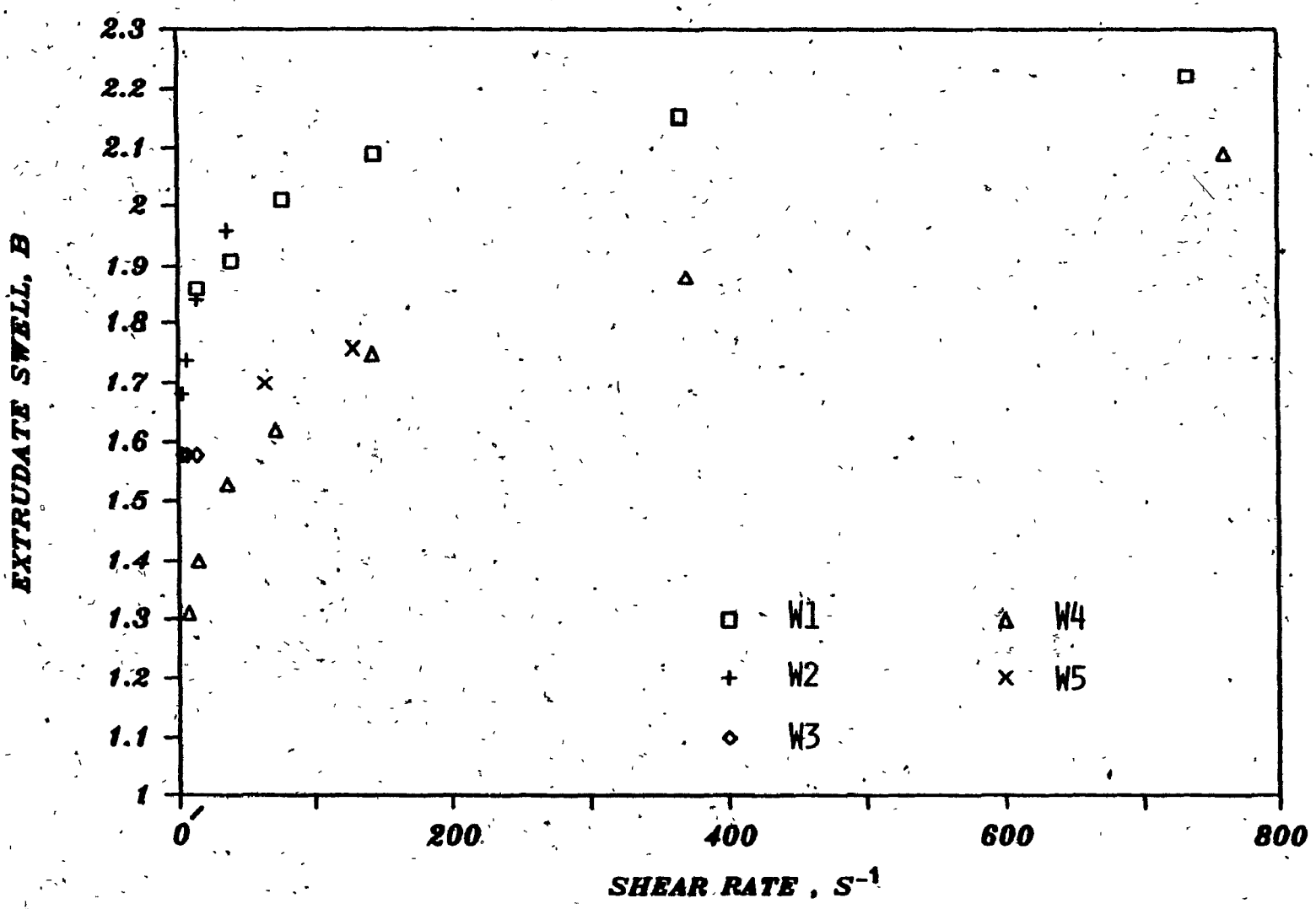

FIGURE 4.10. Equilibrium Extrudate Swell as a Function of Shear Rate, $\dot{\gamma}_w$, for Five Polyethylene Resins Extruded at 190°C.

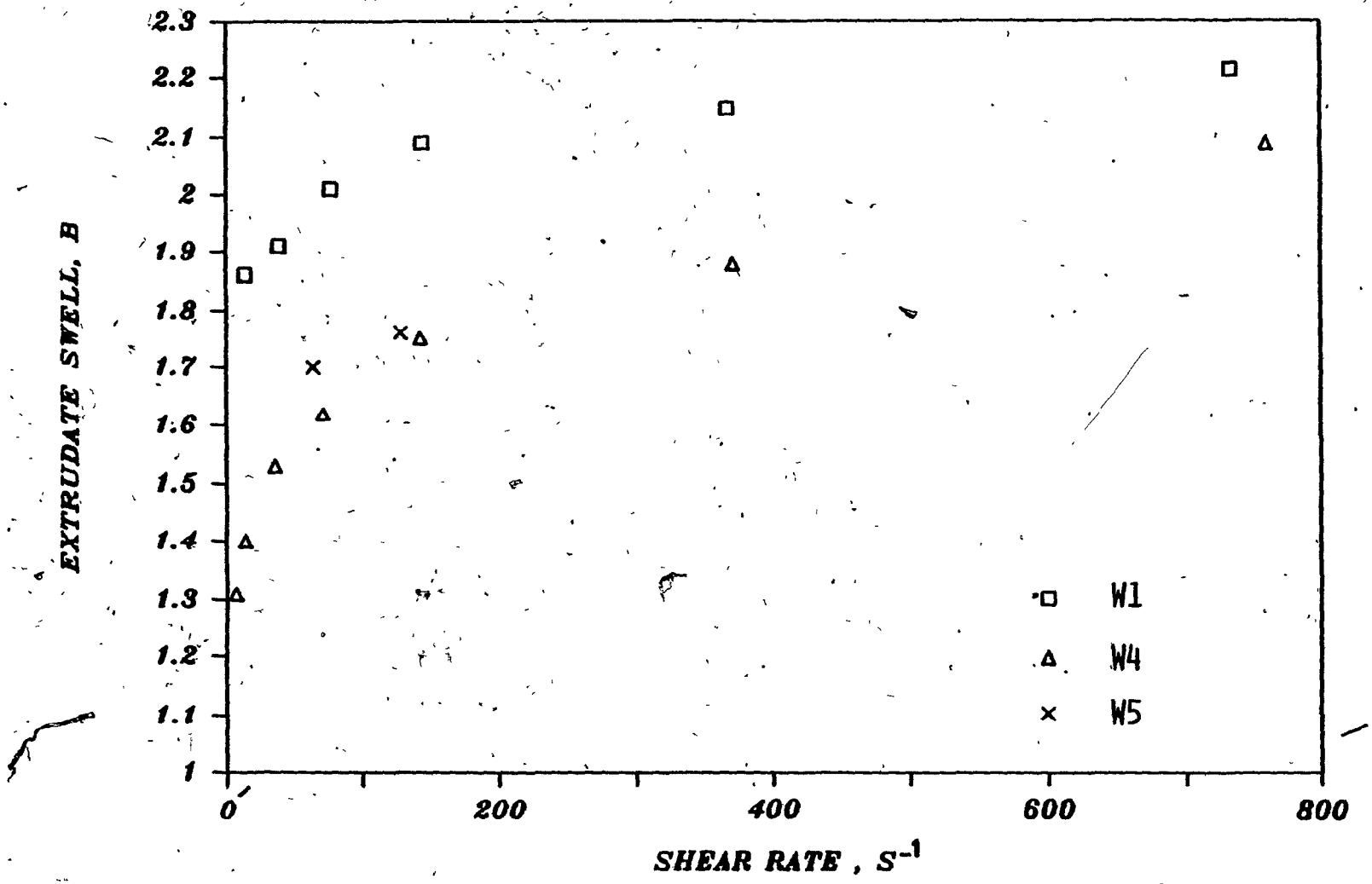

FIGURE 4.11. Equilibrium Extrudate Swell as a Function of Shear Rate, $\dot{\gamma}_w$, for Resins (W1, W4 and W5) Extruded at 190°C.

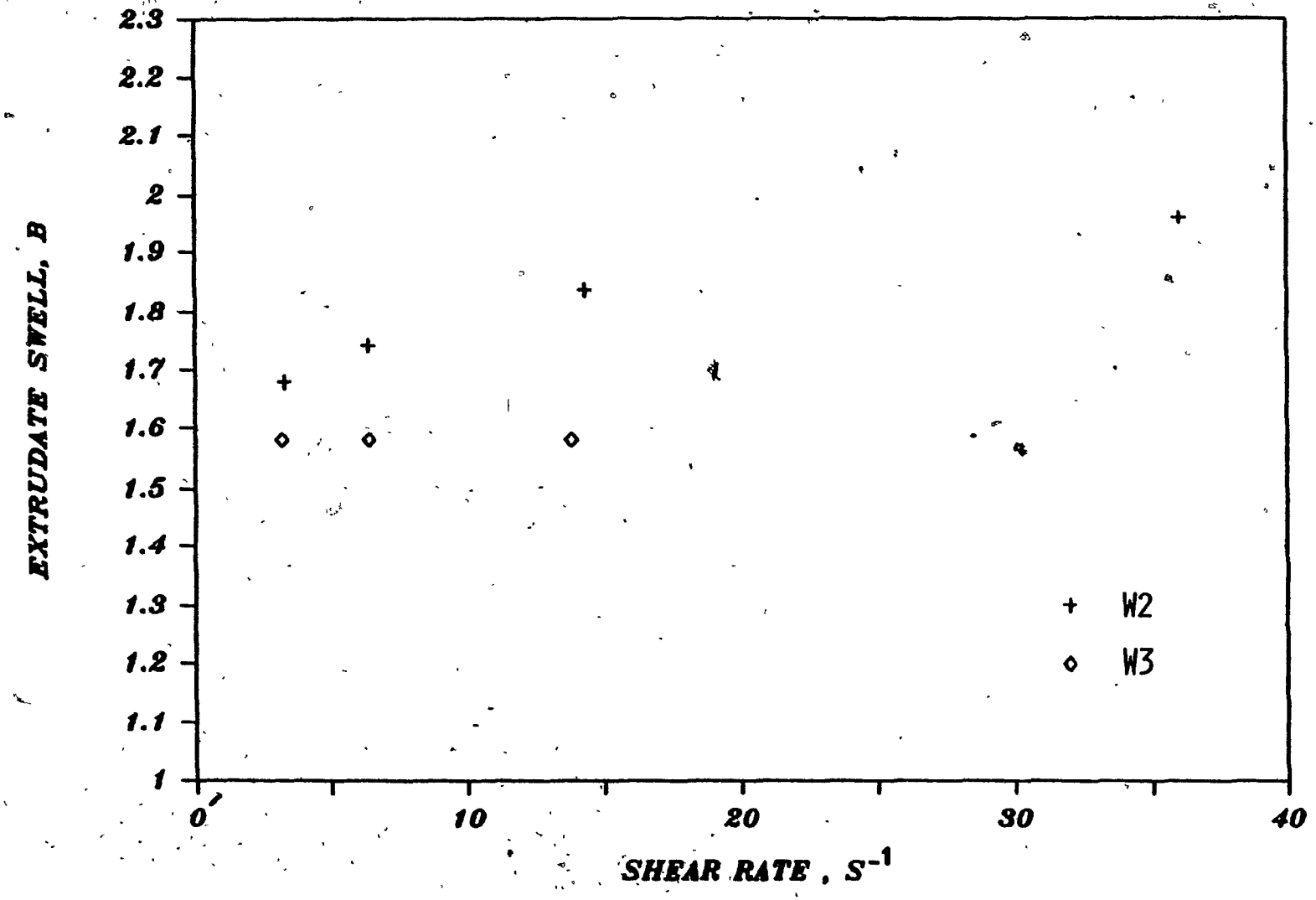

FIGURE 4.12. Equilibrium Extrudate Swell as a Function of Shear Rate, $\dot{\gamma}_w$, for Resins (W2 and W3) Extruded at 190°C.

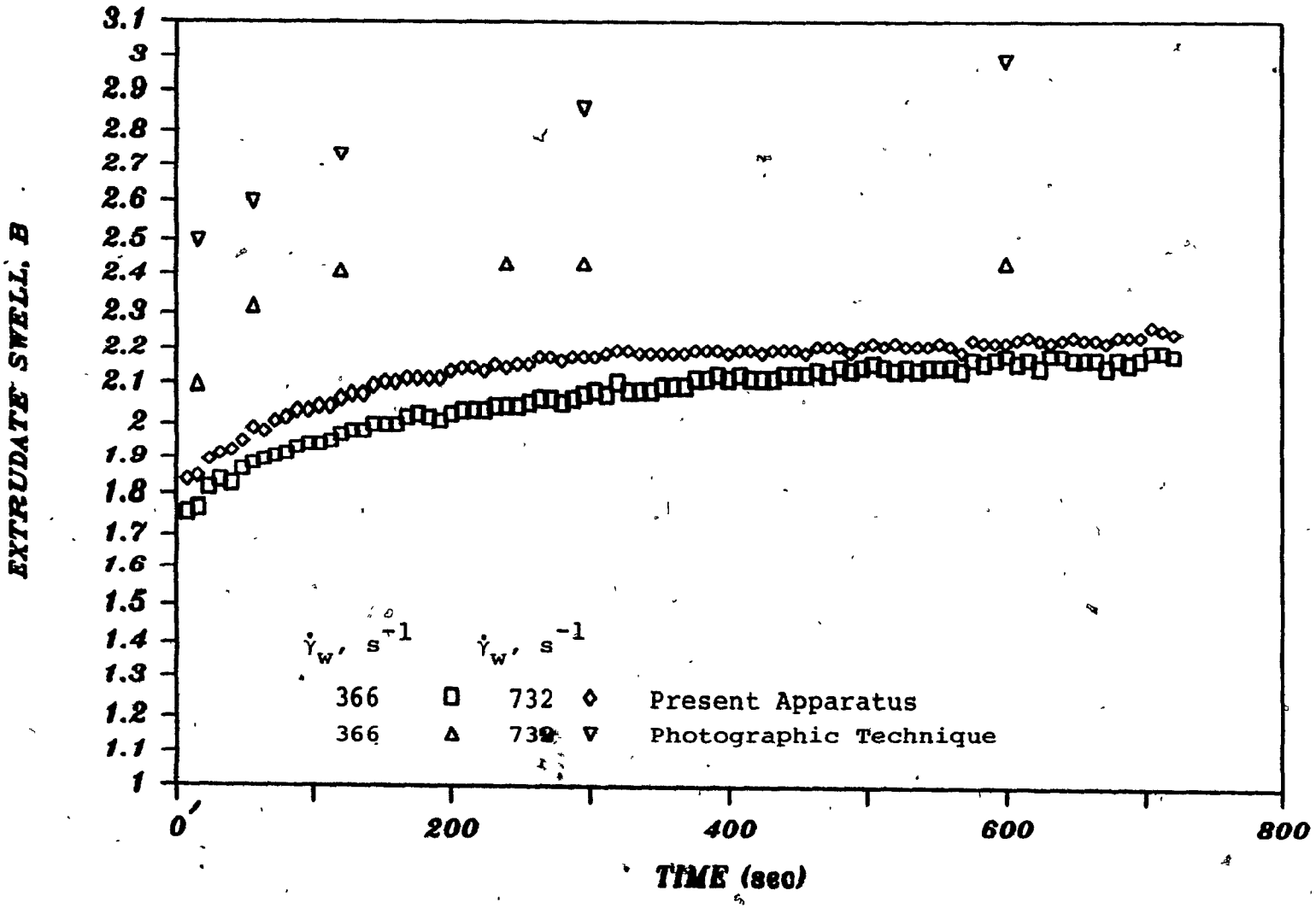

FIGURE 4.13. Time-Dependent Extrudate Swell Data Obtained Using Two Different Techniques. Resin W1. T_M = 190°C.

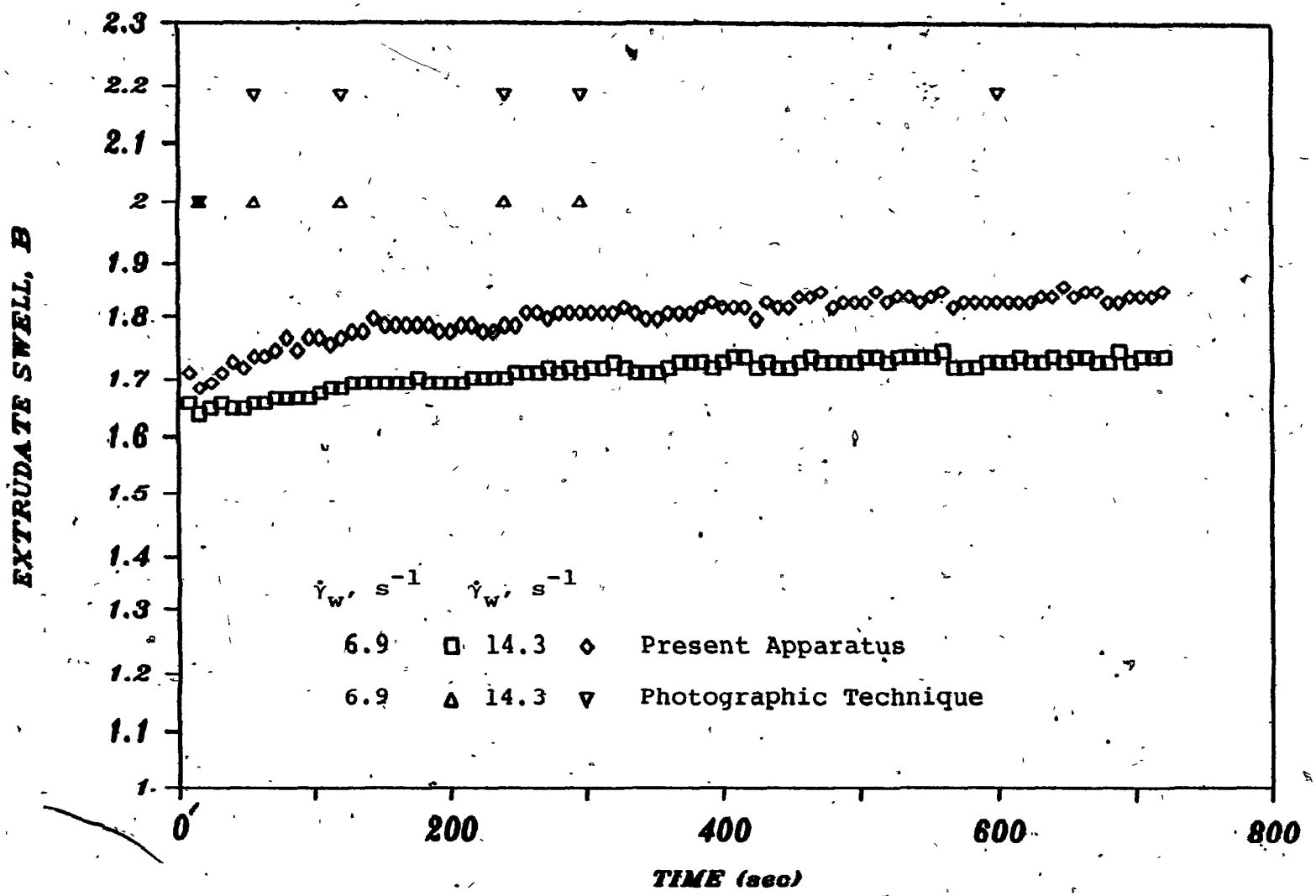

FIGURE 4.14. Time-Dependent Extrudate Swell Data Obtained Using Two Different Techniques. Resin W2. T_M = 190°C.

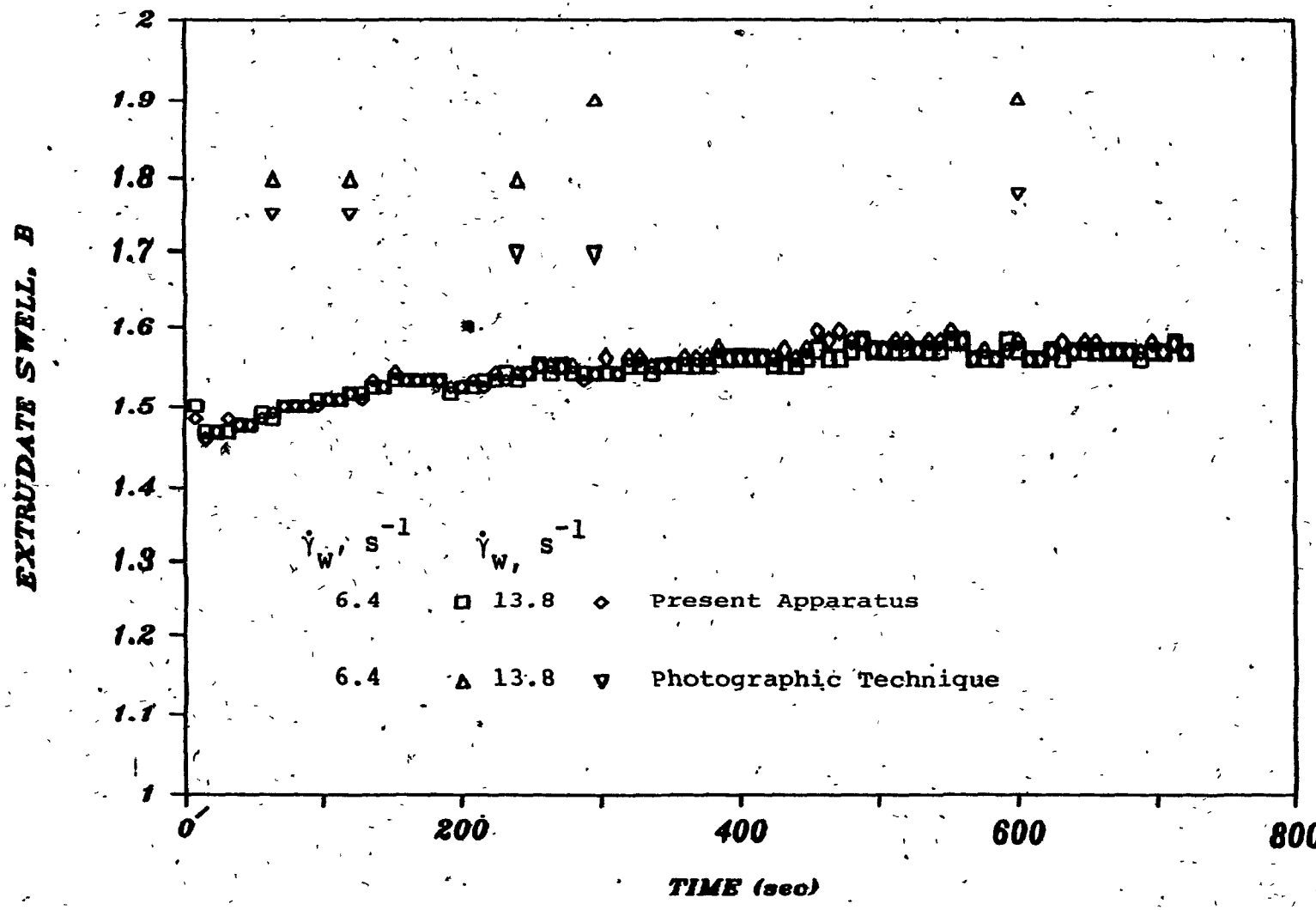

FIGURE 4.15. Time-Dependent Extrudate Swell Data Obtained Using Two Different Techniques. Resin W3. T_M = 190°C.

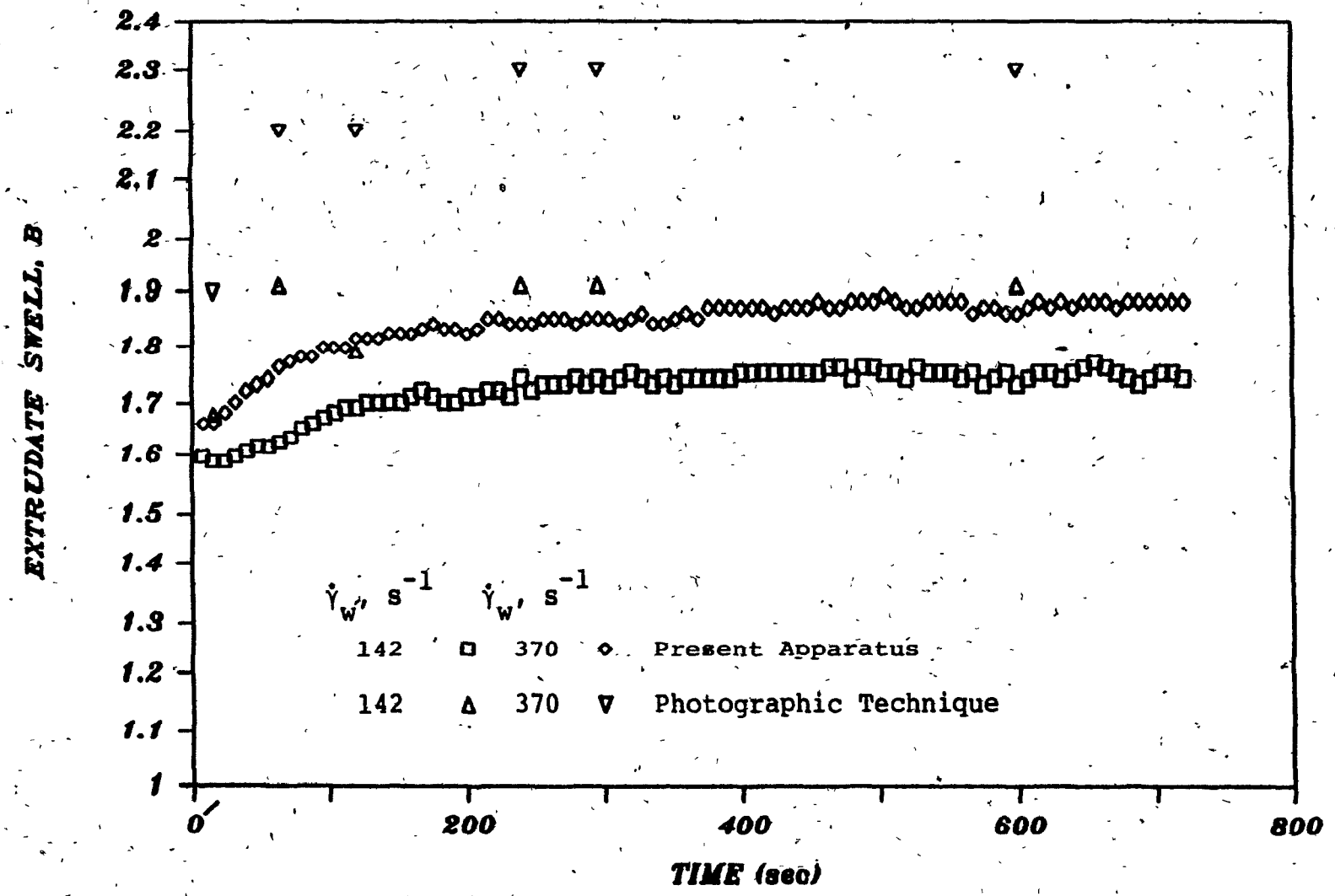

FIGURE 4.16. Time-Dependent Extrudate Swell Data Obtained Using Two Different Techniques. Resin W4. T_M = 190°C.

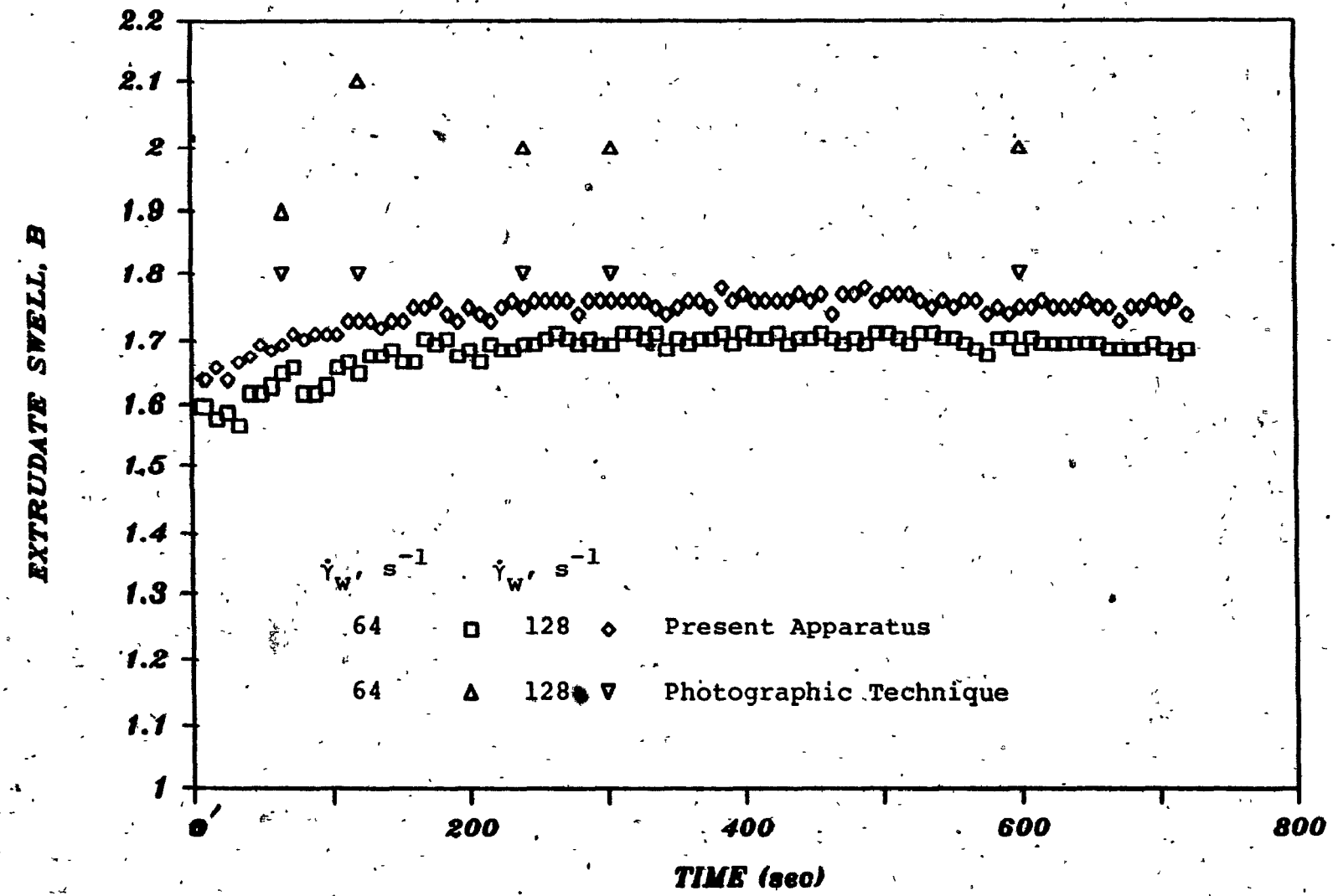

FIGURE 4.17. Time-Dependent Extrudate Swell Data Obtained Using Two Different Techniques. Resin W5. T_M = 190°C.

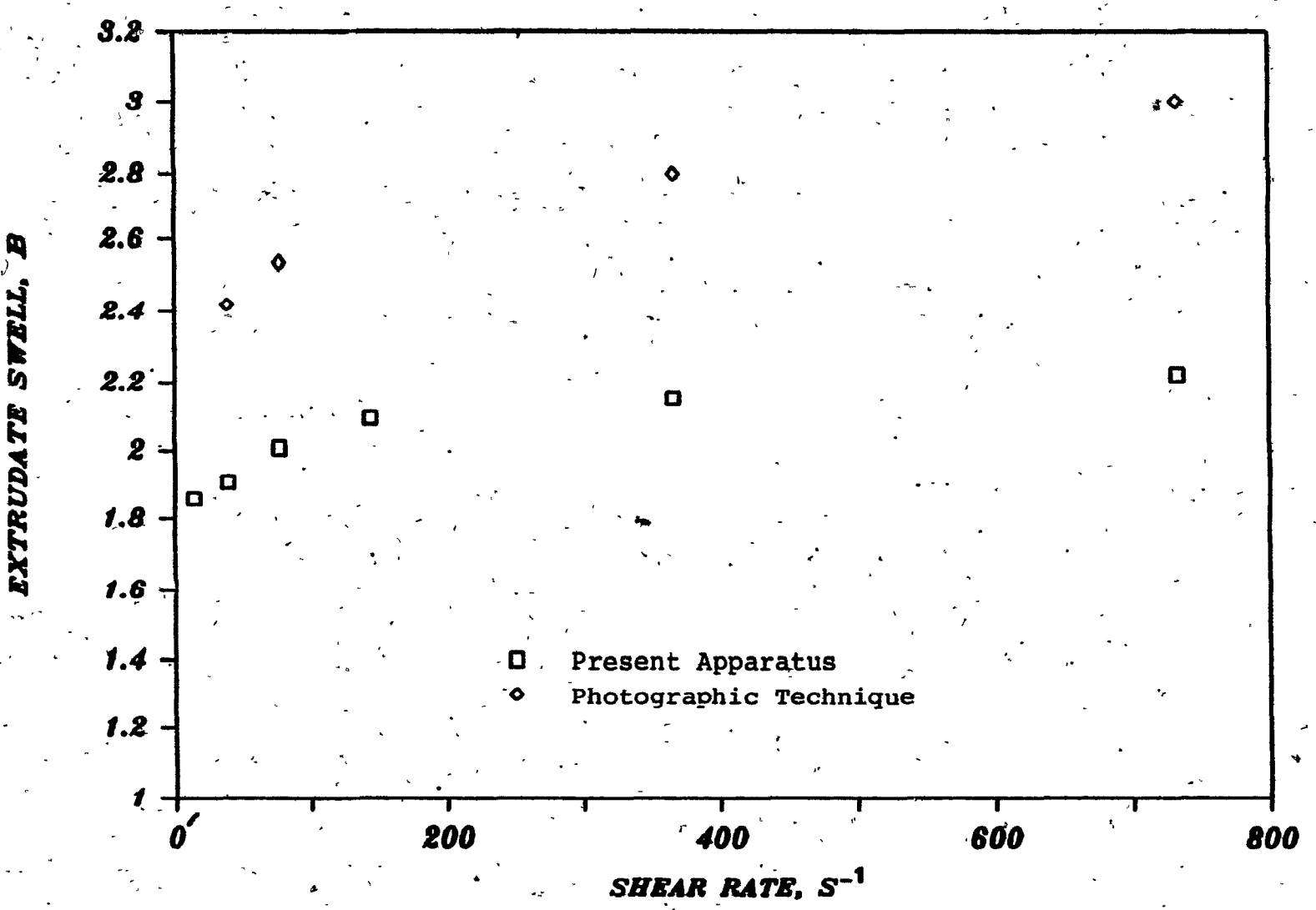

FIGURE 4.18. Equilibrium Extrudate Swell Data for Resin WI. T_M = 190°C.

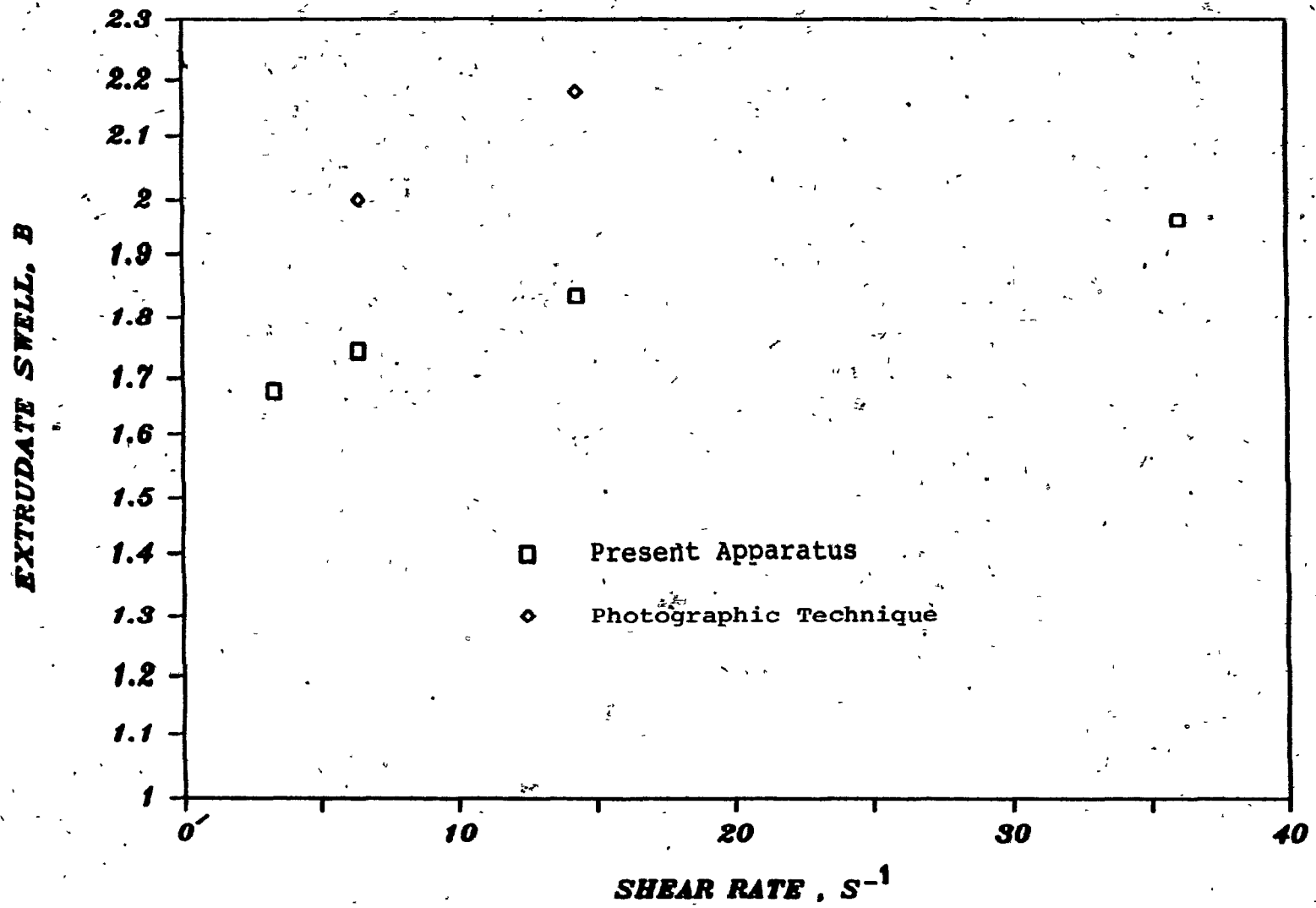

FIGURE 4.19. Equilibrium Extrudate Swell Data for Resin W2. T_M = 190°C.

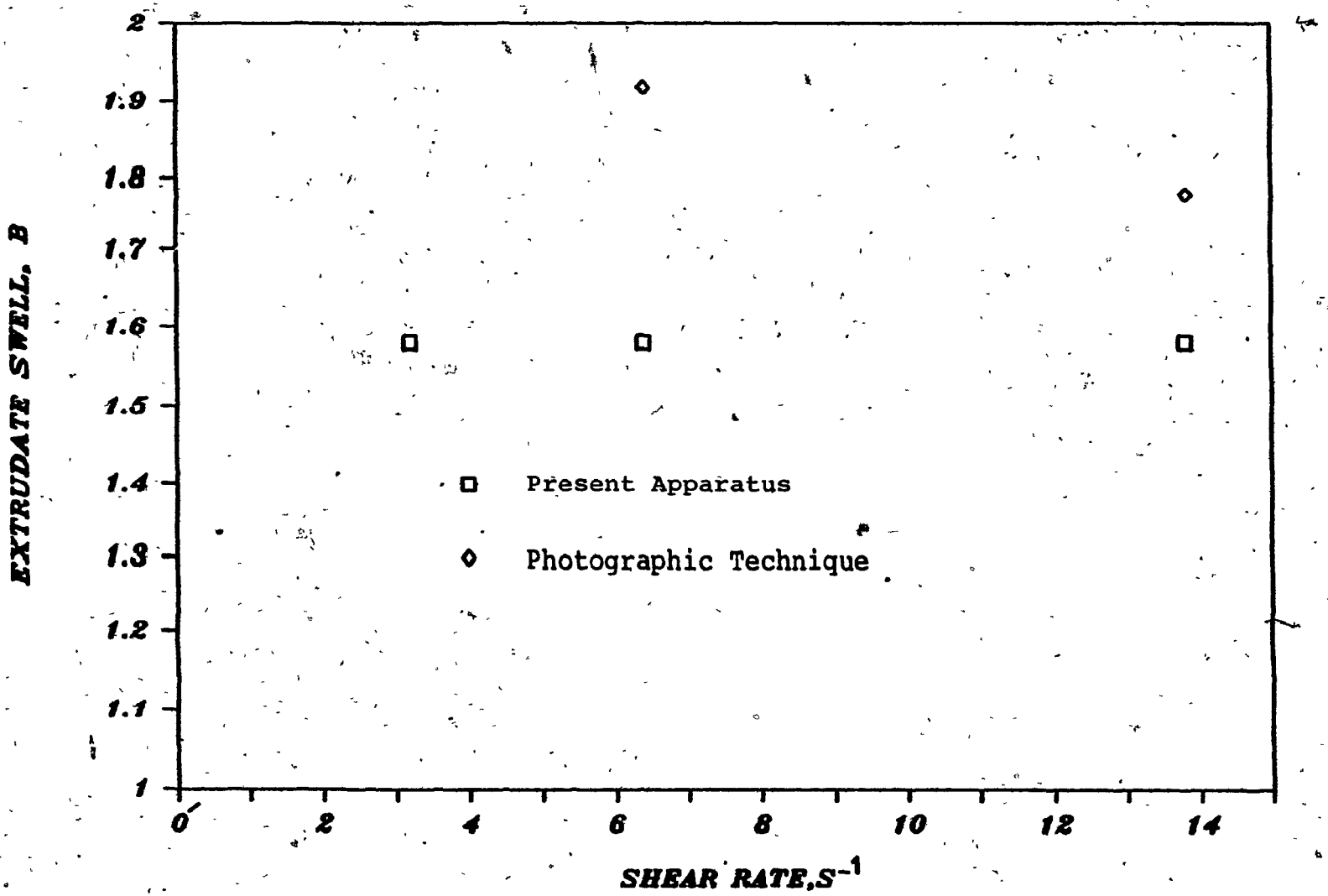

FIGURE 4.20. Equilibrium Extrudate Swell Data for Resin W3. T_M = 190°C.

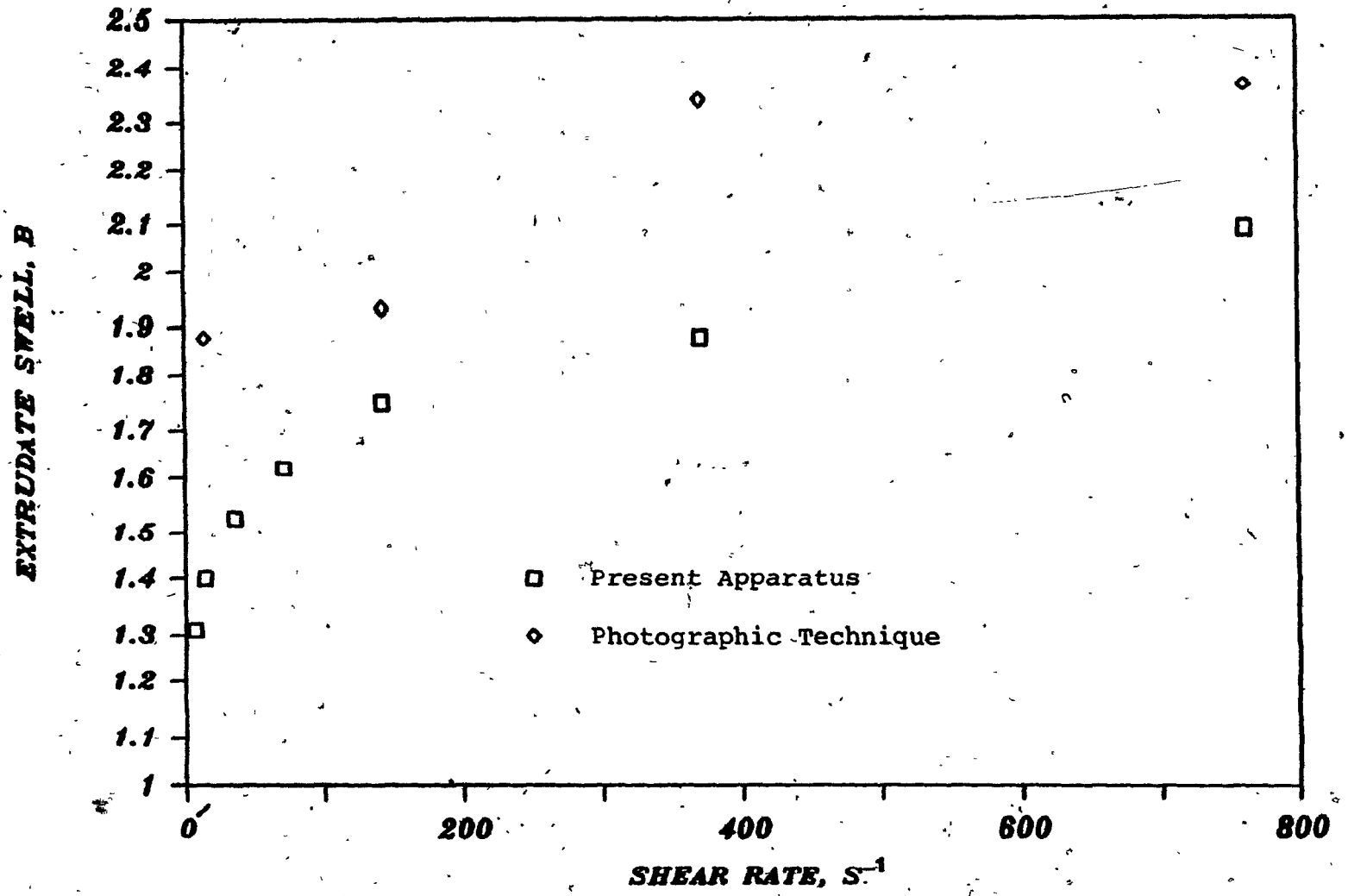

FIGURE 4.21. Equilibrium Extrudate Swell Data for Resin W4. T_M = 190°C.

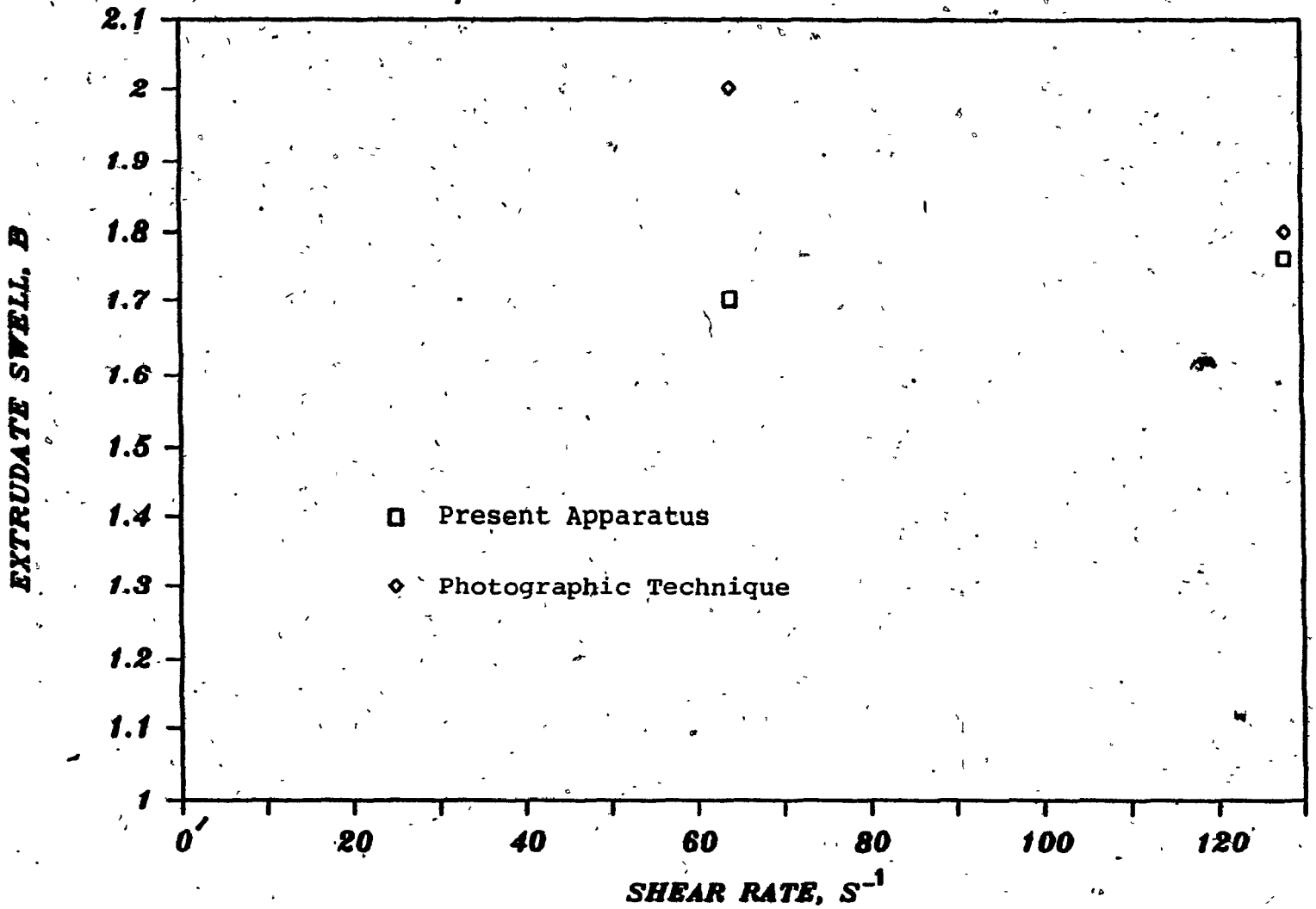

FIGURE 4.22. Equilibrium Extrudate Swell Data for Resin W5. $T_M = 190^{\circ}C$.

4.2.3 Effect of Temperature

Resin W1 was extruded at 210°C and the swell was measured. The time-dependent swell at different shear rates is shown in Figure 4.23. The same trend is observed as at 190°C. Time-dependent swell data, at the two different temperatures (210° and 190°C), are compared in Figures 4.24 to 4.27.

The equilibrium swell data at both temperatures and for different shear rates are presented in Table 4.3. The equilibrium swell data, as a function of apparent shear rate, $\dot{\gamma}$, for both temperatures are plotted in Figure 4.28.

The results confirm that extrudate swell decreases, though slightly in this case, when extrusion temperature increases.

4.3 Polypropylene and the Effect of Glass Fibers

Both the unfilled polypropylene (PP) resin and the fiber-reinforced resin (30% short glass-fiber content) were extruded at 200°C. For the unfilled PP, the inner compartments of the thermostating chamber were filled with a mixture of low viscosity silicone oils. The mixture consisted of 43% (volume) 2 cS and 57% 5 cS oils. For the filled PP, the compartments were filled with 20 cS silicone oil. The temperature of the compartments was maintained at 160°C. Equilibrium swell of PP was reached in about 5 minutes, after the experiment had started. Therefore, the effect of oil absorption was considered to be negligible. This needs to be confirmed.

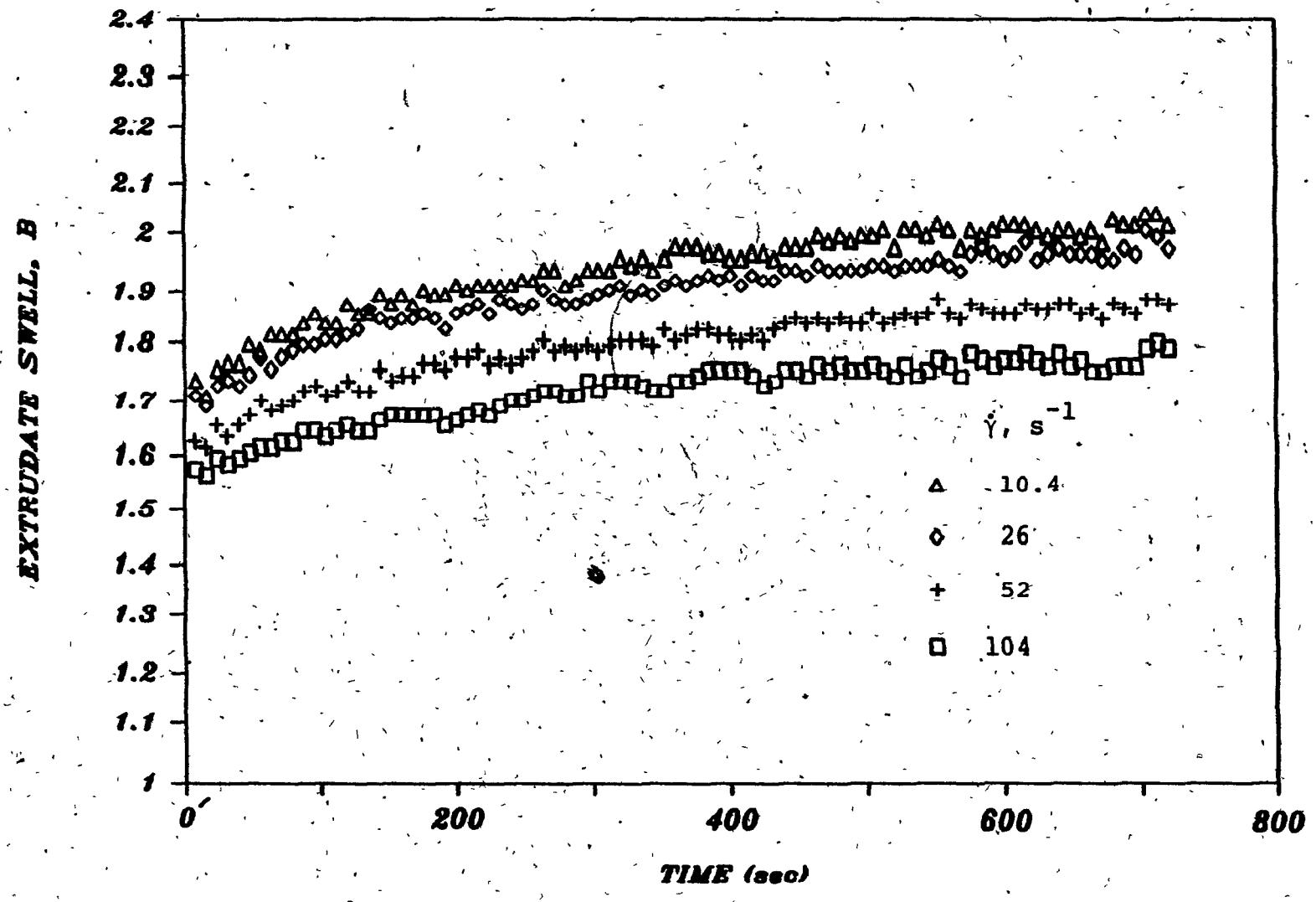

FIGURE 4.23. Time-Dependent Extrudate Swell of Resin W1 at 210°C for Different Shear Rates, $\dot{\gamma}$.

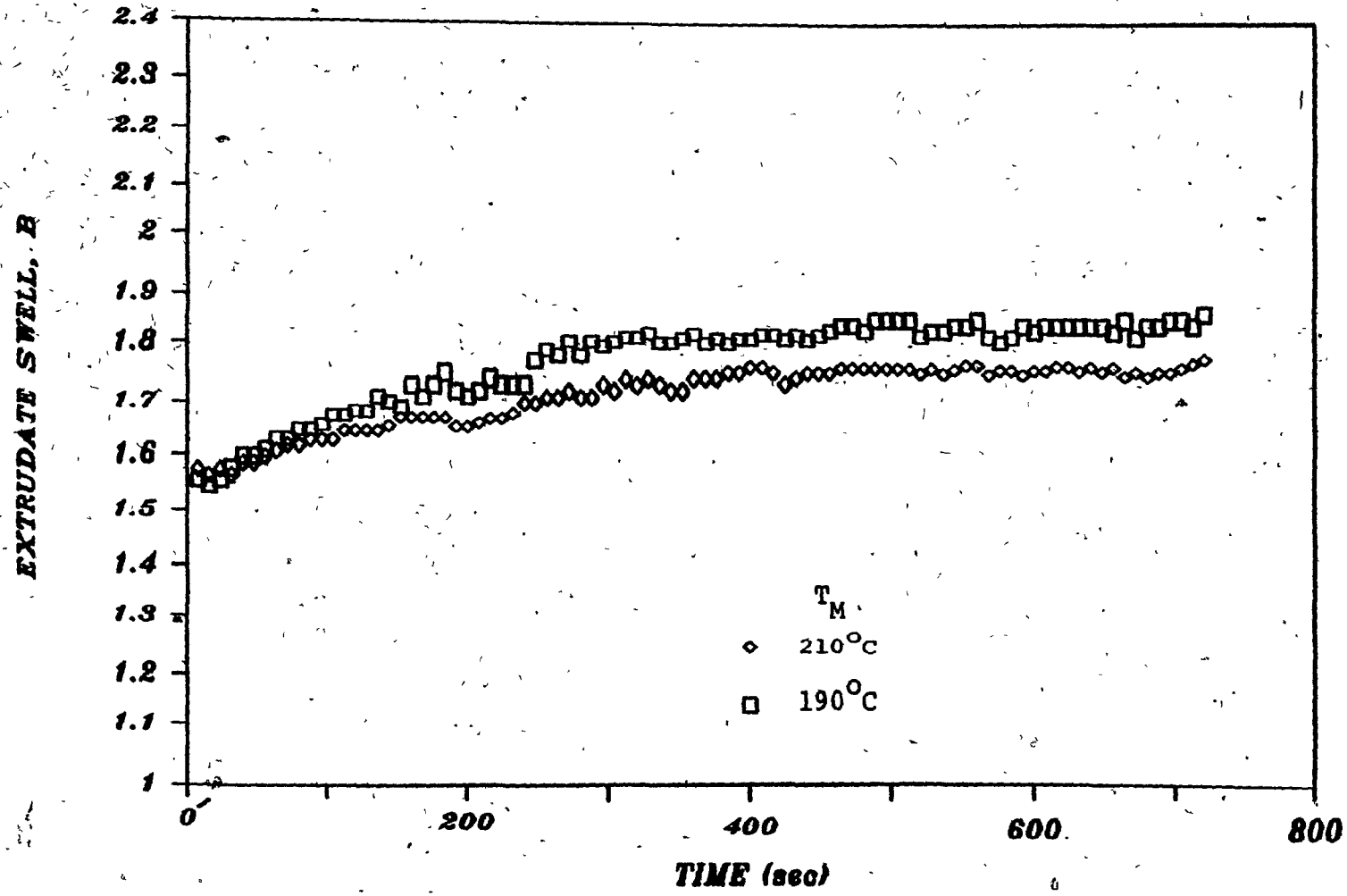

FIGURE 4.24. Time-Dependent Extrudate Swell at Two Extrusion Temperatures. Apparent Shear Rate, $\dot{\gamma} = 10.4\ s^{-1}$. Resin W1.

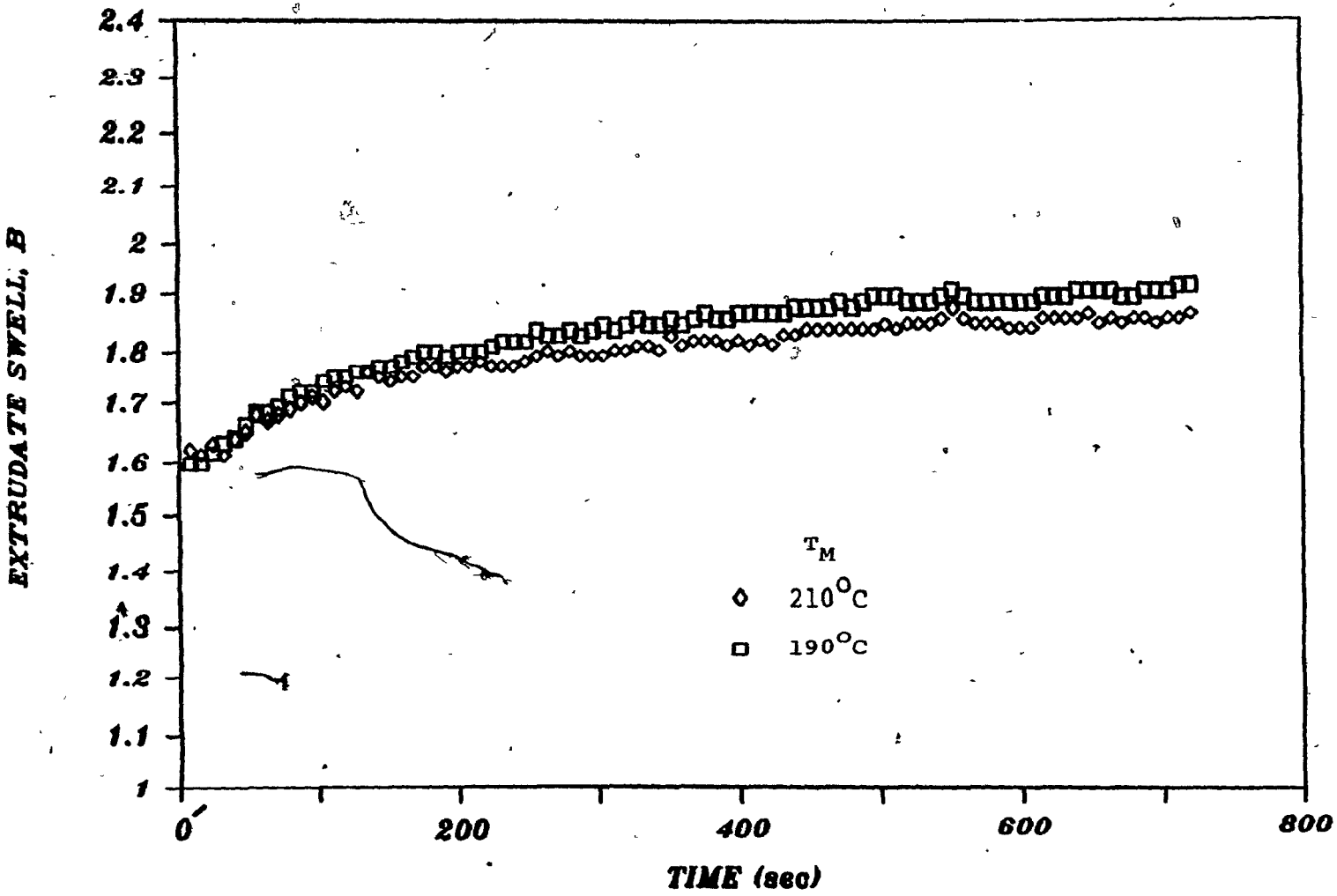

FIGURE 4.25. Time-Dependent Extrudate Swell at Two Extrusion Temperatures. Apparent Shear Rate, $\dot{\gamma} = 26\ s^{-1}$. Resin W1.

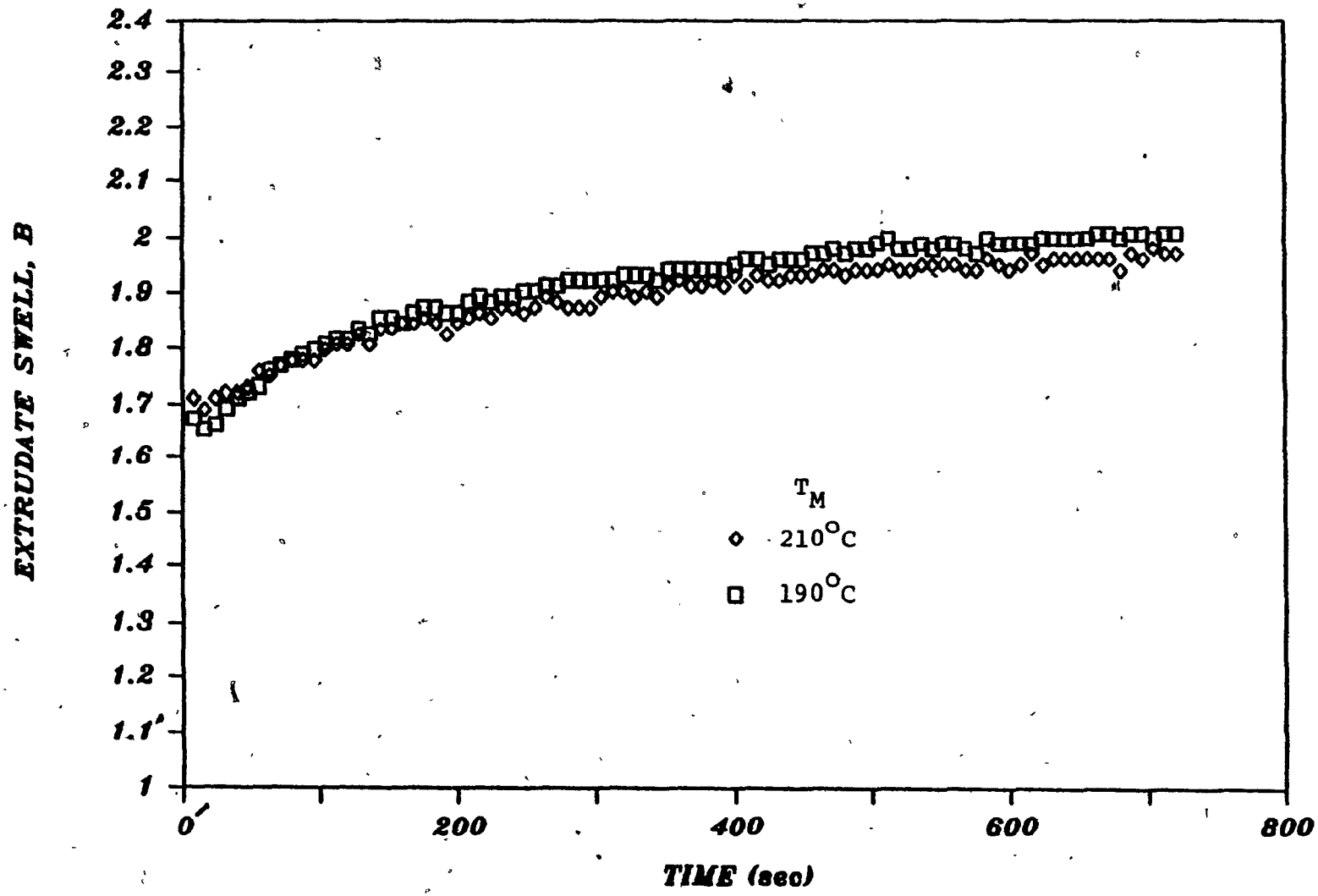

FIGURE 4.26. Time-Dependent Extrudate Swell at Two Extrusion Temperatures. Apparent Shear Rate, $\dot{\gamma} = 52\ s^{-1}$. Resin W1.

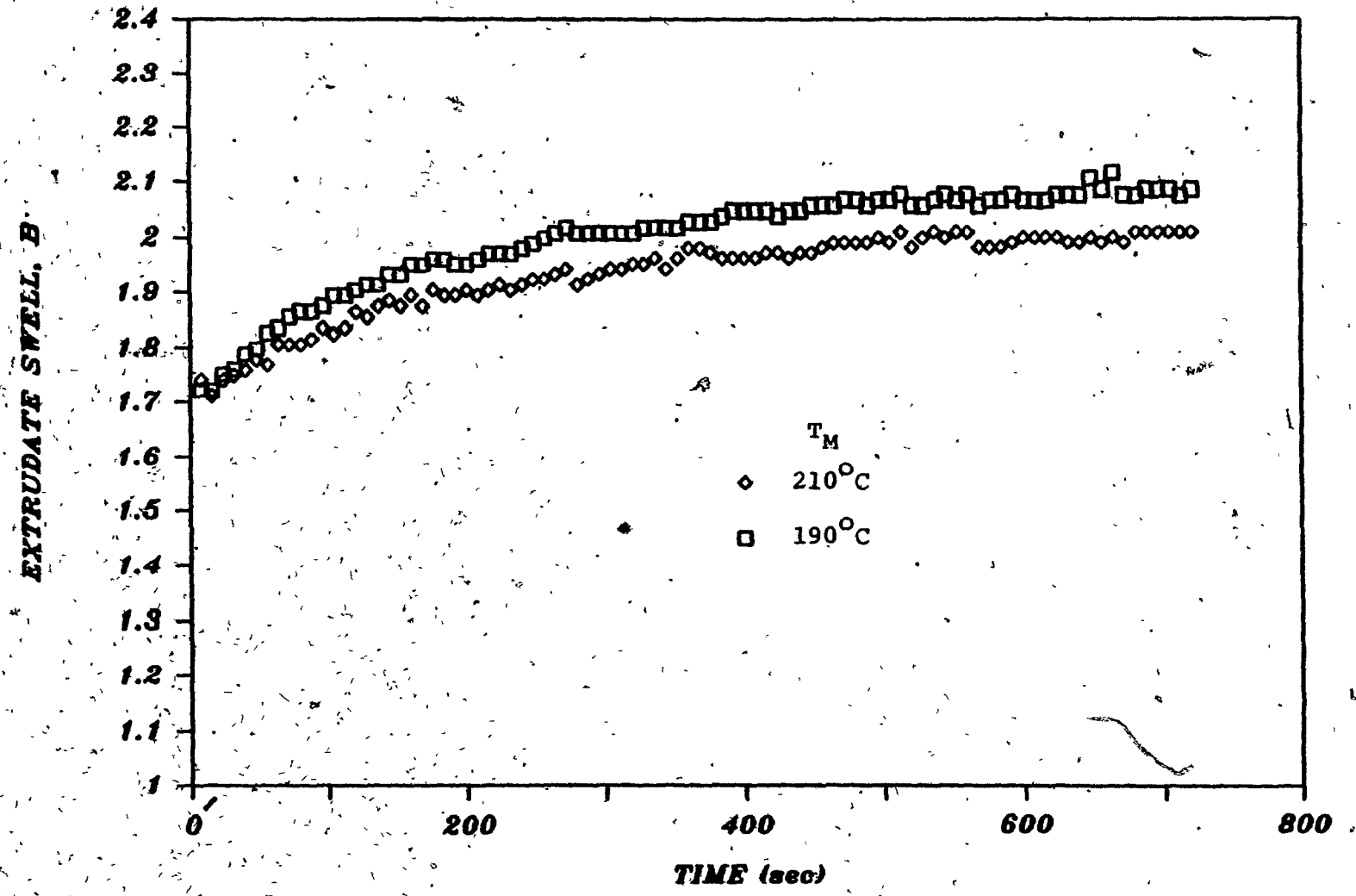

FIGURE 4.27. Time-Dependent Extrudate Swell at Two Extrusion Temperatures. Apparent Shear Rate, $\dot{\gamma} = 104\ s^{-1}$. Resin W1.

TABLE 4.3

Equilibrium Extrudate Swell Values for Resin W1 Extruded at 210° and 190°C

Apparent Shear Rate $\dot{\gamma}$, s^{-1}	Swell, B at 190°C	Swell, B at 210°C
10.4	1.86	1.76
26	1.91	1.85
52	2.01	1.97

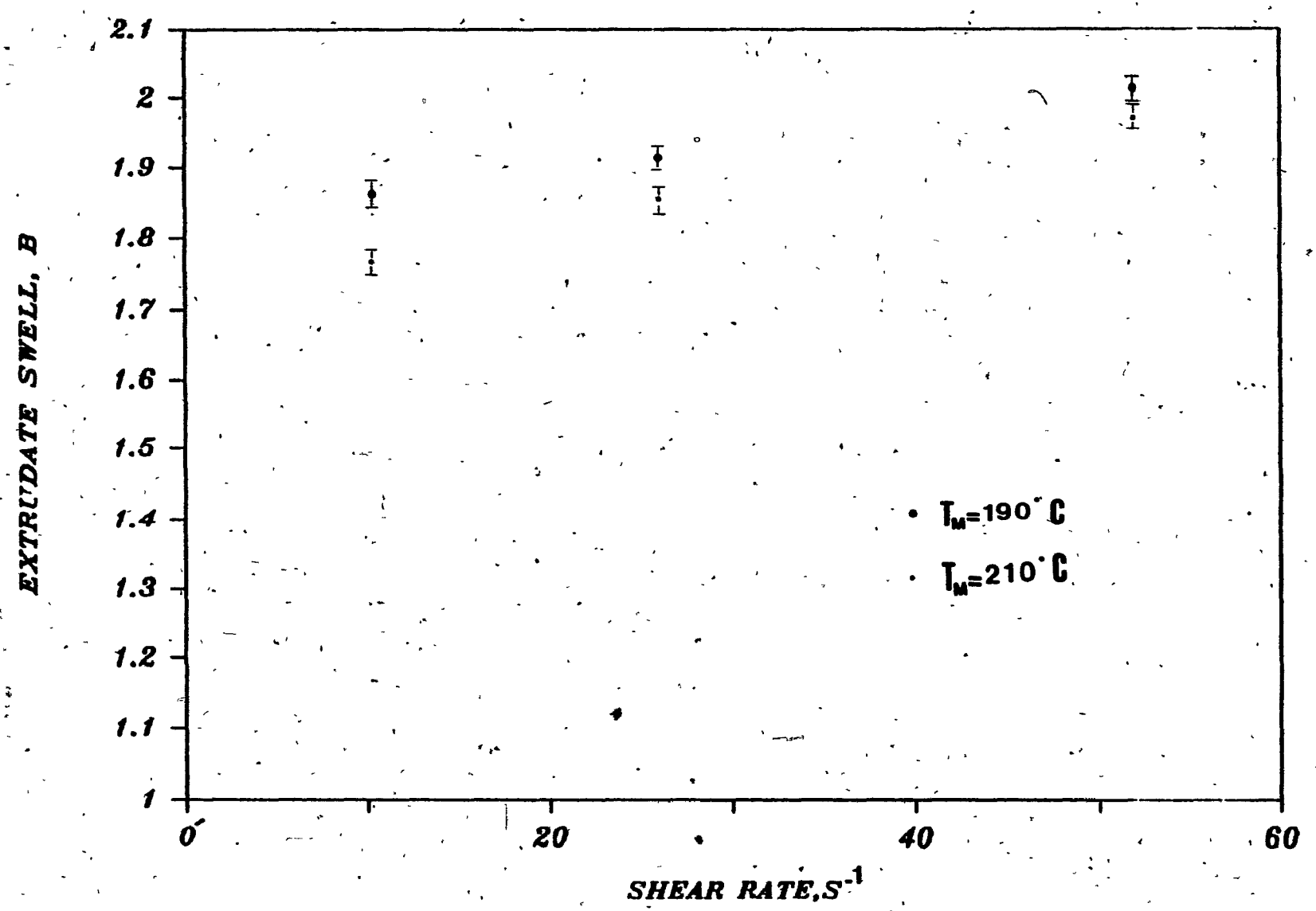

FIGURE 4.28. Equilibrium Extrudate Swell of Resin W1 as a Function of Apparent Shear Rate at Two Extrusion Temperatures.

Extrudate swell of unfilled PP was measured at 3 different shear rates. The time-dependent swell is shown in Figure 4.29. It is seen that extrudate swell increases with shear rate. The true shear rates are indicated in the figure.

The filled PP exhibited no detectable swell under the indicated conditions. This can be seen in Figure 4.30, where the time-dependent swell data for the filled as well as the unfilled resins are shown at comparable shear rates. Only the apparent shear rates for the filled PP are indicated.

The results on the swell of polypropylene support the general belief that the addition of fillers to the polymer melt reduces extrudate swell substantially. In this case, the swell is effectively eliminated, because of the high filler content. The relatively large scatter in the data is probably due to the rough surface of the extrudate.

4.4 Liquid Crystal Polymer (LCP 2000)

LCP 2000 resin was extruded at 300°C. The inner compartments were filled with 20 cS silicone oil and heated up to 200°C.

Extrudate swell was measured at 3 different shear rates. The results for apparent shear rates 26 s^{-1} and 104 s^{-1} are shown in Figure 4.31. Extrudate swell at 52 s^{-1} was measured, but the result is not shown because it showed similar behaviour. No extrudate swell was detected. This is in general agreement with the results obtained by White (103), who found

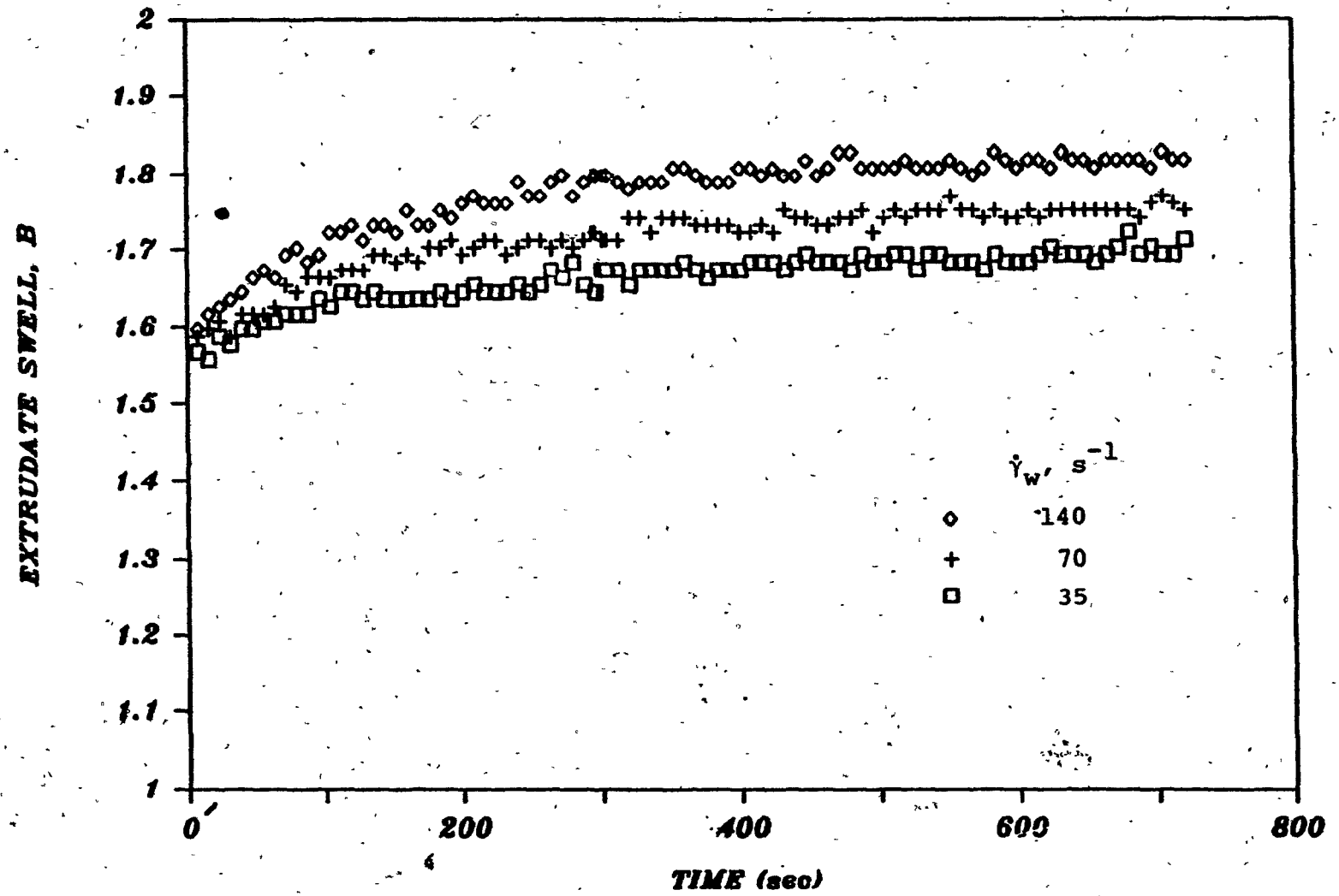

FIGURE 4.29. Extrudate Swell of Unfilled Polypropylene Resin at Different Shear Rates, $\dot{\gamma}_w$. Extrusion Temperature, T_M = 200°C.

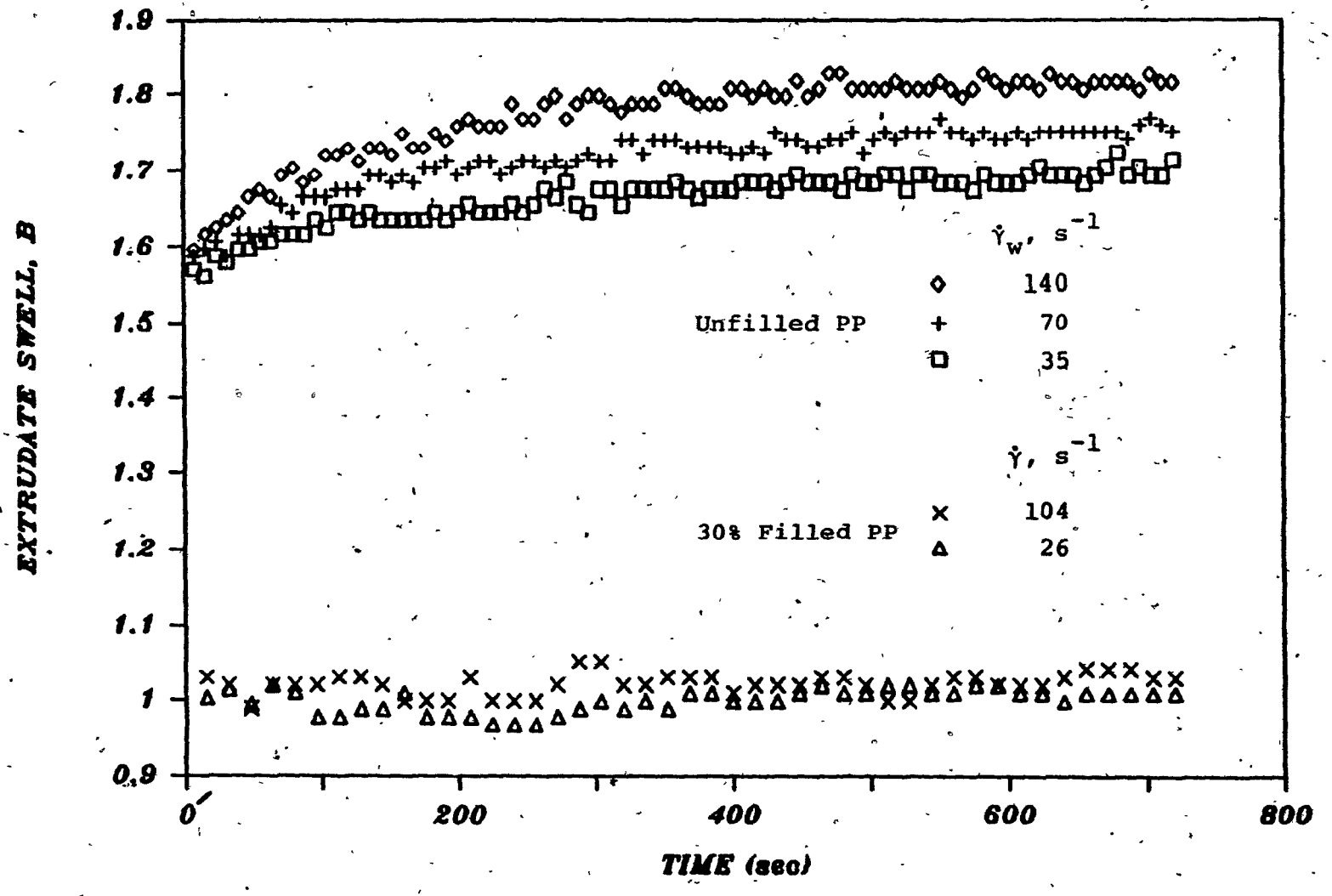

FIGURE 4.30. The Effect of Glass Fibers on Extrudate Swell of PP. Extrusion Temperature, T_M = 200°C.

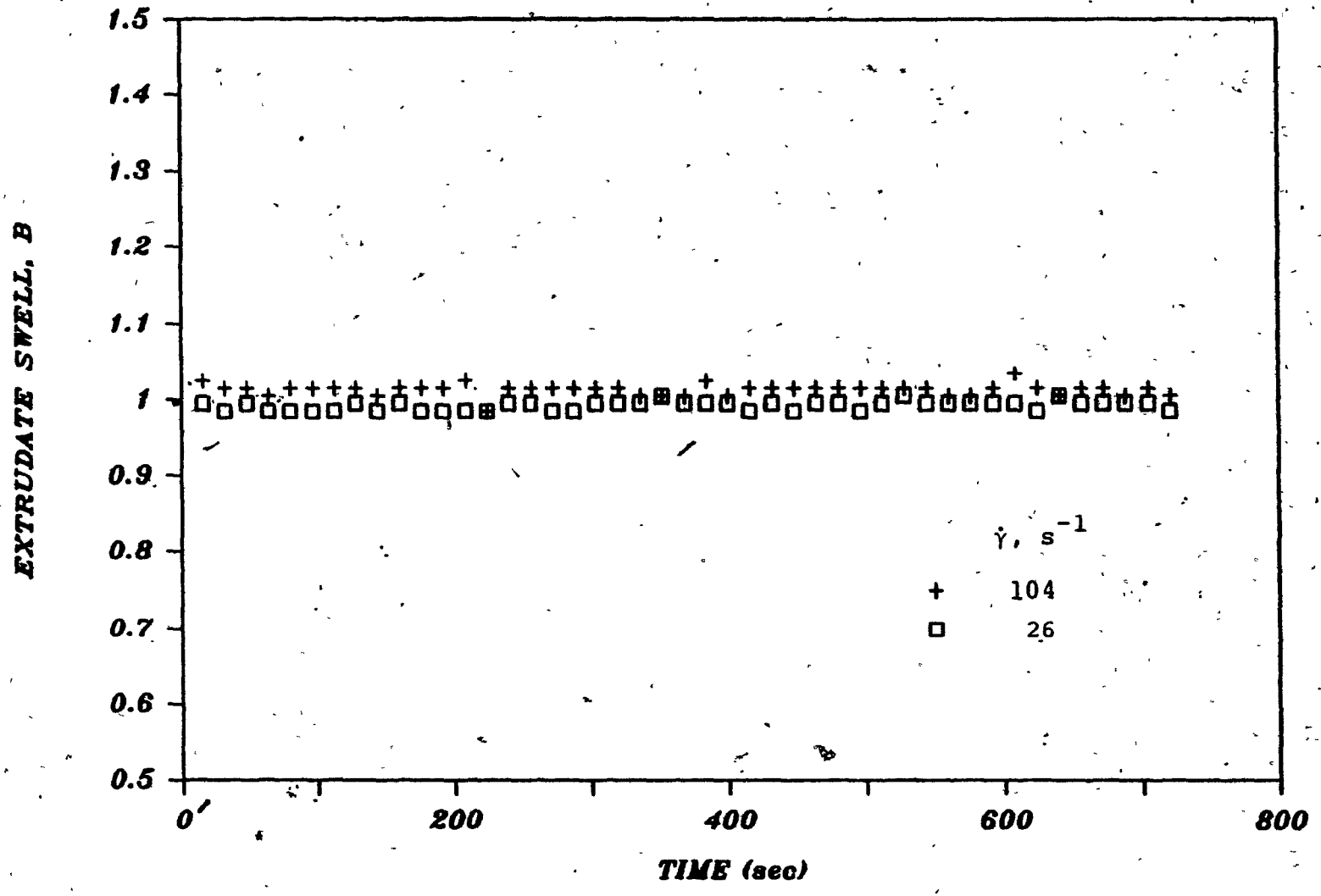

FIGURE 4.31. Extrudate Swell of LCP at 300°C.

that LCP melts exhibit a behaviour similar to the behaviour of fiber-filled melts. It is important to note that the thermostating chamber temperature was only 200°C, while the melting point of the resin is around 280°C. Therefore, the effects of thermal expansion and frozen stresses are not accounted for. More detailed studies are needed to confirm these results.

CHAPTER 5

CONCLUSIONS AND RECOMMENDATIONS

(1) A new semi-automatic apparatus to measure true capillary extrudate swell of polymer melts was designed, constructed and tested.

(2) The apparatus provides two kinds of output. An analog output capable of driving a chart recorder and a digital output. The digital output is passed through a data logger to an IBM PC, where the data can be analyzed and stored.

(3) It was illustrated that consistent and reliable data can be obtained using the proposed apparatus.

(4) Time-dependent as well as equilibrium extrudate swell data could be obtained with good reproducibility. The spread in the measured values of the diameter obtained from different runs, under the same conditions, did not exceed 37.5 μm.

(5) The apparatus was used in conjunction with an Instron Capillary Rheometer. However, the apparatus can be easily used with any capillary extrusion system that offers an unobstructed view of the extrudate.

(6) The apparatus can be used without any modification to measure extrudate swell as well as to monitor dimensions

of products in the rubber and in the wire coating industries.

(7) The die-barrel assembly should be modified in such a way as to provide a view of the tip of the die through the glass windows of the thermostating chamber. This would enable the measurement of the swelling as soon as the extrudate emerges from the die.

(8) To take full advantage of the previous suggestion, it is recommended to acquire a Direct Memory Access (DMA) device. Such a device would enable the logging of data into the IBM PC at high speed. In this way, the early stages of swell can be studied. In the present configuration, the maximum rate of data acquisition by the computer is one line scan every 0.53 seconds. The data can be collected by the camera module at a maximum speed of 4000 line scans per second.

(9) Using a stepper-motor, one can scan the extrudate vertically. This would permit measurement of the diameter at different locations below the die.

(10) It is important to continue the search for a proper thermostating medium. The medium should match the density of the polymer melt but not interact with it. It should also be transparent and thermally stable.

NOMENCLATURE

B	Extrudate swell ratio
D	Diameter
D_c	Diameter of the capillary
D_e	Diameter of the extrudate
D_s	Diameter of the solidified extrudate
G'	Storage modulus
G''	Loss modulus
J_e	Steady state shear compliance
L	Length of the capillary
$\bar{M}_n$	Number average molecular weight
$\bar{M}_w$	Weight average molecular weight
$\bar{M}_z$	z-average molecular weight
N_1	First normal stress difference
S_R	Recoverable shear strain

Greek Letters

$\dot{\gamma}$	Shear rate
$\dot{\gamma}$	Apparent shear rate
$\dot{\gamma}_w$	True wall shear rate
η^*	Complex viscosity
λ	Relaxation time
ρ	Density
ρ_s	Density of the solid polymer

REFERENCES

1. N. Al-Bastaki, M.Eng. Thesis, McGill University, Montreal (1982).
2. S. Middleman, "Fundamentals of Polymer Processing", McGraw-Hill, New York (1977).
3. J. Vlachopoulos, Reviews on the Deformation Behaviour of Materials, III, 4, 219 (1981).
4. L.L. Chapoy and S. Pedersen, Polym. Eng. Sci., 17, 724 (1977).
5. B. Maxwell and M. Nguyen, Polym. Eng. Sci., 19, 1140 (1979).
6. E.B. Bagley and H.J. Duffey, Trans. Soc. Rheol., 14, 545 (1970).
7. R. Bird, R. Armstrong and O. Hassager, "Dynamics of Polymeric Liquids: Volume I", Fluid Mechanics, John Wiley & Sons, New York (1977).
8. T. Nishimura and T. Kataoka, Rheol. Acta, 23, 40 (1984).
9. J. Leblanc, Rubber Chem. Technol., 54, 905 (1981).
10. G.R. Cotten, Rubber Chem. Technol., 54, 61 (1981).
11. G.R. Cotten, Rubber Chem. Technol., 52, 187 (1979).
12. R.I. Tanner, J. Non-Newt. Fluid Mech., 6, 289 (1980).
13. C.D. Han and M. Charles, Trans. Soc. Rheol., 14, 213 (1970).
14. C.D. Han, "Rheology in Polymer Processing", Academic Press, New York (1976).
15. W. Graessley, S.D. Glasscock and R.L. Crawley, Trans. Soc. Rheol., 14, 519 (1970).
16. J. Vlachopoulos, M. Horie and S. Lidarikis, Trans. Soc. Rheol., 16, 669 (1972).
17. E. Bagley, J. Storey and D. West, J. Appl. Polym. Sci., 7, 1661 (1963).

18. L. Chapoy, Rheol. Acta, 8, 4, 33 (1969).

19. M. Rogers, J. Appl. Polym. Sci., 14, 1979 (1970).

20. A.S. Anand and I.S. Bhardwaj, Rheol. Acta, 19, 614 (1980).

21. R. Racin and D.C. Bogue, Trans. Soc. Rheol., 23, 263 (1979).

22. F.P. La Mantia, A. Valenza and D. Acierno, Rheol. Acta, 22, 308 (1983).

23. D. Romanini and G. Pezzin, Rheol. Acta, 21, 699 (1982).

24. N. Alle, F.E. Andersen and J. Lyngaae-Jorgensen, Rheol. Acta, 20, 222 (1981).

25. G. Pezzin, "Proc. 2nd World Congr. Chem. Eng.", Montreal, 6, 273 (1981).

26. N. Minagawa and J.L. White, J. Appl. Polym. Sci., 20, 501 (1976).

27. A.K. Bagchi and K.K. Sirkar, J. Appl. Polym. Sci., 23, 1653 (1979).

28. P.K. Agarwal, E.B. Bagley and C.T. Hill, Polym. Eng. Sci., 18, 282 (1978).

29. G.R. Cotten, Rubber Chem. Technol., 52, 199 (1979).

30. I. Pliskin, Rubber Chem. Technol., 46, 1210 (1973).

31. M. Fleissner, Angew. Makromol. Chem., 33, 75 (1973).

32. R.N. Shroff and M. Shida, Soc. Plastics Engrs. ANTIC Preprints, Montreal, April (1977).

33. R.A. Mendelson and F.L. Finger, J. Appl. Polym. Sci., 19, 1061 (1975).

34. R.A. Mendelson and F.L. Finger, J. Appl. Polym. Sci., 17, 797 (1973).

35. L.A. Hamielec and J. Vlachopoulos, J. Appl. Polym. Sci., 28, 2389 (1983).

36. M. Rokudai, J. Appl. Polym. Sci., 26, 1427 (1981).

37. J.M. Dealy, "Rheometers for Molten Polymers", Van Nostran Reinhold Company, New York (1982).

38. R.A. Stratton and A.F. Butcher, J. Polym. Sci., A-2, 9, 1703 (1971).

39. L.A. Utracki, Z. Bakerdjian and M.R. Kamal, J. Appl. Polym. Sci., 19, 481 (1975).

40. G.V. Vinogradov et al., Mekhanika Polimerov, 1, 116 (1977).

41. R. Spencer and R. Dillon, J. Colloid Sci., 3, 163 (1948).

42. N. Nakajima and M. Shida, Trans. Soc. Rheol., 10, 299 (1966).

43. R.A. Mendelson, F.L. Finger and E.B. Bagley, J. Polym. Sci., Part C, 35, 177 (1971).

44. Z. Rigbi, SPE J., 22 (1953).

45. R. Spencer, "Physics of Plastics", P. Ritchie, Editor, Butterworth, London (1965).

46. F. Cogswell, Plast. and Polym., 391 (1970).

47. R.I. Tanner, J. Polym. Sci., A-2, 8, 2067 (1970).

48. B.A. Whipple and C.T. Hill, AIChE J., 24, 664 (1978).

49. J. Batchelor, J.P. Berry and F. Horsfall, Polymer, 14, 297 (1973).

50. R.I. Tanner, Appl. Polym. Symp., 20, 201 (1973).

51. R.E. Nickell, R.I. Tanner and B. Caswell, J. Fluid Mech., 65, 189 (1974).

52. W. Allan, Int. J. Num. Meth. Eng., 11, 1621 (1977).

53. M.E. Ryan and A. Dutta, Proc. 2nd World Congr. Chem. Eng., Montreal, 6, 277 (1981).

54. P.W. Chang, P.W. Patten and B.A. Finlayson, Comp. Fluids, 7, 267 (1979).

55. C.J. Coleman, J. Non.-Newt. Fluid Mech., 8, 261 (1981).

56. M.J. Crochet and R. Keunings, J. Non-Newt. Fluid Mech., 7, 199 (1980).

57. M.J. Crochet and R. Keunings, Proc. 2nd World Congr. Chem. Eng., Montreal, 285 (1981).

58. M.J. Crochet and R. Keunings, J. Non-Newt. Fluid Mech., 10, 339 (1982).

59. M.J. Crochet and R. Keunings, J. Non-Newt. Fluid Mech., 10, 85 (1982).

60. K.R. Reddy and R.I. Tanner, J. Rheol., 22, 661 (1978).

61. H.B. Phouc and R.I. Tanner, J. Fluid Mech., 98, 253 (1980).

62. E. Mitsoulis, Ph.D. Thesis, McMaster University, Hamilton (1984).

63. R.I. Tanner, "Computational Analysis of Polymer Processing", J.R.A. Pearson and F.M. Richardson, Editors, Applied Science, Essex, England (1983).

64. J.L. White and J.F. Roman, J. Appl. Polym. Sci., 20, 1005 (1976).

65. J.M. Dealy, A. Garcia-Rejon and M.R. Kamal, Can. J. Chem. Eng., 55, 651 (1977).

66. D. Kalyon, Ph.D. Thesis, McGill University, Montreal (1980).

67. N. Orby, Ph.D. Thesis, McGill University, Montreal (1983).

68. J.M. Dealy and A. Garcia-Rejon, Proc. VIIIth Int. Congr. Rheol., 3:63, Plenum Press, New York (1980).

69. N. Tokita, Rubber Chem. Technol., 54, 439 (1981).

70. P.S. Johnson, Rubber Chem. Technol., 56, 575 (1983).

71. R.H. Norman and P.S. Johnson, Rubber Chem. Technol., 54, 493 (1981).

72. "Monsanto Trade Bulletin G-14", Monsanto Company, 947 West Road, Akron, Ohio 44314, U.S.A.

73. J. Leblanc, Rheol. Acta, 20, 95 (1981).

74 "Trade Bulletin", C.W. Brabender Instruments, Inc., 50 E. Wesley Street, S. Hackensack, New Jersey 07606, U.S.A.

75. "Trade Bulletin (1982)", Optikon Corporation Ltd., 410 Conestago Road, Waterloo, Ontario N2L 4E2.

76. "Trade Bulletin", Metrelic Sarl., 44 Rue de Teurre-Neuve, 72020, Paris, France.

77. A. Magnin, Doctoral Thesis, Strassbourgh (1983).

78. J.F. Agassant, Private Communications (1984).

79. R.W. Pfoutz, Proc. SPIE, 60, 110 (1975).

80. I. McFarlane, Proc. SPIE, 145, 50 (1978).

81. P.W. Fry, J. Physics E., 8, 337 (1975).

82. G.F. Amelio, Scientific American, 230, 22 (1974).

83. P.W. Fry, Proc. SPIE, 145, 2 (1978).

84. D.G. Purll, Proc. SPIE, 145, 9 (1978).

85. D. Bertani, M. Cetica, S. Ciliberto and F. Francini, Rev. Sci. Instrum., 55, 8, 1270 (1984).

86. "Trade Bulletin (1982)", EG & G Reticon, 345 Portrero Avenue, Sunnyvale, CA 94086, U.S.A.

87. "Trade Bulletin (1981). CCD: The Solid State Image Technology", Fairchild CCD Imaging, 4001 Miranda Avenue, Palo Alto, CA 94304, U.S.A.

88. J.F, Claridge, Proc. SPIE, 145, 58 (1978).

89. L.T. Clarke, Proc. SPIE, 145, 28 (1978).

90. B.D. Clay, Proc. SPIE, 145, 45 (1978).

91. D.J. Purll, Proc. SPIE, 145, 18 (1978).

92. R.B. Lewis, Proc. SPIE, 145, 38 (1978).

93. R.K. Hopwood, Proc. SPIE, 230, 72 (1980).

94. A.G. McGovern, Proc. SPIE, 60, 6 (1975).

95. H.A. Elion, "Laser Systems and Applications", Pergamon Press, New York (1967).

96. D. O'Shea, W. Callen and W.T. Rhodes, "Introduction to Lasers and Their Applications", Addison-Wesley Publish Company, Massachusetts (1978).

97. Instron Capillary Rheometer, Operating and Maintenance Instructions (1976), Instron Co., Canton, MA.

98. L.A. Utracki, A. Catani, J. Lara and M.R. Kamal, "Polymer Processing and Properties", G. Astarita and L. Nicolais, eds., Capri, Italy, p. 79 (June 1983).

99. L.A. Utracki and J. Lara, Inter. Workshop on "Extensional Flow", Mulhouse-La Bress, France (1983).

100. R.A. Orwoll and P.J. Flory, J. Amer. Chem. Soc., 89, 26, 6815 (1967).

101. L.A. Utracki, Private Communications (1984).

102. J. Crank and G.S. Park, "Diffusion in Polymers", Academic Press, London (1968).

103. J.L. White, J. Rheol., 22, 507 (1978).

APPENDIX A

DETAILED DIAGRAMS OF THE CAMERA MODULE

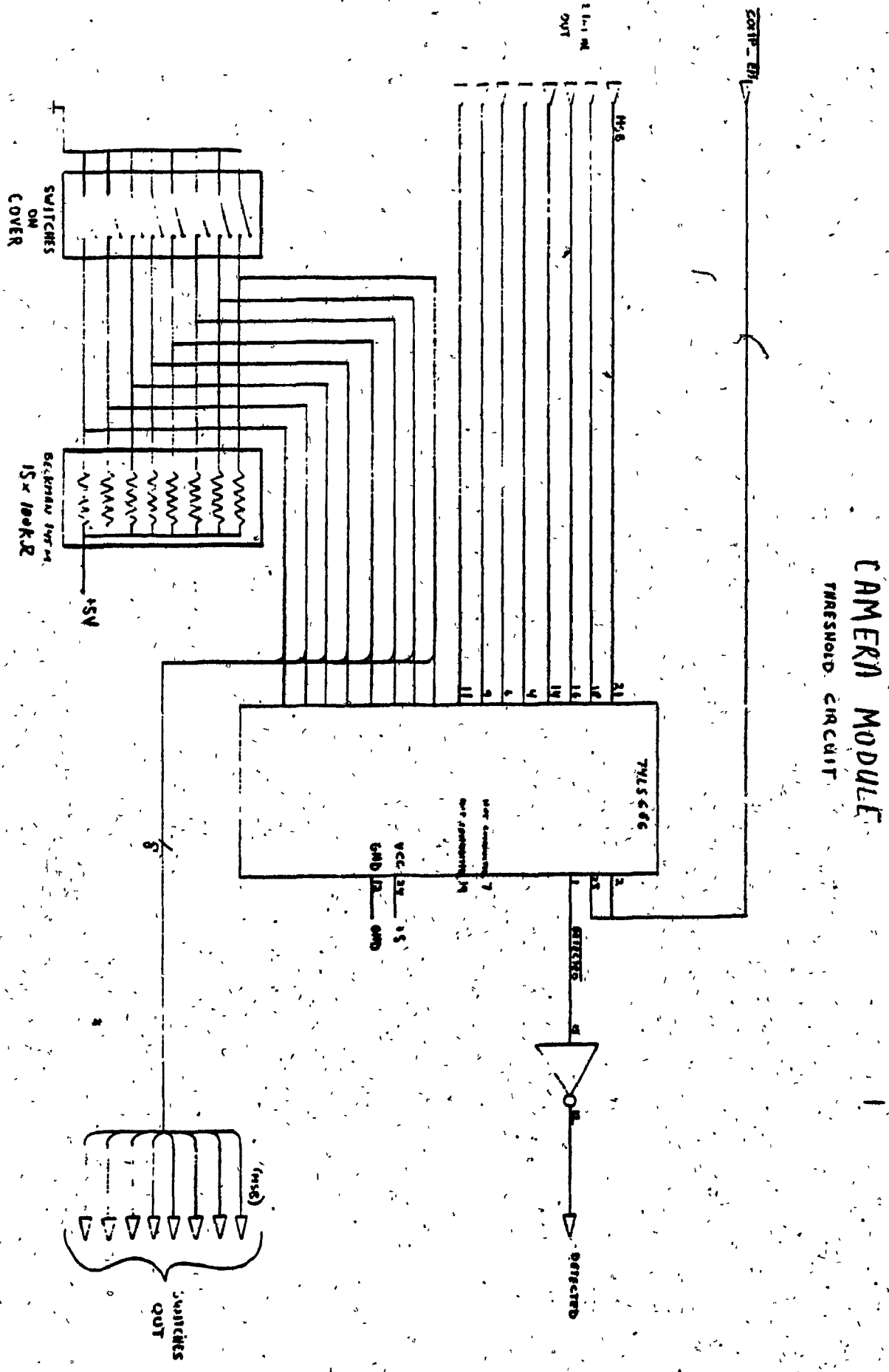

CAMERA MODULE

CLOCK CIRCUITS

A-2

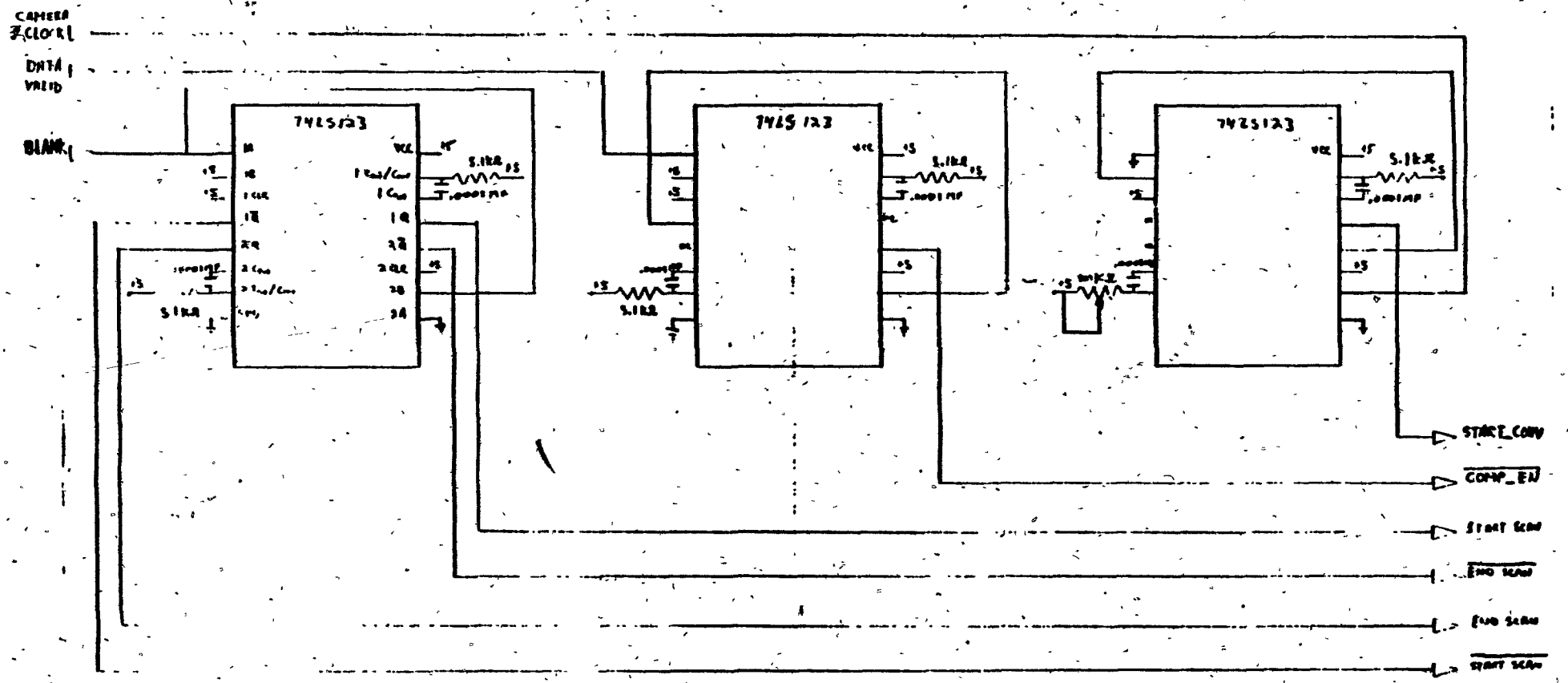

A-3

CAMERA MODULE

SHADOW COUNTER
DIGITAL OUTPUT

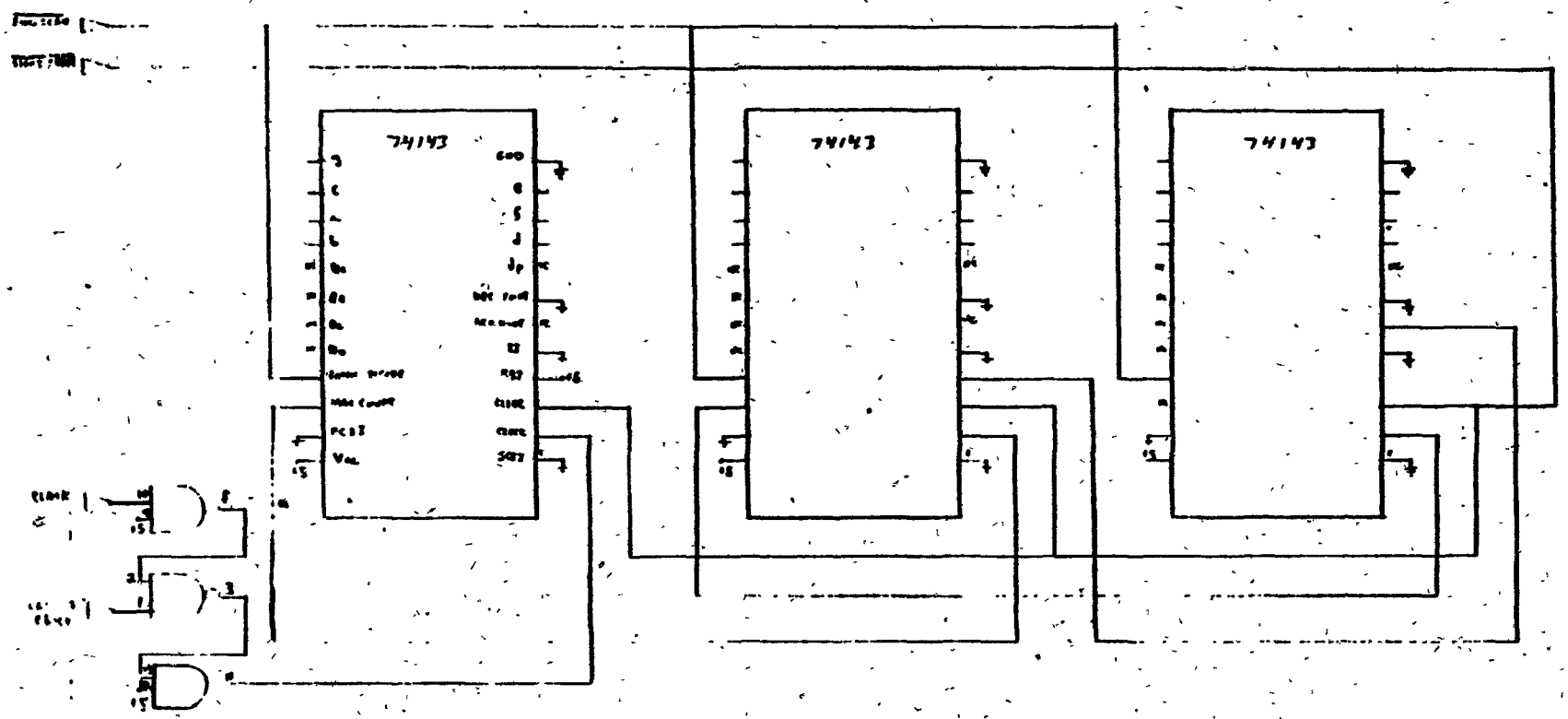

CAMERA MODULE

ANALOG THRESHOLD LEVEL

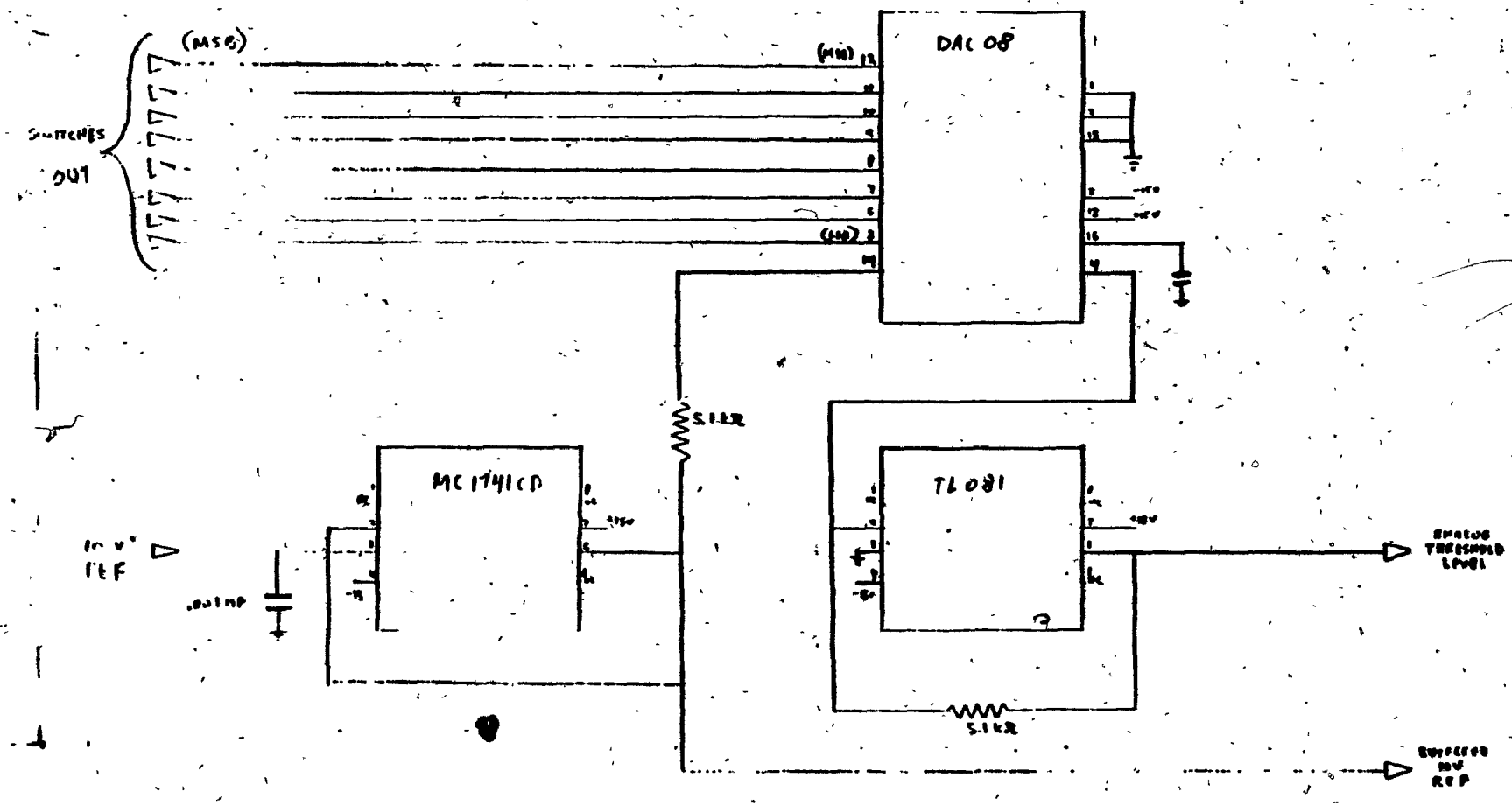

CAMERA MODULE
A/D CIRCUIT

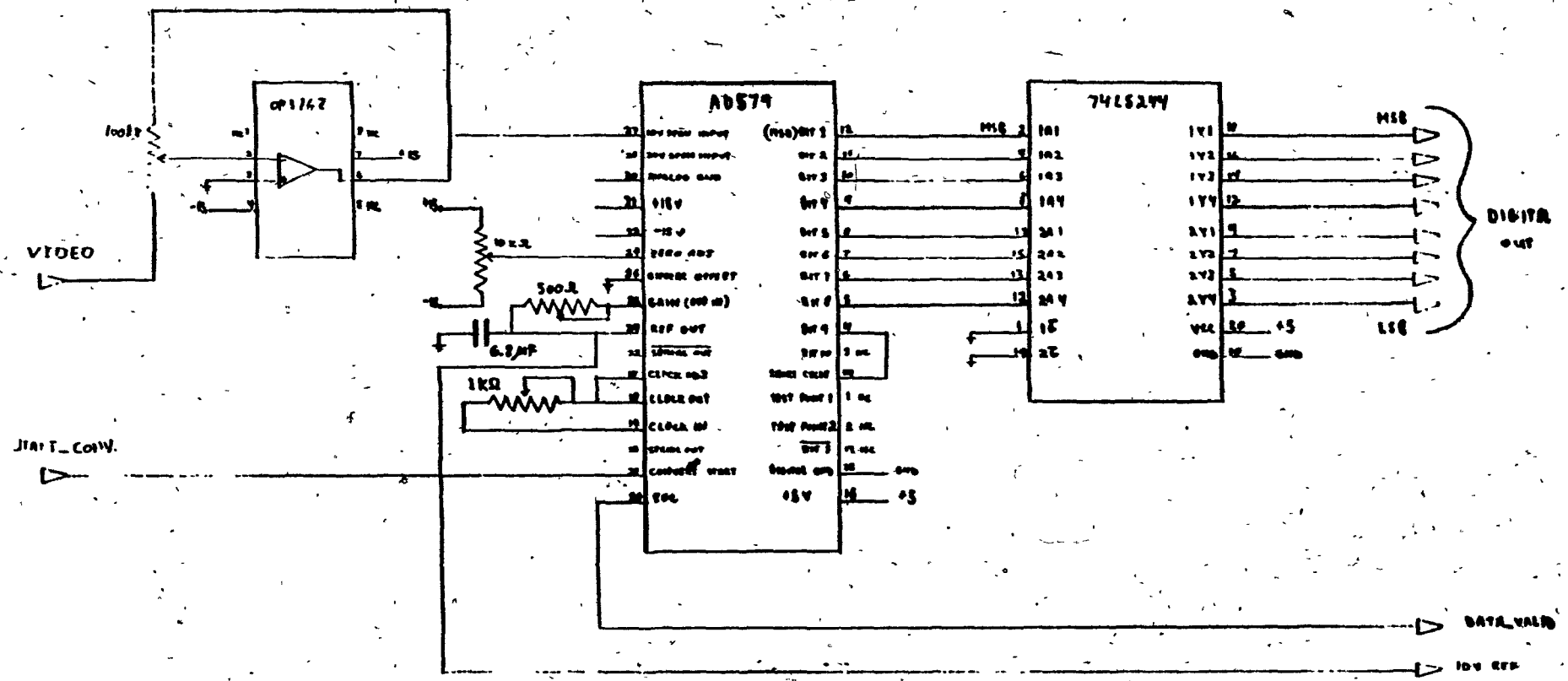

A-8

CAMERA MODULE

SHADOW COUNTER
ANALOG OUTPUT

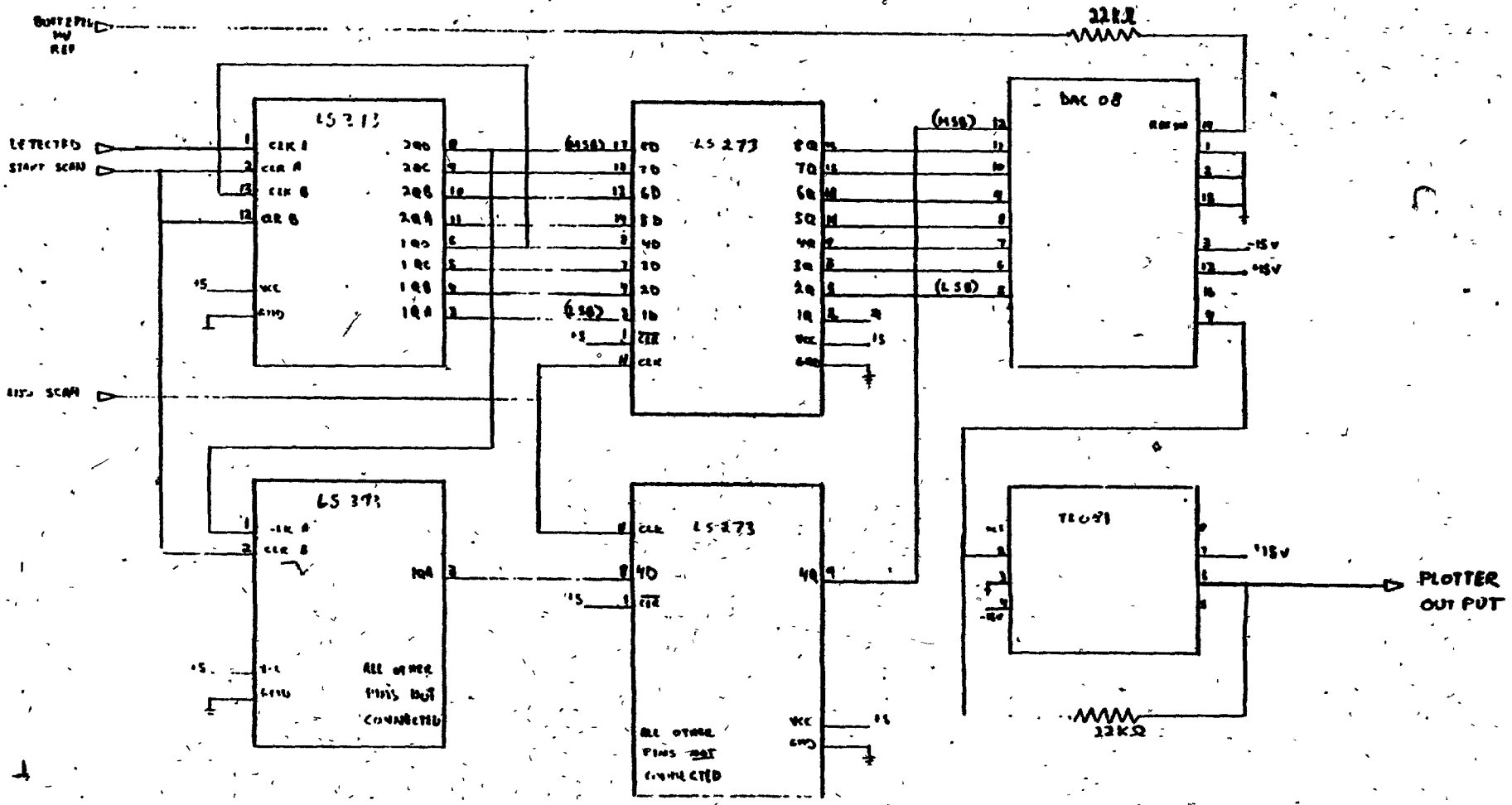

APPENDIX B

ILLUMINATION OF THE CENTRAL PHOTODIODES: AN OPTICAL SOLUTION

As mentioned earlier, when the temperature of the oil was significantly below the freezing point of the resin, the diameter could be measured easily and accurately without problems by setting the appropriate threshold level. However, as soon as the temperature of the oil approached the melting region, the central part of the image became bright. The photodiodes in the central part of the image gave a signal corresponding to full illumination. One approach to overcome this problem involves the use of computer software to compensate for the illumination of the central part. This is the approach which has been employed in the present study.

It would be desirable to overcome the above problem by using optical means only. Under such conditions, it would be possible to use a chart recorder to measure the swell of an unpigmented molten extrudate. Therefore, an attempt was made to obtain an optical solution.

The insertion of a pinhole between the photodiode array and the magnifying lens, at the focal point of the latter, might filter out the light originating from the central part of the extrudate, as shown schematically in Figure B-1.

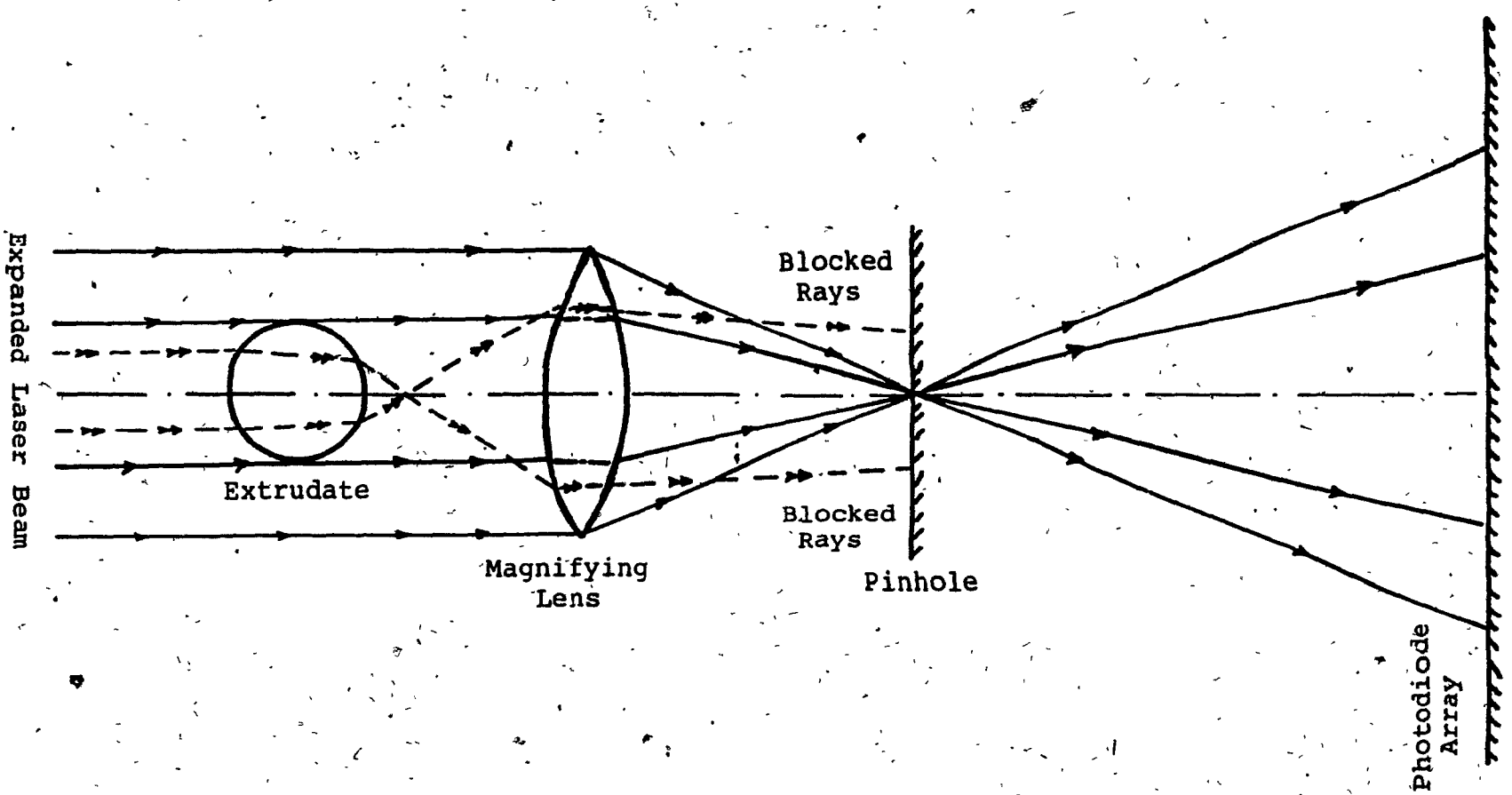

FIGURE B-1. An Illustration of the Proposed Optical Solution

Four pinholes of different diameters (100, 300, 500 and 1000 μm) were tried. The pinholes were held, one at a time, on a lateral-transverse slide. The slide could be moved on an optical bench. Thus, the position of the pinhole could be adjusted in all three directions. The 1000 and 500 μm pinholes reduced the central bright part of the image substantially, but did not eliminate it completely. No optical noise was observed, when these two pinholes were used. The 100 μm pinhole practically eliminated the central bright part of the image. However, the optical noise increased drastically, making it very difficult to make reliable measurements. This noise might be due to very small mechanical vibrations. The 300 μm pinhole performed somewhere in the middle between the two extremes.

The noise could probably be eliminated, if the experiment is performed on an optical table and if very precise positioning equipment was used. However, this would make the apparatus expensive and sensitive, if not impractical. However, it would be of interest to pursue a practical optical solution to this problem.

APPENDIX C

DETAILED DIAGRAMS OF THE DATA LOGGER

Input DB-25 pin Assignment

Pin 1 — D0 (LSB)
Pin 2 — D1
Pin 3 — D2
Pin 4 — D3
Pin 5 — D4
Pin 6 — D5
Pin 7 — D6
Pin 8 — D7 (MSB)
Pin 9 — Ground
Pin 10 — Ground
Pin 11 — Byte Ready(L)
Pin 12 — Block Ready(L)
Pin 13 — Ground
Pin 14 — Ground

Command Byte Definition

Bit 0 — Reserved for future definition/expansion.
(LSB)

Bit 1 — The next 3 bits define the number of 512-byte blocks to be captured
Bit 2 — during the next possible moment. It must be borne in mind that
Bit 3 — a maximum of 7 512-byte blocks can remain in memory at any time.
— If this is somehow exceeded, the ERROR light will come on. This
— condition will persist until the reset button is hit (hardware
— reset), by the abort command whose definition will follow.

Bit 4 — The last 4 bits define the number of half-second (0.5s) intervals
Bit 5 — at which the sampling is done. Thus the shortest interval at
Bit 6 — which the sampling can occur is 0.5s. The longest defined within
Bit 7 — one command byte is then 7.5 seconds. However, nearly any multiple
(MSB) — of 0.5 second can be achieved under the supervision of the host.

Since the function of the command word is quintessential, its integrity has to be pre-

served. To this end, the command byte is to be repeated, and the data-logger will compare both transmissions. If the command integrity is intact, then it will respond with one "A" (41H) - for acknowledge, ie 01000001. Otherwise, one "N" (4EH), ie 01001110 comes back, and the host should repeat the commmand byte twice again.

Should an unexpected condition occur from which the data-logger cannot recover, or if the host wishes to abort a command or reset the machine, it can be done in software by sending to it 2 (two) bytes of 00. Note that a before change to sampling modes can be effected, the data-logger has to receive these two bytes of 00's, and then the new command twice.

Note that the data-logger transmits the 512-byte block immediately upon completion of capture. No provision has been made to store the captured block in memory until instructed by the host to send.

Switch Settings

Four baud rates are switch selectable from the DIP-swich on the back of the unit. The first switch corresponds to bit 0 (LSB). When thrown in the OPEN position, it means that that particular switch setting is a 1.

00 - 1200 Baud; K1135 setting — 0111 (7H)
01 - 2400 Baud; K1135 setting — 1100 (CH)
10 - 9600 Baud; K1135 setting — 1110 (EH)
11 - 19K2 Baud; K1135 setting — 1111 (FH)

Together with the four selectable baud rates, are four selectable settings for parity. These are set via switches 3 and 4.

Switch 3 - Parity Even (0) / Parity Odd(1)
Switch 4 - Parity Enable (0) / Parity Disable (1)

Port and Bit Assignments

Write Command Port — 0CH
Run(H) - Bit 0
Light Error Lamp(H) - Bit 1

SIO Base — 1CH

Lo Counter Bank

Port 04H

Hi Counter Bank
Port 08H

Baud Rate Initialization
Port 00H

Status Read Port
Port 00H
Job Done(L) - Bit 0
Error (L) - Bit 1

The table in the following pages indicate combinations of baud rates and the rates at which 512-byte blocks can be sampled AND transmitted at the specified baud rates. Combinations that cannot be carried out due to any incompatibility in the input and output rates are flagged by the label "IMPOSSIBLE". Execution of any of these combinations will result in the error lamp being turned on. Combinations that are possible, on the other hand, have the entry labelled "Next" inserted into the location (400H + the asscociated "Loc" of the entry) of the EPROM.

Considerations for Increased Throughput

Given the current environment in which the data-logging is to take place, the speed at which data can be acquired is severely constrained by the speed at which it can be acquired by the IBM PC from the RS-232 line. Current operation of the IBM PC serial port is at 9600 baud. If this can be speeded up to 19.2k baud, the rate of sampling can be increased to more than twice that at 9600 baud. This is an attractive option as no modification on the data-logger is needed for operation at that baud rate. Baud rate settings of the data-logger for various rates of communication are described above.

Should even higher baud rates be needed, hardware, and maybe, software modifications have to be effected. The receive and transmit clock rates of the SIO have to be speeded up for increased throughput. One possibility would be to feed the receive and transmit clocks with some fraction of the 2.0MHz CPU clock such that its speed is compatible with that of the receiving hardware. Considerations must be given to the fact that the SIO used has a maximum frequency of operation of 2.0MHz, or the equivalent of 500Kbits/second.

It is likely that with higher speeds of operation, there would be a need to change the communication protocols. Little more can be said about this without having yet obtained the documentation for the receiving hardware except that the receive protocol should be understood well, before effecting any changes to the current transmission protocol.

Considerations for Increased Timing Accuracy

Although much careful thought has been given to the design of the timing loops, there may be occassions that require higher criticality in timing. On board the data-logger, the

```
Baud Rate =    0  Total time =  5.000 secs # of blocks =  3 # of bytes =  1536 Time needed = 12.800 IMPOSSIBLE
Baud Rate = 1200  Total time =  5.000 secs # of blocks =  4 # of bytes =  2048 Time needed = 17.067 IMPOSSIBLE
Baud Rate = 1200  Total time =  5.000 secs # of blocks =  5 # of bytes =  2560 Time needed = 21.333 IMPOSSIBLE
Baud Rate = 1200  Total time =  5.000 secs # of blocks =  6 # of bytes =  3072 Time needed = 25.600 IMPOSSIBLE
Baud Rate = 1200  Total time =  5.000 secs # of blocks =  7 # of bytes =  3584 Time needed = 29.867 IMPOSSIBLE
Baud Rate = 1200  Time avail. =  5.500 secs # of blocks =  1 # of bytes =   512 Time needed =  4.267 Next =  5
Baud Rate = 1200  Total time =  5.500 secs # of blocks =  2 # of bytes =  1024 Time needed =  8.533 IMPOSSIBLE
Baud Rate = 1200  Total time =  5.500 secs # of blocks =  3 # of bytes =  1536 Time needed = 12.800 IMPOSSIBLE
Baud Rate = 1200  Total time =  5.500 secs # of blocks =  4 # of bytes =  2048 Time needed = 17.067 IMPOSSIBLE
Baud Rate = 1200  Total time =  5.500 secs # of blocks =  5 # of bytes =  2560 Time needed = 21.333 IMPOSSIBLE
Baud Rate = 1200  Total time =  5.500 secs # of blocks =  6 # of bytes =  3072 Time needed = 25.600 IMPOSSIBLE
Baud Rate = 1200  Total time =  5.500 secs # of blocks =  7 # of bytes =  3584 Time needed = 29.867 IMPOSSIBLE
Baud Rate = 1200  Time avail. =  6.000 secs # of blocks =  1 # of bytes =   512 Time needed =  4.267 Next =  7
Baud Rate = 1200  Total time =  6.000 secs # of blocks =  2 # of bytes =  1024 Time needed =  8.533 IMPOSSIBLE
Baud Rate = 1200  Total time =  6.000 secs # of blocks =  3 # of bytes =  1536 Time needed = 12.800 IMPOSSIBLE
Baud Rate = 1200  Total time =  6.000 secs # of blocks =  4 # of bytes =  2048 Time needed = 17.067 IMPOSSIBLE
Baud Rate = 1200  Total time =  6.000 secs # of blocks =  5 # of bytes =  2560 Time needed = 21.333 IMPOSSIBLE
Baud Rate = 1200  Total time =  6.000 secs # of blocks =  6 # of bytes =  3072 Time needed = 25.600 IMPOSSIBLE
Baud Rate = 1200  Total time =  6.000 secs # of blocks =  7 # of bytes =  3584 Time needed = 29.867 IMPOSSIBLE
Baud Rate = 1200  Time avail. =  6.500 secs # of blocks =  1 # of bytes =   512 Time needed =  4.267 Next =  9
Baud Rate = 1200  Total time =  6.500 secs # of blocks =  2 # of bytes =  1024 Time needed =  8.533 IMPOSSIBLE
Baud Rate = 1200  Total time =  6.500 secs # of blocks =  3 # of bytes =  1536 Time needed = 12.800 IMPOSSIBLE
Baud Rate = 1200  Total time =  6.500 secs # of blocks =  4 # of bytes =  2048 Time needed = 17.067 IMPOSSIBLE
Baud Rate = 1200  Total time =  6.500 secs # of blocks =  5 # of bytes =  2560 Time needed = 21.333 IMPOSSIBLE
Baud Rate = 1200  Total time =  6.500 secs # of blocks =  6 # of bytes =  3072 Time needed = 25.600 IMPOSSIBLE
Baud Rate = 1200  Total time =  6.500 secs # of blocks =  7 # of bytes =  3584 Time needed = 29.867 IMPOSSIBLE
Baud Rate = 1200  Time avail. =  7.000 secs # of blocks =  1 # of bytes =   512 Time needed =  4.267 Next = 11
Baud Rate = 1200  Total time =  7.000 secs # of blocks =  2 # of bytes =  1024 Time needed =  8.533 IMPOSSIBLE
Baud Rate = 1200  Total time =  7.000 secs # of blocks =  3 # of bytes =  1536 Time needed = 12.800 IMPOSSIBLE
Baud Rate = 1200  Total time =  7.000 secs # of blocks =  4 # of bytes =  2048 Time needed = 17.067 IMPOSSIBLE
Baud Rate = 1200  Total time =  7.000 secs # of blocks =  5 # of bytes =  2560 Time needed = 21.333 IMPOSSIBLE
Baud Rate = 1200  Total time =  7.000 secs # of blocks =  6 # of bytes =  3072 Time needed = 25.600 IMPOSSIBLE
Baud Rate = 1200  Total time =  7.000 secs # of blocks =  7 # of bytes =  3584 Time needed = 29.867 IMPOSSIBLE
Baud Rate = 1200  Time avail. =  7.500 secs # of blocks =  1 # of bytes =   512 Time needed =  4.267 Next = 13
Baud Rate = 1200  Total time =  7.500 secs # of blocks =  2 # of bytes =  1024 Time needed =  8.533 IMPOSSIBLE
Baud Rate = 1200  Total time =  7.500 secs # of blocks =  3 # of bytes =  1536 Time needed = 12.800 IMPOSSIBLE
Baud Rate = 1200  Total time =  7.500 secs # of blocks =  4 # of bytes =  2048 Time needed = 17.067 IMPOSSIBLE
Baud Rate = 1200  Total time =  7.500 secs # of blocks =  5 # of bytes =  2560 Time needed = 21.333 IMPOSSIBLE
Baud Rate = 1200  Total time =  7.500 secs # of blocks =  6 # of bytes =  3072 Time needed = 25.600 IMPOSSIBLE
Baud Rate = 1200  Total time =  7.500 secs # of blocks =  7 # of bytes =  3584 Time needed = 29.867 IMPOSSIBLE
Baud Rate = 4800  Total time =  0.500 secs # of blocks =  1 # of bytes =   512 Time needed =  1.067 IMPOSSIBLE
Baud Rate = 4800  Total time =  0.500 secs # of blocks =  2 # of bytes =  1024 Time needed =  2.133 IMPOSSIBLE
Baud Rate = 4800  Total time =  0.500 secs # of blocks =  3 # of bytes =  1536 Time needed =  3.200 IMPOSSIBLE
Baud Rate = 4800  Total time =  0.500 secs # of blocks =  4 # of bytes =  2048 Time needed =  4.267 IMPOSSIBLE
Baud Rate = 4800  Total time =  0.500 secs # of blocks =  5 # of bytes =  2560 Time needed =  5.333 IMPOSSIBLE
Baud Rate = 4800  Total time =  0.500 secs # of blocks =  6 # of bytes =  3072 Time needed =  6.400 IMPOSSIBLE
Baud Rate = 4800  Total time =  0.500 secs # of blocks =  7 # of bytes =  3584 Time needed =  7.467 IMPOSSIBLE
Baud Rate = 4800  Total time =  1.000 secs # of blocks =  1 # of bytes =   512 Time needed =  1.067 IMPOSSIBLE
Baud Rate = 4800  Total time =  1.000 secs # of blocks =  2 # of bytes =  1024 Time needed =  2.133 IMPOSSIBLE
Baud Rate = 4800  Total time =  1.000 secs # of blocks =  3 # of bytes =  1536 Time needed =  3.200 IMPOSSIBLE
Baud Rate = 4800  Total time =  1.000 secs # of blocks =  4 # of bytes =  2048 Time needed =  4.267 IMPOSSIBLE
Baud Rate = 4800  Total time =  1.000 secs # of blocks =  5 # of bytes =  2560 Time needed =  5.333 IMPOSSIBLE
Baud Rate = 4800  Total time =  1.000 secs # of blocks =  6 # of bytes =  3072 Time needed =  6.400 IMPOSSIBLE
Baud Rate = 4800  Total time =  1.000 secs # of blocks =  7 # of bytes =  3584 Time needed =  7.467 IMPOSSIBLE
Baud Rate = 4800  Time avail. =  1.500 secs # of blocks =  1 # of bytes =   512 Time needed =  1.067 Next =  2
Baud Rate = 4800  Total time =  1.500 secs # of blocks =  2 # of bytes =  1024 Time needed =  2.133 IMPOSSIBLE
Baud Rate = 4800  Total time =  1.500 secs # of blocks =  3 # of bytes =  1536 Time needed =  3.200 IMPOSSIBLE
Baud Rate = 4800  Total time =  1.500 secs # of blocks =  4 # of bytes =  2048 Time needed =  4.267 IMPOSSIBLE
Baud Rate = 4800  Total time =  1.500 secs # of blocks =  5 # of bytes =  2560 Time needed =  5.333 IMPOSSIBLE
Baud Rate = 4800  Total time =  1.500 secs # of blocks =  6 # of bytes =  3072 Time needed =  6.400 IMPOSSIBLE
Baud Rate = 4800  Total time =  1.500 secs # of blocks =  7 # of bytes =  3584 Time needed =  7.467 IMPOSSIBLE
Baud Rate = 4800  Time avail. =  2.000 secs # of blocks =  1 # of bytes =   512 Time needed =  1.067 Next =  4
Baud Rate = 4800  Total time =  2.000 secs # of blocks =  2 # of bytes =  1024 Time needed =  2.133 IMPOSSIBLE
Baud Rate = 4800  Total time =  2.000 secs # of blocks =  3 # of bytes =  1536 Time needed =  3.200 IMPOSSIBLE
Baud Rate = 4800  Total time =  2.000 secs # of blocks =  4 # of bytes =  2048 Time needed =  4.267 IMPOSSIBLE
Baud Rate = 4800  Total time =  2.000 secs # of blocks =  5 # of bytes =  2560 Time needed =  5.333 IMPOSSIBLE
```

```
Baud Rate =    0  Total time =  2.000 secs # of blocks =  6 # of bytes =    2 Time needed =  6.400 IMPOSSIBLE
Baud Rate = 4800  Total time =  2.000 secs # of blocks =  7 # of bytes =   14 Time needed =  7.467 IMPOSSIBLE
Baud Rate = 4800  Time avail. =  2.500 secs # of blocks =  1 # of bytes =  512 Time needed =  1.067 Next =  6
Baud Rate = 4800  Time avail. =  2.500 secs # of blocks =  2 # of bytes = 1024 Time needed =  2.133 Next =  2
Baud Rate = 4800  Total time =  2.500 secs # of blocks =  3 # of bytes = 1536 Time needed =  3.200 IMPOSSIBLE
Baud Rate = 4800  Total time =  2.500 secs # of blocks =  4 # of bytes = 2048 Time needed =  4.267 IMPOSSIBLE
Baud Rate = 4800  Total time =  2.500 secs # of blocks =  5 # of bytes = 2560 Time needed =  5.333 IMPOSSIBLE
Baud Rate = 4800  Total time =  2.500 secs # of blocks =  6 # of bytes = 3072 Time needed =  6.400 IMPOSSIBLE
Baud Rate = 4800  Total time =  2.500 secs # of blocks =  7 # of bytes = 3584 Time needed =  7.467 IMPOSSIBLE
Baud Rate = 4800  Time avail. =  3.000 secs # of blocks =  1 # of bytes =  512 Time needed =  1.067 Next =  8
Baud Rate = 4800  Time avail. =  3.000 secs # of blocks =  2 # of bytes = 1024 Time needed =  2.133 Next =  4
Baud Rate = 4800  Total time =  3.000 secs # of blocks =  3 # of bytes = 1536 Time needed =  3.200 IMPOSSIBLE
Baud Rate = 4800  Total time =  3.000 secs # of blocks =  4 # of bytes = 2048 Time needed =  4.267 IMPOSSIBLE
Baud Rate = 4800  Total time =  3.000 secs # of blocks =  5 # of bytes = 2560 Time needed =  5.333 IMPOSSIBLE
Baud Rate = 4800  Total time =  3.000 secs # of blocks =  6 # of bytes = 3072 Time needed =  6.400 IMPOSSIBLE
Baud Rate = 4800  Total time =  3.000 secs # of blocks =  7 # of bytes = 3584 Time needed =  7.467 IMPOSSIBLE
Baud Rate = 4800  Time avail. =  3.500 secs # of blocks =  1 # of bytes =  512 Time needed =  1.067 Next = 10
Baud Rate = 4800  Time avail. =  3.500 secs # of blocks =  2 # of bytes = 1024 Time needed =  2.133 Next =  6
Baud Rate = 4800  Time avail. =  3.500 secs # of blocks =  3 # of bytes = 1536 Time needed =  3.200 Next =  1
Baud Rate = 4800  Total time =  3.500 secs # of blocks =  4 # of bytes = 2048 Time needed =  4.267 IMPOSSIBLE
Baud Rate = 4800  Total time =  3.500 secs # of blocks =  5 # of bytes = 2560 Time needed =  5.333 IMPOSSIBLE
Baud Rate = 4800  Total time =  3.500 secs # of blocks =  6 # of bytes = 3072 Time needed =  6.400 IMPOSSIBLE
Baud Rate = 4800  Total time =  3.500 secs # of blocks =  7 # of bytes = 3584 Time needed =  7.467 IMPOSSIBLE
Baud Rate = 4800  Time avail. =  4.000 secs # of blocks =  1 # of bytes =  512 Time needed =  1.067 Next = 12
Baud Rate = 4800  Time avail. =  4.000 secs # of blocks =  2 # of bytes = 1024 Time needed =  2.133 Next =  8
Baud Rate = 4800  Time avail. =  4.000 secs # of blocks =  3 # of bytes = 1536 Time needed =  3.200 Next =  3
Baud Rate = 4800  Total time =  4.000 secs # of blocks =  4 # of bytes = 2048 Time needed =  4.267 IMPOSSIBLE
Baud Rate = 4800  Total time =  4.000 secs # of blocks =  5 # of bytes = 2560 Time needed =  5.333 IMPOSSIBLE
Baud Rate = 4800  Total time =  4.000 secs # of blocks =  6 # of bytes = 3072 Time needed =  6.400 IMPOSSIBLE
Baud Rate = 4800  Total time =  4.000 secs # of blocks =  7 # of bytes = 3584 Time needed =  7.467 IMPOSSIBLE
Baud Rate = 4800  Time avail. =  4.500 secs # of blocks =  1 # of bytes =  512 Time needed =  1.067 Next = 14
Baud Rate = 4800  Time avail. =  4.500 secs # of blocks =  2 # of bytes = 1024 Time needed =  2.133 Next = 10
Baud Rate = 4800  Time avail. =  4.500 secs # of blocks =  3 # of bytes = 1536 Time needed =  3.200 Next =  5
Baud Rate = 4800  Time avail. =  4.500 secs # of blocks =  4 # of bytes = 2048 Time needed =  4.267 Next =  1
Baud Rate = 4800  Total time =  4.500 secs # of blocks =  5 # of bytes = 2560 Time needed =  5.333 IMPOSSIBLE
Baud Rate = 4800  Total time =  4.500 secs # of blocks =  6 # of bytes = 3072 Time needed =  6.400 IMPOSSIBLE
Baud Rate = 4800  Total time =  4.500 secs # of blocks =  7 # of bytes = 3584 Time needed =  7.467 IMPOSSIBLE
Baud Rate = 4800  Time avail. =  5.000 secs # of blocks =  1 # of bytes =  512 Time needed =  1.067 Next = 16
Baud Rate = 4800  Time avail. =  5.000 secs # of blocks =  2 # of bytes = 1024 Time needed =  2.133 Next = 12
Baud Rate = 4800  Time avail. =  5.000 secs # of blocks =  3 # of bytes = 1536 Time needed =  3.200 Next =  7
Baud Rate = 4800  Time avail. =  5.000 secs # of blocks =  4 # of bytes = 2048 Time needed =  4.267 Next =  3
Baud Rate = 4800  Total time =  5.000 secs # of blocks =  5 # of bytes = 2560 Time needed =  5.333 IMPOSSIBLE
Baud Rate = 4800  Total time =  5.000 secs # of blocks =  6 # of bytes = 3072 Time needed =  6.400 IMPOSSIBLE
Baud Rate = 4800  Total time =  5.000 secs # of blocks =  7 # of bytes = 3584 Time needed =  7.467 IMPOSSIBLE
Baud Rate = 4800  Time avail. =  5.500 secs # of blocks =  1 # of bytes =  512 Time needed =  1.067 Next = 18
Baud Rate = 4800  Time avail. =  5.500 secs # of blocks =  2 # of bytes = 1024 Time needed =  2.133 Next = 14
Baud Rate = 4800  Time avail. =  5.500 secs # of blocks =  3 # of bytes = 1536 Time needed =  3.200 Next =  9
Baud Rate = 4800  Time avail. =  5.500 secs # of blocks =  4 # of bytes = 2048 Time needed =  4.267 Next =  5
Baud Rate = 4800  Time avail. =  5.500 secs # of blocks =  5 # of bytes = 2560 Time needed =  5.333 Next =  1
Baud Rate = 4800  Total time =  5.500 secs # of blocks =  6 # of bytes = 3072 Time needed =  6.400 IMPOSSIBLE
Baud Rate = 4800  Total time =  5.500 secs # of blocks =  7 # of bytes = 3584 Time needed =  7.467 IMPOSSIBLE
Baud Rate = 4800  Time avail. =  6.000 secs # of blocks =  1 # of bytes =  512 Time needed =  1.067 Next = 20
Baud Rate = 4800  Time avail. =  6.000 secs # of blocks =  2 # of bytes = 1024 Time needed =  2.133 Next = 16
Baud Rate = 4800  Time avail. =  6.000 secs # of blocks =  3 # of bytes = 1536 Time needed =  3.200 Next = 11
Baud Rate = 4800  Time avail. =  6.000 secs # of blocks =  4 # of bytes = 2048 Time needed =  4.267 Next =  7
Baud Rate = 4800  Time avail. =  6.000 secs # of blocks =  5 # of bytes = 2560 Time needed =  5.333 Next =  3
Baud Rate = 4800  Total time =  6.000 secs # of blocks =  6 # of bytes = 3072 Time needed =  6.400 IMPOSSIBLE
Baud Rate = 4800  Total time =  6.000 secs # of blocks =  7 # of bytes = 3584 Time needed =  7.467 IMPOSSIBLE
Baud Rate = 4800  Time avail. =  6.500 secs # of blocks =  1 # of bytes =  512 Time needed =  1.067 Next = 22
Baud Rate = 4800  Time avail. =  6.500 secs # of blocks =  2 # of bytes = 1024 Time needed =  2.133 Next = 18
Baud Rate = 4800  Time avail. =  6.500 secs # of blocks =  3 # of bytes = 1536 Time needed =  3.200 Next = 13
Baud Rate = 4800  Time avail. =  6.500 secs # of blocks =  4 # of bytes = 2048 Time needed =  4.267 Next =  9
Baud Rate = 4800  Time avail. =  6.500 secs # of blocks =  5 # of bytes = 2560 Time needed =  5.333 Next =  5
Baud Rate = 4800  Time avail. =  6.500 secs # of blocks =  6 # of bytes = 3072 Time needed =  6.400 Next =  0
Baud Rate = 4800  Total time =  6.500 secs # of blocks =  7 # of bytes = 3584 Time needed =  7.467 IMPOSSIBLE
Baud Rate = 4800  Time avail. =  7.000 secs # of blocks =  1 # of bytes =  512 Time needed =  1.067 Next = 24
```

```
Baud Rate = 120   Total time =  0.500 secs # of blocks =  1 # of bytes =  512 Time needed =  4.267 IMPOSSIBLE
Baud Rate = 1200  Total time =  0.500 secs # of blocks =  2 # of bytes = 1024 Time needed =  8.533 IMPOSSIBLE
Baud Rate = 1200  Total time =  0.500 secs # of blocks =  3 # of bytes = 1536 Time needed = 12.800 IMPOSSIBLE
Baud Rate = 1200  Total time =  0.500 secs # of blocks =  4 # of bytes = 2048 Time needed = 17.067 IMPOSSIBLE
Baud Rate = 1200  Total time =  0.500 secs # of blocks =  5 # of bytes = 2560 Time needed = 21.333 IMPOSSIBLE
Baud Rate = 1200  Total time =  0.500 secs # of blocks =  6 # of bytes = 3072 Time needed = 25.600 IMPOSSIBLE
Baud Rate = 1200  Total time =  0.500 secs # of blocks =  7 # of bytes = 3584 Time needed = 29.867 IMPOSSIBLE
Baud Rate = 1200  Total time =  1.000 secs # of blocks =  1 # of bytes =  512 Time needed =  4.267 IMPOSSIBLE
Baud Rate = 1200  Total time =  1.000 secs # of blocks =  2 # of bytes = 1024 Time needed =  8.533 IMPOSSIBLE
Baud Rate = 1200  Total time =  1.000 secs # of blocks =  3 # of bytes = 1536 Time needed = 12.800 IMPOSSIBLE
Baud Rate = 1200  Total time =  1.000 secs # of blocks =  4 # of bytes = 2048 Time needed = 17.067 IMPOSSIBLE
Baud Rate = 1200  Total time =  1.000 secs # of blocks =  5 # of bytes = 2560 Time needed = 21.333 IMPOSSIBLE
Baud Rate = 1200  Total time =  1.000 secs # of blocks =  6 # of bytes = 3072 Time needed = 25.600 IMPOSSIBLE
Baud Rate = 1200  Total time =  1.000 secs # of blocks =  7 # of bytes = 3584 Time needed = 29.867 IMPOSSIBLE
Baud Rate = 1200  Total time =  1.500 secs # of blocks =  1 # of bytes =  512 Time needed =  4.267 IMPOSSIBLE
Baud Rate = 1200  Total time =  1.500 secs # of blocks =  2 # of bytes = 1024 Time needed =  8.533 IMPOSSIBLE
Baud Rate = 1200  Total time =  1.500 secs # of blocks =  3 # of bytes = 1536 Time needed = 12.800 IMPOSSIBLE
Baud Rate = 1200  Total time =  1.500 secs # of blocks =  4 # of bytes = 2048 Time needed = 17.067 IMPOSSIBLE
Baud Rate = 1200  Total time =  1.500 secs # of blocks =  5 # of bytes = 2560 Time needed = 21.333 IMPOSSIBLE
Baud Rate = 1200  Total time =  1.500 secs # of blocks =  6 # of bytes = 3072 Time needed = 25.600 IMPOSSIBLE
Baud Rate = 1200  Total time =  1.500 secs # of blocks =  7 # of bytes = 3584 Time needed = 29.867 IMPOSSIBLE
Baud Rate = 1200  Total time =  2.000 secs # of blocks =  1 # of bytes =  512 Time needed =  4.267 IMPOSSIBLE
Baud Rate = 1200  Total time =  2.000 secs # of blocks =  2 # of bytes = 1024 Time needed =  8.533 IMPOSSIBLE
Baud Rate = 1200  Total time =  2.000 secs # of blocks =  3 # of bytes = 1536 Time needed = 12.800 IMPOSSIBLE
Baud Rate = 1200  Total time =  2.000 secs # of blocks =  4 # of bytes = 2048 Time needed = 17.067 IMPOSSIBLE
Baud Rate = 1200  Total time =  2.000 secs # of blocks =  5 # of bytes = 2560 Time needed = 21.333 IMPOSSIBLE
Baud Rate = 1200  Total time =  2.000 secs # of blocks =  6 # of bytes = 3072 Time needed = 25.600 IMPOSSIBLE
Baud Rate = 1200  Total time =  2.000 secs # of blocks =  7 # of bytes = 3584 Time needed = 29.867 IMPOSSIBLE
Baud Rate = 1200  Total time =  2.500 secs # of blocks =  1 # of bytes =  512 Time needed =  4.267 IMPOSSIBLE
Baud Rate = 1200  Total time =  2.500 secs # of blocks =  2 # of bytes = 1024 Time needed =  8.533 IMPOSSIBLE
Baud Rate = 1200  Total time =  2.500 secs # of blocks =  3 # of bytes = 1536 Time needed = 12.800 IMPOSSIBLE
Baud Rate = 1200  Total time =  2.500 secs # of blocks =  4 # of bytes = 2048 Time needed = 17.067 IMPOSSIBLE
Baud Rate = 1200  Total time =  2.500 secs # of blocks =  5 # of bytes = 2560 Time needed = 21.333 IMPOSSIBLE
Baud Rate = 1200  Total time =  2.500 secs # of blocks =  6 # of bytes = 3072 Time needed = 25.600 IMPOSSIBLE
Baud Rate = 1200  Total time =  2.500 secs # of blocks =  7 # of bytes = 3584 Time needed = 29.867 IMPOSSIBLE
Baud Rate = 1200  Total time =  3.000 secs # of blocks =  1 # of bytes =  512 Time needed =  4.267 IMPOSSIBLE
Baud Rate = 1200  Total time =  3.000 secs # of blocks =  2 # of bytes = 1024 Time needed =  8.533 IMPOSSIBLE
Baud Rate = 1200  Total time =  3.000 secs # of blocks =  3 # of bytes = 1536 Time needed = 12.800 IMPOSSIBLE
Baud Rate = 1200  Total time =  3.000 secs # of blocks =  4 # of bytes = 2048 Time needed = 17.067 IMPOSSIBLE
Baud Rate = 1200  Total time =  3.000 secs # of blocks =  5 # of bytes = 2560 Time needed = 21.333 IMPOSSIBLE
Baud Rate = 1200  Total time =  3.000 secs # of blocks =  6 # of bytes = 3072 Time needed = 25.600 IMPOSSIBLE
Baud Rate = 1200  Total time =  3.000 secs # of blocks =  7 # of bytes = 3584 Time needed = 29.867 IMPOSSIBLE
Baud Rate = 1200  Total time =  3.500 secs # of blocks =  1 # of bytes =  512 Time needed =  4.267 IMPOSSIBLE
Baud Rate = 1200  Total time =  3.500 secs # of blocks =  2 # of bytes = 1024 Time needed =  8.533 IMPOSSIBLE
Baud Rate = 1200  Total time =  3.500 secs # of blocks =  3 # of bytes = 1536 Time needed = 12.800 IMPOSSIBLE
Baud Rate = 1200  Total time =  3.500 secs # of blocks =  4 # of bytes = 2048 Time needed = 17.067 IMPOSSIBLE
Baud Rate = 1200  Total time =  3.500 secs # of blocks =  5 # of bytes = 2560 Time needed = 21.333 IMPOSSIBLE
Baud Rate = 1200  Total time =  3.500 secs # of blocks =  6 # of bytes = 3072 Time needed = 25.600 IMPOSSIBLE
Baud Rate = 1200  Total time =  3.500 secs # of blocks =  7 # of bytes = 3584 Time needed = 29.867 IMPOSSIBLE
Baud Rate = 1200  Total time =  4.000 secs # of blocks =  1 # of bytes =  512 Time needed =  4.267 IMPOSSIBLE
Baud Rate = 1200  Total time =  4.000 secs # of blocks =  2 # of bytes = 1024 Time needed =  8.533 IMPOSSIBLE
Baud Rate = 1200  Total time =  4.000 secs # of blocks =  3 # of bytes = 1536 Time needed = 12.800 IMPOSSIBLE
Baud Rate = 1200  Total time =  4.000 secs # of blocks =  4 # of bytes = 2048 Time needed = 17.067 IMPOSSIBLE
Baud Rate = 1200  Total time =  4.000 secs # of blocks =  5 # of bytes = 2560 Time needed = 21.333 IMPOSSIBLE
Baud Rate = 1200  Total time =  4.000 secs # of blocks =  6 # of bytes = 3072 Time needed = 25.600 IMPOSSIBLE
Baud Rate = 1200  Total time =  4.000 secs # of blocks =  7 # of bytes = 3584 Time needed = 29.867 IMPOSSIBLE
Baud Rate = 1200  Time avail. =  4.500 secs # of blocks =  1 # of bytes =  512 Time needed =  4.267 Next =  1
Baud Rate = 1200  Total time =  4.500 secs # of blocks =  2 # of bytes = 1024 Time needed =  8.533 IMPOSSIBLE
Baud Rate = 1200  Total time =  4.500 secs # of blocks =  3 # of bytes = 1536 Time needed = 12.800 IMPOSSIBLE
Baud Rate = 1200  Total time =  4.500 secs # of blocks =  4 # of bytes = 2048 Time needed = 17.067 IMPOSSIBLE
Baud Rate = 1200  Total time =  4.500 secs # of blocks =  5 # of bytes = 2560 Time needed = 21.333 IMPOSSIBLE
Baud Rate = 1200  Total time =  4.500 secs # of blocks =  6 # of bytes = 3072 Time needed = 25.600 IMPOSSIBLE
Baud Rate = 1200  Total time =  4.500 secs # of blocks =  7 # of bytes = 3584 Time needed = 29.867 IMPOSSIBLE
Baud Rate = 1200  Time avail. =  5.000 secs # of blocks =  1 # of bytes =  512 Time needed =  4.267 Next =  3
Baud Rate = 1200  Total time =  5.000 secs # of blocks =  2 # of bytes = 1024 Time needed =  8.533 IMPOSSIBLE
```

```
Baud Rate =  [illegible]  Time avail. =  7.000 secs # of blocks =  2 # of byt[illegible]  024 Time needed =  2.133 Next = 20
Baud Rate = 300  Time avail. =  7.000 secs # of blocks =  3 # of bytes =  536 Time needed =  3.200 Next = 15
Baud Rate = 4800  Time avail. =  7.000 secs # of blocks =  4 # of bytes = 2048 Time needed =  4.267 Next = 11
Baud Rate = 4800  Time avail. =  7.000 secs # of blocks =  5 # of bytes = 2560 Time needed =  5.333 Next =  7
Baud Rate = 4800  Time avail. =  7.000 secs # of blocks =  6 # of bytes = 3072 Time needed =  6.400 Next =  2
Baud Rate = 4800  Total time =  7.000 secs # of blocks =  7 # of bytes = 3584 Time needed =  7.467 IMPOSSIBLE
Baud Rate = 4800  Time avail. =  7.500 secs # of blocks =  1 # of bytes =  512 Time needed =  1.067 Next = 26
Baud Rate = 4800  Time avail. =  7.500 secs # of blocks =  2 # of bytes = 1024 Time needed =  2.133 Next = 22
Baud Rate = 4800  Time avail. =  7.500 secs # of blocks =  3 # of bytes = 1536 Time needed =  3.200 Next = 17
Baud Rate = 4800  Time avail. =  7.500 secs # of blocks =  4 # of bytes = 2048 Time needed =  4.267 Next = 13
Baud Rate = 4800  Time avail. =  7.500 secs # of blocks =  5 # of bytes = 2560 Time needed =  5.333 Next =  9
Baud Rate = 4800  Time avail. =  7.500 secs # of blocks =  6 # of bytes = 3072 Time needed =  6.400 Next =  4
Baud Rate = 4800  Time avail. =  7.500 secs # of blocks =  7 # of bytes = 3584 Time needed =  7.467 Next =  0
Baud Rate = 9600  Total time =  0.500 secs # of blocks =  1 # of bytes =  512 Time needed =  0.533 IMPOSSIBLE
Baud Rate = 9600  Total time =  0.500 secs # of blocks =  2 # of bytes = 1024 Time needed =  1.067 IMPOSSIBLE
Baud Rate = 9600  Total time =  0.500 secs # of blocks =  3 # of bytes = 1536 Time needed =  1.600 IMPOSSIBLE
Baud Rate = 9600  Total time =  0.500 secs # of blocks =  4 # of bytes = 2048 Time needed =  2.133 IMPOSSIBLE
Baud Rate = 9600  Total time =  0.500 secs # of blocks =  5 # of bytes = 2560 Time needed =  2.667 IMPOSSIBLE
Baud Rate = 9600  Total time =  0.500 secs # of blocks =  6 # of bytes = 3072 Time needed =  3.200 IMPOSSIBLE
Baud Rate = 9600  Total time =  0.500 secs # of blocks =  7 # of bytes = 3584 Time needed =  3.733 IMPOSSIBLE
Baud Rate = 9600  Time avail. =  1.000 secs # of blocks =  1 # of bytes =  512 Time needed =  0.533 Next =  2
Baud Rate = 9600  Total time =  1.000 secs # of blocks =  2 # of bytes = 1024 Time needed =  1.067 IMPOSSIBLE
Baud Rate = 9600  Total time =  1.000 secs # of blocks =  3 # of bytes = 1536 Time needed =  1.600 IMPOSSIBLE
Baud Rate = 9600  Total time =  1.000 secs # of blocks =  4 # of bytes = 2048 Time needed =  2.133 IMPOSSIBLE
Baud Rate = 9600  Total time =  1.000 secs # of blocks =  5 # of bytes = 2560 Time needed =  2.667 IMPOSSIBLE
Baud Rate = 9600  Total time =  1.000 secs # of blocks =  6 # of bytes = 3072 Time needed =  3.200 IMPOSSIBLE
Baud Rate = 9600  Total time =  1.000 secs # of blocks =  7 # of bytes = 3584 Time needed =  3.733 IMPOSSIBLE
Baud Rate = 9600  Time avail. =  1.500 secs # of blocks =  1 # of bytes =  512 Time needed =  0.533 Next =  4
Baud Rate = 9600  Time avail. =  1.500 secs # of blocks =  2 # of bytes = 1024 Time needed =  1.067 Next =  2
Baud Rate = 9600  Total time =  1.500 secs # of blocks =  3 # of bytes = 1536 Time needed =  1.600 IMPOSSIBLE
Baud Rate = 9600  Total time =  1.500 secs # of blocks =  4 # of bytes = 2048 Time needed =  2.133 IMPOSSIBLE
Baud Rate = 9600  Total time =  1.500 secs # of blocks =  5 # of bytes = 2560 Time needed =  2.667 IMPOSSIBLE
Baud Rate = 9600  Total time =  1.500 secs # of blocks =  6 # of bytes = 3072 Time needed =  3.200 IMPOSSIBLE
Baud Rate = 9600  Total time =  1.500 secs # of blocks =  7 # of bytes = 3584 Time needed =  3.733 IMPOSSIBLE
Baud Rate = 9600  Time avail. =  2.000 secs # of blocks =  1 # of bytes =  512 Time needed =  0.533 Next =  6
Baud Rate = 9600  Time avail. =  2.000 secs # of blocks =  2 # of bytes = 1024 Time needed =  1.067 Next =  4
Baud Rate = 9600  Time avail. =  2.000 secs # of blocks =  3 # of bytes = 1536 Time needed =  1.600 Next =  2
Baud Rate = 9600  Total time =  2.000 secs # of blocks =  4 # of bytes = 2048 Time needed =  2.133 IMPOSSIBLE
Baud Rate = 9600  Total time =  2.000 secs # of blocks =  5 # of bytes = 2560 Time needed =  2.667 IMPOSSIBLE
Baud Rate = 9600  Total time =  2.000 secs # of blocks =  6 # of bytes = 3072 Time needed =  3.200 IMPOSSIBLE
Baud Rate = 9600  Total time =  2.000 secs # of blocks =  7 # of bytes = 3584 Time needed =  3.733 IMPOSSIBLE
Baud Rate = 9600  Time avail. =  2.500 secs # of blocks =  1 # of bytes =  512 Time needed =  0.533 Next =  8
Baud Rate = 9600  Time avail. =  2.500 secs # of blocks =  2 # of bytes = 1024 Time needed =  1.067 Next =  6
Baud Rate = 9600  Time avail. =  2.500 secs # of blocks =  3 # of bytes = 1536 Time needed =  1.600 Next =  4
Baud Rate = 9600  Time avail. =  2.500 secs # of blocks =  4 # of bytes = 2048 Time needed =  2.133 Next =  2
Baud Rate = 9600  Total time =  2.500 secs # of blocks =  5 # of bytes = 2560 Time needed =  2.667 IMPOSSIBLE
Baud Rate = 9600  Total time =  2.500 secs # of blocks =  6 # of bytes = 3072 Time needed =  3.200 IMPOSSIBLE
Baud Rate = 9600  Total time =  2.500 secs # of blocks =  7 # of bytes = 3584 Time needed =  3.733 IMPOSSIBLE
Baud Rate = 9600  Time avail. =  3.000 secs # of blocks =  1 # of bytes =  512 Time needed =  0.533 Next = 10
Baud Rate = 9600  Time avail. =  3.000 secs # of blocks =  2 # of bytes = 1024 Time needed =  1.067 Next =  8
Baud Rate = 9600  Time avail. =  3.000 secs # of blocks =  3 # of bytes = 1536 Time needed =  1.600 Next =  6
Baud Rate = 9600  Time avail. =  3.000 secs # of blocks =  4 # of bytes = 2048 Time needed =  2.133 Next =  4
Baud Rate = 9600  Time avail. =  3.000 secs # of blocks =  5 # of bytes = 2560 Time needed =  2.667 Next =  1
Baud Rate = 9600  Total time =  3.000 secs # of blocks =  6 # of bytes = 3072 Time needed =  3.200 IMPOSSIBLE
Baud Rate = 9600  Total time =  3.000 secs # of blocks =  7 # of bytes = 3584 Time needed =  3.733 IMPOSSIBLE
Baud Rate = 9600  Time avail. =  3.500 secs # of blocks =  1 # of bytes =  512 Time needed =  0.533 Next = 12
Baud Rate = 9600  Time avail. =  3.500 secs # of blocks =  2 # of bytes = 1024 Time needed =  1.067 Next = 10
Baud Rate = 9600  Time avail. =  3.500 secs # of blocks =  3 # of bytes = 1536 Time needed =  1.600 Next =  8
Baud Rate = 9600  Time avail. =  3.500 secs # of blocks =  4 # of bytes = 2048 Time needed =  2.133 Next =  6
Baud Rate = 9600  Time avail. =  3.500 secs # of blocks =  5 # of bytes = 2560 Time needed =  2.667 Next =  3
Baud Rate = 9600  Time avail. =  3.500 secs # of blocks =  6 # of bytes = 3072 Time needed =  3.200 Next =  1
Baud Rate = 9600  Total time =  3.500 secs # of blocks =  7 # of bytes = 3584 Time needed =  3.733 IMPOSSIBLE
Baud Rate = 9600  Time avail. =  4.000 secs # of blocks =  1 # of bytes =  512 Time needed =  0.533 Next = 14
Baud Rate = 9600  Time avail. =  4.000 secs # of blocks =  2 # of bytes = 1024 Time needed =  1.067 Next = 12
Baud Rate = 9600  Time avail. =  4.000 secs # of blocks =  3 # of bytes = 1536 Time needed =  1.600 Next = 10
Baud Rate = 9600  Time avail. =  4.000 secs # of blocks =  4 # of bytes = 2048 Time needed =  2.133 Next =  8
```

```
Baud Rate =  [illegible]  Time avail. =  4.000 secs # of blocks =  5 # of byt[illegible]  160 Time needed =  2.667 Next =  5
Baud Rate = 9600  Time avail. =  4.000 secs # of blocks =  6 # of bytes =  J72 Time needed =  3.200 Next =  3
Baud Rate = 9600  Time avail. =  4.000 secs # of blocks =  7 # of bytes = 8584 Time needed =  3.733 Next =  1
Baud Rate = 9600  Time avail. =  4.500 secs # of blocks =  1 # of bytes =  512 Time needed =  0.533 Next = 16
Baud Rate = 9600  Time avail. =  4.500 secs # of blocks =  2 # of bytes = 1024 Time needed =  1.067 Next = 14
Baud Rate = 9600  Time avail. =  4.500 secs # of blocks =  3 # of bytes = 1536 Time needed =  1.600 Next = 12
Baud Rate = 9600  Time avail. =  4.500 secs # of blocks =  4 # of bytes = 2048 Time needed =  2.133 Next = 10
Baud Rate = 9600  Time avail. =  4.500 secs # of blocks =  5 # of bytes = 2560 Time needed =  2.667 Next =  7
Baud Rate = 9600  Time avail. =  4.500 secs # of blocks =  6 # of bytes = 3072 Time needed =  3.200 Next =  5
Baud Rate = 9600  Time avail. =  4.500 secs # of blocks =  7 # of bytes = 3584 Time needed =  3.733 Next =  3
Baud Rate = 9600  Time avail. =  5.000 secs # of blocks =  1 # of bytes =  512 Time needed =  0.533 Next = 18
Baud Rate = 9600  Time avail. =  5.000 secs # of blocks =  2 # of bytes = 1024 Time needed =  1.067 Next = 16
Baud Rate = 9600  Time avail. =  5.000 secs # of blocks =  3 # of bytes = 1536 Time needed =  1.600 Next = 14
Baud Rate = 9600  Time avail. =  5.000 secs # of blocks =  4 # of bytes = 2048 Time needed =  2.133 Next = 12
Baud Rate = 9600  Time avail. =  5.000 secs # of blocks =  5 # of bytes = 2560 Time needed =  2.667 Next =  9
Baud Rate = 9600  Time avail. =  5.000 secs # of blocks =  6 # of bytes = 3072 Time needed =  3.200 Next =  7
Baud Rate = 9600  Time avail. =  5.000 secs # of blocks =  7 # of bytes = 3584 Time needed =  3.733 Next =  5
Baud Rate = 9600  Time avail. =  5.500 secs # of blocks =  1 # of bytes =  512 Time needed =  0.533 Next = 20
Baud Rate = 9600  Time avail. =  5.500 secs # of blocks =  2 # of bytes = 1024 Time needed =  1.067 Next = 18
Baud Rate = 9600  Time avail. =  5.500 secs # of blocks =  3 # of bytes = 1536 Time needed =  1.600 Next = 16
Baud Rate = 9600  Time avail. =  5.500 secs # of blocks =  4 # of bytes = 2048 Time needed =  2.133 Next = 14
Baud Rate = 9600  Time avail. =  5.500 secs # of blocks =  5 # of bytes = 2560 Time needed =  2.667 Next = 11
Baud Rate = 9600  Time avail. =  5.500 secs # of blocks =  6 # of bytes = 3072 Time needed =  3.200 Next =  9
Baud Rate = 9600  Time avail. =  5.500 secs # of blocks =  7 # of bytes = 3584 Time needed =  3.733 Next =  7
Baud Rate = 9600  Time avail. =  6.000 secs # of blocks =  1 # of bytes =  512 Time needed =  0.533 Next = 22
Baud Rate = 9600  Time avail. =  6.000 secs # of blocks =  2 # of bytes = 1024 Time needed =  1.067 Next = 20
Baud Rate = 9600  Time avail. =  6.000 secs # of blocks =  3 # of bytes = 1536 Time needed =  1.600 Next = 18
Baud Rate = 9600  Time avail. =  6.000 secs # of blocks =  4 # of bytes = 2048 Time needed =  2.133 Next = 16
Baud Rate = 9600  Time avail. =  6.000 secs # of blocks =  5 # of bytes = 2560 Time needed =  2.667 Next = 13
Baud Rate = 9600  Time avail. =  6.000 secs # of blocks =  6 # of bytes = 3072 Time needed =  3.200 Next = 11
Baud Rate = 9600  Time avail. =  6.000 secs # of blocks =  7 # of bytes = 3584 Time needed =  3.733 Next =  9
Baud Rate = 9600  Time avail. =  6.500 secs # of blocks =  1 # of bytes =  512 Time needed =  0.533 Next = 24
Baud Rate = 9600  Time avail. =  6.500 secs # of blocks =  2 # of bytes = 1024 Time needed =  1.067 Next = 22
Baud Rate = 9600  Time avail. =  6.500 secs # of blocks =  3 # of bytes = 1536 Time needed =  1.600 Next = 20
Baud Rate = 9600  Time avail. =  6.500 secs # of blocks =  4 # of bytes = 2048 Time needed =  2.133 Next = 18
Baud Rate = 9600  Time avail. =  6.500 secs # of blocks =  5 # of bytes = 2560 Time needed =  2.667 Next = 15
Baud Rate = 9600  Time avail. =  6.500 secs # of blocks =  6 # of bytes = 3072 Time needed =  3.200 Next = 13
Baud Rate = 9600  Time avail. =  6.500 secs # of blocks =  7 # of bytes = 3584 Time needed =  3.733 Next = 11
Baud Rate = 9600  Time avail. =  7.000 secs # of blocks =  1 # of bytes =  512 Time needed =  0.533 Next = 26
Baud Rate = 9600  Time avail. =  7.000 secs # of blocks =  2 # of bytes = 1024 Time needed =  1.067 Next = 24
Baud Rate = 9600  Time avail. =  7.000 secs # of blocks =  3 # of bytes = 1536 Time needed =  1.600 Next = 22
Baud Rate = 9600  Time avail. =  7.000 secs # of blocks =  4 # of bytes = 2048 Time needed =  2.133 Next = 20
Baud Rate = 9600  Time avail. =  7.000 secs # of blocks =  5 # of bytes = 2560 Time needed =  2.667 Next = 17
Baud Rate = 9600  Time avail. =  7.000 secs # of blocks =  6 # of bytes = 3072 Time needed =  3.200 Next = 15
Baud Rate = 9600  Time avail. =  7.000 secs # of blocks =  7 # of bytes = 3584 Time needed =  3.733 Next = 13
Baud Rate = 9600  Time avail. =  7.500 secs # of blocks =  1 # of bytes =  512 Time needed =  0.533 Next = 28
Baud Rate = 9600  Time avail. =  7.500 secs # of blocks =  2 # of bytes = 1024 Time needed =  1.067 Next = 26
Baud Rate = 9600  Time avail. =  7.500 secs # of blocks =  3 # of bytes = 1536 Time needed =  1.600 Next = 24
Baud Rate = 9600  Time avail. =  7.500 secs # of blocks =  4 # of bytes = 2048 Time needed =  2.133 Next = 22
Baud Rate = 9600  Time avail. =  7.500 secs # of blocks =  5 # of bytes = 2560 Time needed =  2.667 Next = 19
Baud Rate = 9600  Time avail. =  7.500 secs # of blocks =  6 # of bytes = 3072 Time needed =  3.200 Next = 17
Baud Rate = 9600  Time avail. =  7.500 secs # of blocks =  7 # of bytes = 3584 Time needed =  3.733 Next = 15
Baud Rate = 19K2  Time avail. =  0.500 secs # of blocks =  1 # of bytes =  512 Time needed =  0.267 Next =  1
Baud Rate = 19K2  Total time =  0.500 secs # of blocks =  2 # of bytes = 1024 Time needed =  0.533 IMPOSSIBLE
Baud Rate = 19K2  Total time =  0.500 secs # of blocks =  3 # of bytes = 1536 Time needed =  0.800 IMPOSSIBLE
Baud Rate = 19K2  Total time =  0.500 secs # of blocks =  4 # of bytes = 2048 Time needed =  1.067 IMPOSSIBLE
Baud Rate = 19K2  Total time =  0.500 secs # of blocks =  5 # of bytes = 2560 Time needed =  1.333 IMPOSSIBLE
Baud Rate = 19K2  Total time =  0.500 secs # of blocks =  6 # of bytes = 3072 Time needed =  1.600 IMPOSSIBLE
Baud Rate = 19K2  Total time =  0.500 secs # of blocks =  7 # of bytes = 3584 Time needed =  1.867 IMPOSSIBLE
Baud Rate = 19K2  Time avail. =  1.000 secs # of blocks =  1 # of bytes =  512 Time needed =  0.267 Next =  3
Baud Rate = 19K2  Time avail. =  1.000 secs # of blocks =  2 # of bytes = 1024 Time needed =  0.533 Next =  2
Baud Rate = 19K2  Time avail. =  1.000 secs # of blocks =  3 # of bytes = 1536 Time needed =  0.800 Next =  1
Baud Rate = 19K2  Total time =  1.000 secs # of blocks =  4 # of bytes = 2048 Time needed =  1.067 IMPOSSIBLE
Baud Rate = 19K2  Total time =  1.000 secs # of blocks =  5 # of bytes = 2560 Time needed =  1.333 IMPOSSIBLE
Baud Rate = 19K2  Total time =  1.000 secs # of blocks =  6 # of bytes = 3072 Time needed =  1.600 IMPOSSIBLE
Baud Rate = 19K2  Total time =  1.000 secs # of blocks =  7 # of bytes = 3584 Time needed =  1.867 IMPOSSIBLE
```

```
Baud Rate =  (2  Time avail. =  1.500 secs # of blocks =  1 # of byt  =    12 Time needed =  0.267 Next =  5
Baud Rate =  _K2  ime avail. =  1.500 secs # of blocks =  2 # of bytes =    24 Time needed =  0.533 Next =  4
Baud Rate = 19K2  Time avail. =  1.500 secs # of blocks =  3 # of bytes =  1536 Time needed =  0.800 Next =  3
Baud Rate = 19K2  Time avail. =  1.500 secs # of blocks =  4 # of bytes =  2048 Time needed =  1.067 Next =  2
Baud Rate = 19K2  Time avail. =  1.500 secs # of blocks =  5 # of bytes =  2560 Time needed =  1.333 Next =  1
Baud Rate = 19K2  Total time =  1.500 secs # of blocks =  6 # of bytes =  3072 Time needed =  1.600 IMPOSSIBLE
Baud Rate = 19K2  Total time =  1.500 secs # of blocks =  7 # of bytes =  3584 Time needed =  1.867 IMPOSSIBLE
Baud Rate = 19K2  Time avail. =  2.000 secs # of blocks =  1 # of bytes =   512 Time needed =  0.267 Next =  7
Baud Rate = 19K2  Time avail  =  2.000 secs # of blocks =  2 # of bytes =  1024 Time needed =  0.533 Next =  6
Baud Rate = 19K2  Time avail. =  2.000 secs # of blocks =  3 # of bytes =  1536 Time needed =  0.800 Next =  5
Baud Rate = 19K2  Time avail. =  2.000 secs # of blocks =  4 # of bytes =  2048 Time needed =  1.067 Next =  4
Baud Rate = 19K2  Time avail. =  2.000 secs # of blocks =  5 # of bytes =  2560 Time needed =  1.333 Next =  3
Baud Rate = 19K2  Time avail. =  2.000 secs # of blocks =  6 # of bytes =  3072 Time needed =  1.600 Next =  2
Baud Rate = 19K2  Time avail. =  2.000 secs # of blocks =  7 # of bytes =  3584 Time needed =  1.867 Next =  1
Baud Rate = 19K2  Time avail. =  2.500 secs # of blocks =  1 # of bytes =   512 Time needed =  0.267 Next =  9
Baud Rate = 19K2  Time avail. =  2.500 secs # of blocks =  2 # of bytes =  1024 Time needed =  0.533 Next =  8
Baud Rate = 19K2  Time avail. =  2.500 secs # of blocks =  3 # of bytes =  1536 Time needed =  0.800 Next =  7
Baud Rate = 19K2  Time avail. =  2.500 secs # of blocks =  4 # of bytes =  2048 Time needed =  1.067 Next =  6
Baud Rate = 19K2  Time avail. =  2.500 secs # of blocks =  5 # of bytes =  2560 Time needed =  1.333 Next =  5
Baud Rate = 19K2  Time avail. =  2.500 secs # of blocks =  6 # of bytes =  3072 Time needed =  1.600 Next =  4
Baud Rate = 19K2  Time avail. =  2.500 secs # of blocks =  7 # of bytes =  3584 Time needed =  1.867 Next =  3
Baud Rate = 19K2  Time avail. =  3.000 secs # of blocks =  1 # of bytes =   512 Time needed =  0.267 Next = 11
Baud Rate = 19K2  Time avail. =  3.000 secs # of blocks =  2 # of bytes =  1024 Time needed =  0.533 Next = 10
Baud Rate = 19K2  Time avail. =  3.000 secs # of blocks =  3 # of bytes =  1536 Time needed =  0.800 Next =  9
Baud Rate = 19K2  Time avail. =  3.000 secs # of blocks =  4 # of bytes =  2048 Time needed =  1.067 Next =  8
Baud Rate = 19K2  Time avail. =  3.000 secs # of blocks =  5 # of bytes =  2560 Time needed =  1.333 Next =  7
Baud Rate = 19K2  Time avail. =  3.000 secs # of blocks =  6 # of bytes =  3072 Time needed =  1.600 Next =  6
Baud Rate = 19K2  Time avail. =  3.000 secs # of blocks =  7 # of bytes =  3584 Time needed =  1.867 Next =  5
Baud Rate = 19K2  Time avail. =  3.500 secs # of block  =  1 # of bytes =   512 Time needed =  0.267 Next = 13
Baud Rate = 19K2  Time avail. =  3.500 secs # of blocks =  2 # of bytes =  1024 Time needed =  0.533 Next = 12
Baud Rate = 19K2  Time avail. =  3.500 secs # of blocks =  3 # of bytes =  1536 Time needed =  0.800 Next = 11
Baud Rate = 19K2  Time avail. =  3.500 secs # of blocks =  4 # of bytes =  2048 Time needed =  1.067 Next = 10
Baud Rate = 19K2  Time avail. =  3.500 secs # of blocks =  5 # of bytes =  2560 Time needed =  1.333 Next =  9
Baud Rate = 19K2  Time avail. =  3.500 secs # of blocks =  6 # of bytes =  3072 Time needed =  1.600 Next =  8
Baud Rate = 19K2  Time avail. =  3.500 secs # of blocks =  7 # of bytes =  3584 Time needed =  1.867 Next =  7
Baud Rate = 19K2  Time avail. =  4.000 secs # of blocks =  1 # of bytes =   512 Time needed =  0.267 Next = 15
Baud Rate = 19K2  Time avail. =  4.000 secs # of blocks =  2 # of bytes =  1024 Time needed =  0.533 Next = 14
Baud Rate = 19K2  Time avail. =  4.000 secs # of blocks =  3 # of bytes =  1536 Time needed =  0.800 Next = 13
Baud Rate = 19K2  Time avail. =  4.000 secs # of blocks =  4 # of bytes =  2048 Time needed =  1.067 Next = 12
Baud Rate = 19K2  Time avail. =  4.000 secs # of blocks =  5 # of bytes =  2560 Time needed =  1.333 Next = 11
Baud Rate = 19K2  Time avail. =  4.000 secs # of blocks =  6 # of bytes =  3072 Time needed =  1.600 Next = 10
Baud Rate = 19K2  Time avail. =  4.000 secs # of blocks =  7 # of bytes =  3584 Time needed =  1.867 Next =  9
Baud Rate = 19K2  Time avail. =  4.500 secs # of blocks =  1 # of bytes =   512 Time needed =  0.267 Next = 17
Baud Rate = 19K2  Time avail. =  4.500 secs # of blocks =  2 # of bytes =  1024 Time needed =  0.533 Next = 16
Baud Rate = 19K2  Time avail. =  4.500 secs # of blocks =  3 # of bytes =  1536 Time needed =  0.800 Next = 15
Baud Rate = 19K2  Time avail. =  4.500 secs # of blocks =  4 # of bytes =  2048 Time needed =  1.067 Next = 14
Baud Rate = 19K2  Time avail. =  4.500 secs # of blocks =  5 # of bytes =  2560 Time needed =  1.333 Next = 13
Baud Rate = 19K2  Time avail. =  4.500 secs # of blocks =  6 # of bytes =  3072 Time needed =  1.600 Next = 12
Baud Rate = 19K2  Time avail. =  4.500 secs # of blocks =  7 # of bytes =  3584 Time needed =  1.867 Next = 11
Baud Rate = 19K2  Time avail. =  5.000 secs # of blocks =  1 # of bytes =   512 Time needed =  0.267 Next = 19
Baud Rate = 19K2  Time avail. =  5.000 secs # of blocks =  2 # of bytes =  1024 Time needed =  0.533 Next = 18
Baud Rate = 19K2  Time avail. =  5.000 secs # of blocks =  3 # of bytes =  1536 Time needed =  0.800 Next = 17
Baud Rate = 19K2  Time avail. =  5.000 secs # of blocks =  4 # of bytes =  2048 Time needed =  1.067 Next = 16
Baud Rate = 19K2  Time avail. =  5.000 secs # of blocks =  5 # of bytes =  2560 Time needed =  1.333 Next = 15
Baud Rate = 19K2  Time avail. =  5.000 secs # of blocks =  6 # of bytes =  3072 Time needed =  1.600 Next = 14
Baud Rate = 19K2  Time avail. =  5.000 secs # of blocks =  7 # of bytes =  3584 Time needed =  1.867 Next = 13
Baud Rate = 19K2  Time avail. =  5.500 secs # of blocks =  1 # of bytes =   512 Time needed =  0.267 Next = 21
Baud Rate = 19K2  Time avail. =  5.500 secs # of blocks =  2 # of bytes =  1024 Time needed =  0.533 Next = 20
Baud Rate = 19K2  Time avail. =  5.500 secs # of blocks =  3 # of bytes =  1536 Time needed =  0.800 Next = 19
Baud Rate = 19K2  Time avail. =  5.500 secs # of blocks =  4 # of bytes =  2048 Time needed =  1.067 Next = 18
Baud Rate = 19K2  Time avail. =  5.500 secs # of blocks =  5 # of bytes =  2560 Time needed =  1.333 Next = 17
Baud Rate = 19K2  Time avail. =  5.500 secs # of blocks =  6 # of bytes =  3072 Time needed =  1.600 Next = 16
Baud Rate = 19K2  Time avail. =  5.500 secs # of blocks =  7 # of bytes =  3584 Time needed =  1.867 Next = 15
Baud Rate = 19K2  Time avail. =  6.000 secs # of blocks =  1 # of bytes =   512 Time needed =  0.267 Next = 23
Baud Rate = 19K2  Time avail. =  6.000 secs # of blocks =  2 # of bytes =  1024 Time needed =  0.533 Next = 22
Baud Rate = 19K2  Time avail. =  6.000 secs # of blocks =  3 # of bytes =  1536 Time needed =  0.800 Next = 21
```

```
Baud Rate =     2   Time avail. =  6.000 secs # of blocks =  4 # of bytes =   48 Time needed =  1.067 Next = 20
Baud Rate =     2   Time avail. =  6.000 secs # of blocks =  5 # of bytes =   50 Time needed =  1.333 Next = 19
Baud Rate = 19K2   Time avail. =  6.000 secs # of blocks =  6 # of bytes = 3072 Time needed =  1.600 Next = 18
Baud Rate = 19K2   Time avail. =  6.000 secs # of blocks =  7 # of bytes = 3584 Time needed =  1.867 Next = 17
Baud Rate = 19K2   Time avail. =  6.500 secs # of blocks =  1 # of bytes =  512 Time needed =  0.267 Next = 25
Baud Rate = 19K2   Time avail. =  6.500 secs # of blocks =  2 # of bytes = 1024 Time needed =  0.533 Next = 24
Baud Rate = 19K2   Time avail. =  6.500 secs # of blocks =  3 # of bytes = 1536 Time needed =  0.800 Next = 23
Baud Rate = 19K2   Time avail. =  6.500 secs # of blocks =  4 # of bytes = 2048 Time needed =  1.067 Next = 22
Baud Rate = 19K2   Time avail. =  6.500 secs # of blocks =  5 # of bytes = 2560 Time needed =  1.333 Next = 21
Baud Rate = 19K2   Time avail. =  6.500 secs # of blocks =  6 # of bytes = 3072 Time needed =  1.600 Next = 20
Baud Rate = 19K2   Time avail. =  6.500 secs # of blocks =  7 # of bytes = 3584 Time needed =  1.867 Next = 19
Baud Rate = 19K2   Time avail. =  7.000 secs # of blocks =  1 # of bytes =  512 Time needed =  0.267 Next = 27
Baud Rate = 19K2   Time avail. =  7.000 secs # of blocks =  2 # of bytes = 1024 Time needed =  0.533 Next = 26
Baud Rate = 19K2   Time avail. =  7.000 secs # of blocks =  3 # of bytes = 1536 Time needed =  0.800 Next = 25
Baud Rate = 19K2   Time avail. =  7.000 secs # of blocks =  4 # of bytes = 2048 Time needed =  1.067 Next = 24
Baud Rate = 19K2   Time avail. =  7.000 secs # of blocks =  5 # of bytes = 2560 Time needed =  1.333 Next = 23
Baud Rate = 19K2   Time avail. =  7.000 secs # of blocks =  6 # of bytes = 3072 Time needed =  1.600 Next = 22
Baud Rate = 19K2   Time avail. =  7.000 secs # of blocks =  7 # of bytes = 3584 Time needed =  1.867 Next = 21
Baud Rate = 19K2   Time avail. =  7.500 secs # of blocks =  1 # of bytes =  512 Time needed =  0.267 Next = 29
Baud Rate = 19K2   Time avail. =  7.500 secs # of blocks =  2 # of bytes = 1024 Time needed =  0.533 Next = 28
Baud Rate = 19K2   Time avail. =  7.500 secs # of blocks =  3 # of bytes = 1536 Time needed =  0.800 Next = 27
Baud Rate = 19K2   Time avail. =  7.500 secs # of blocks =  4 # of bytes = 2048 Time needed =  1.067 Next = 26
Baud Rate = 19K2   Time avail. =  7.500 secs # of blocks =  5 # of bytes = 2560 Time needed =  1.333 Next = 25
Baud Rate = 19K2   Time avail. =  7.500 secs # of blocks =  6 # of bytes = 3072 Time needed =  1.600 Next = 24
Baud Rate = 19K2   Time avail. =  7.500 secs # of blocks =  7 # of bytes = 3584 Time needed =  1.867 Next = 23
```

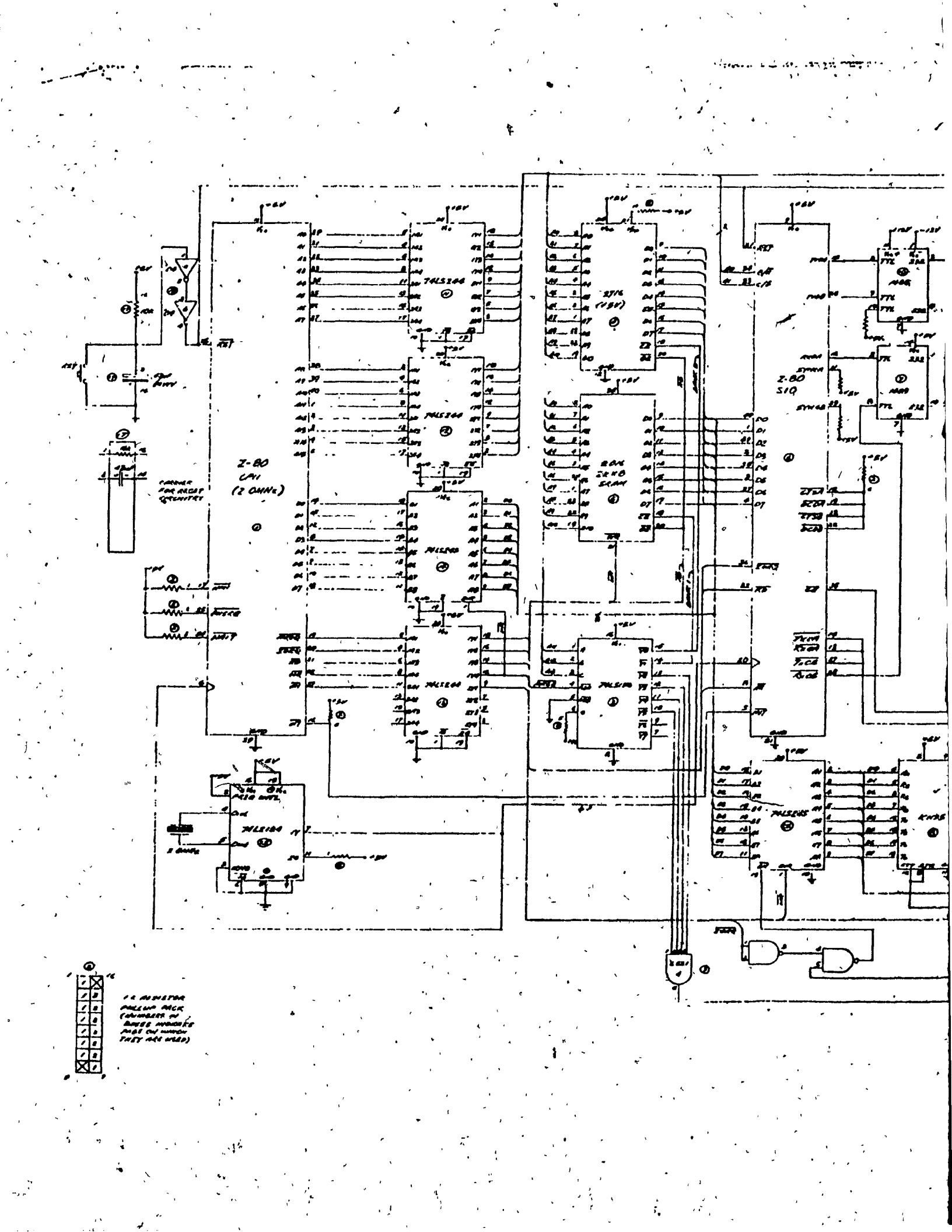
Z-80
CPU
(2 OHMS)
Z-80
SIO
74LS244
74LS245
74LS640
74LS138
74LS08
74LS00
74LS32
74LS04
74LS74
74LS157
74LS367
74LS373
74LS374
74LS393
74LS164
74LS175
74LS273
74LS283
74LS299
74LS373
74LS374
74LS393
74LS164
74LS175
74LS273
74LS283
74LS299

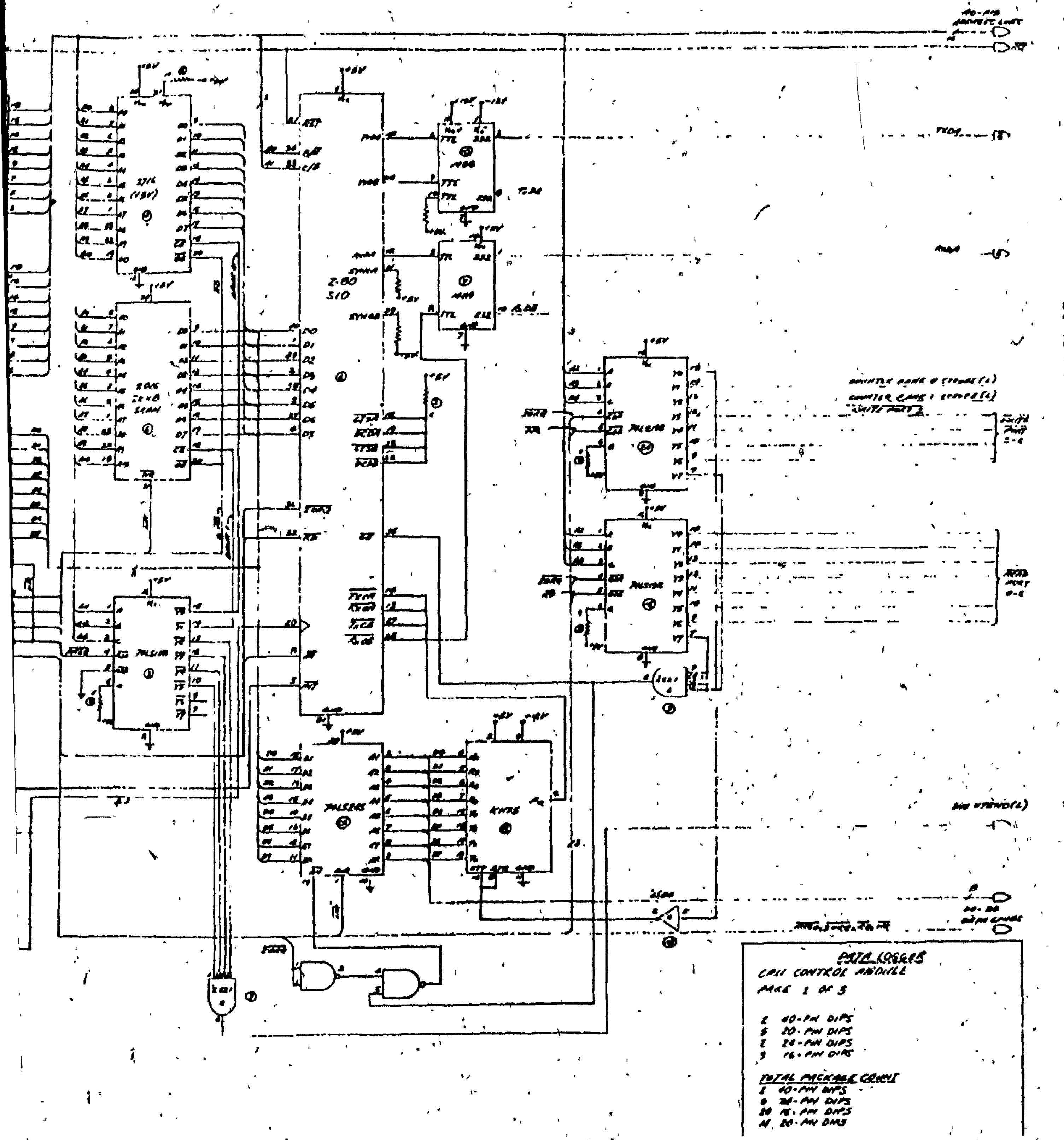
Z-80
SIO
DATA LOGGER
CPU CONTROL MODULE
TOTAL PACKAGE COUNT

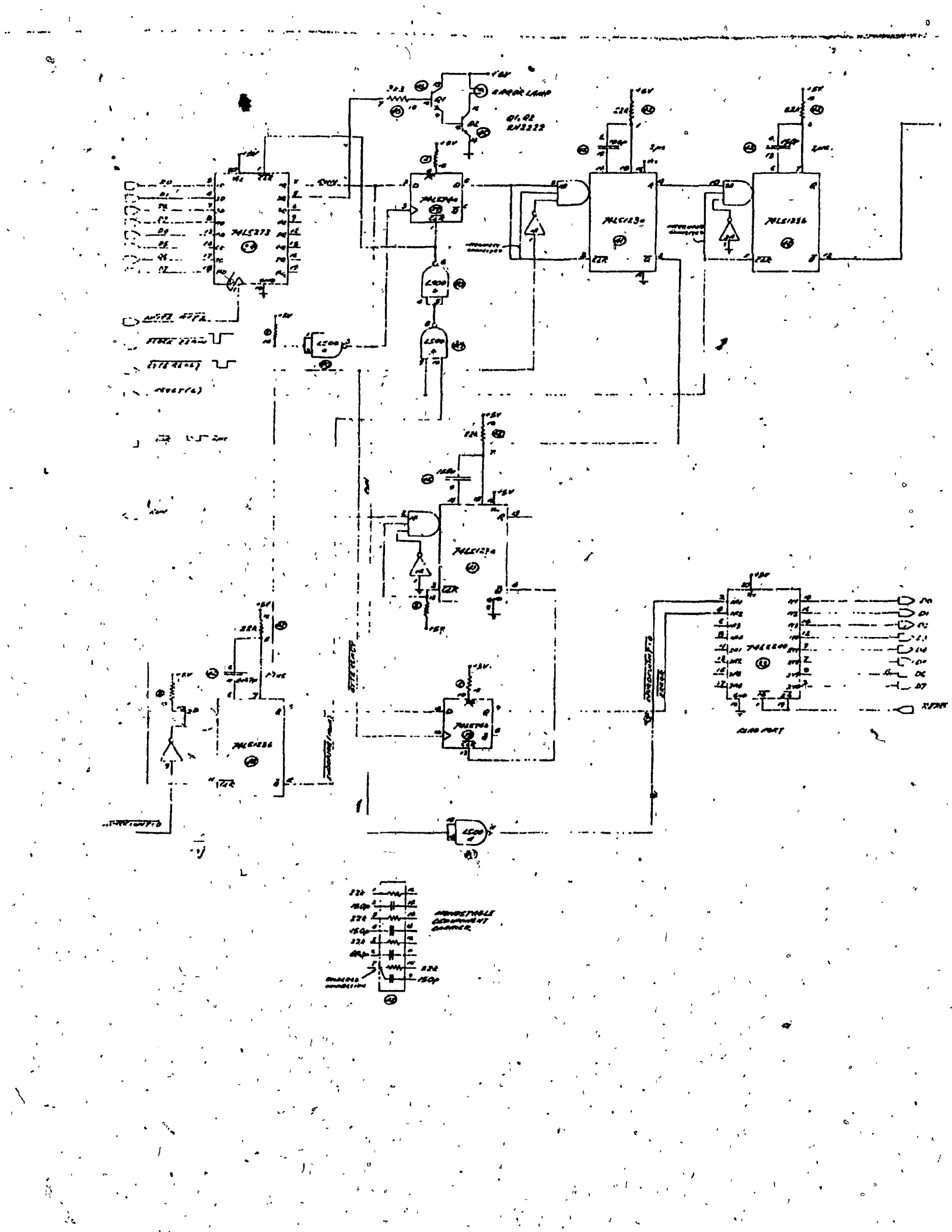

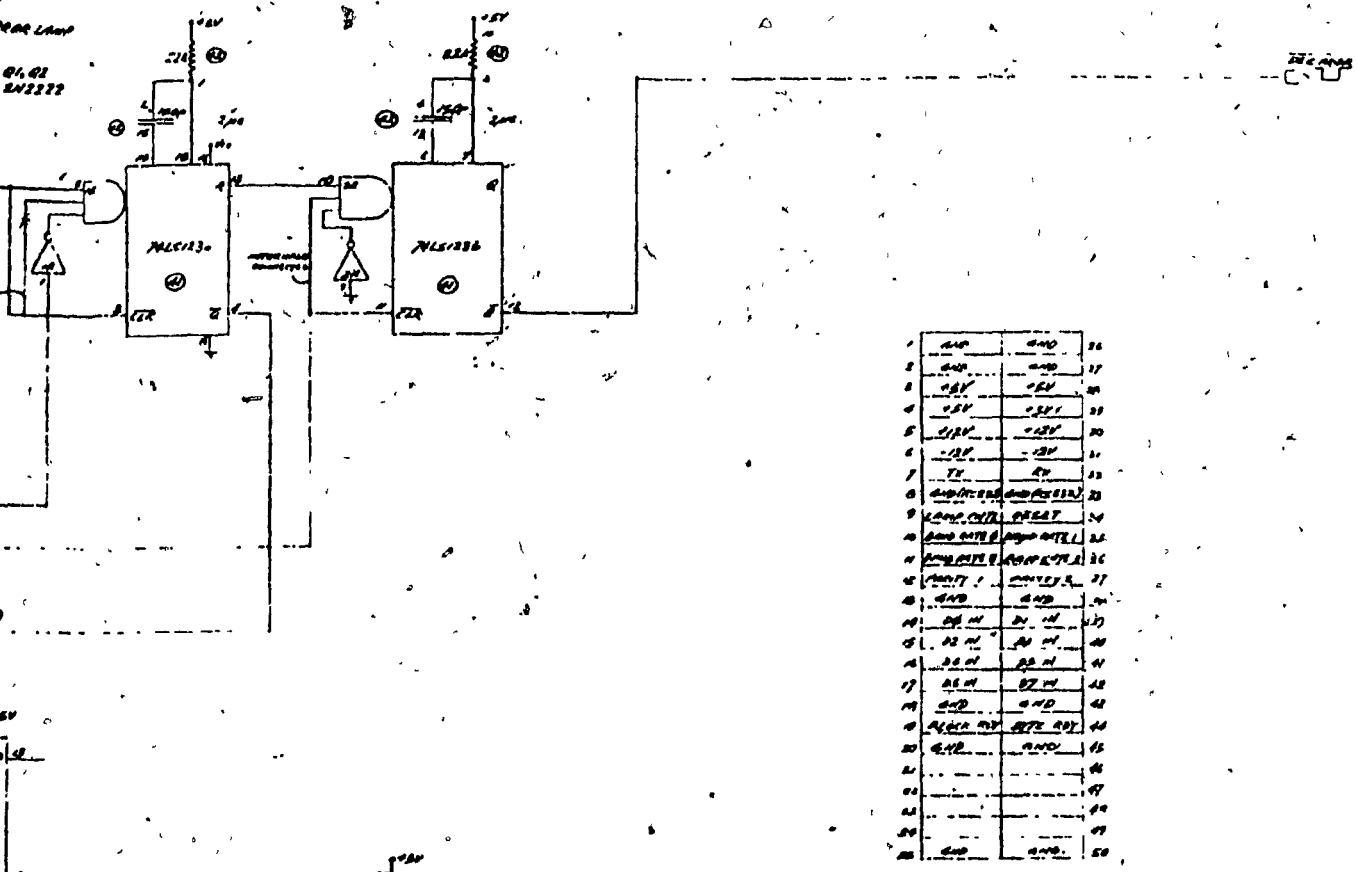

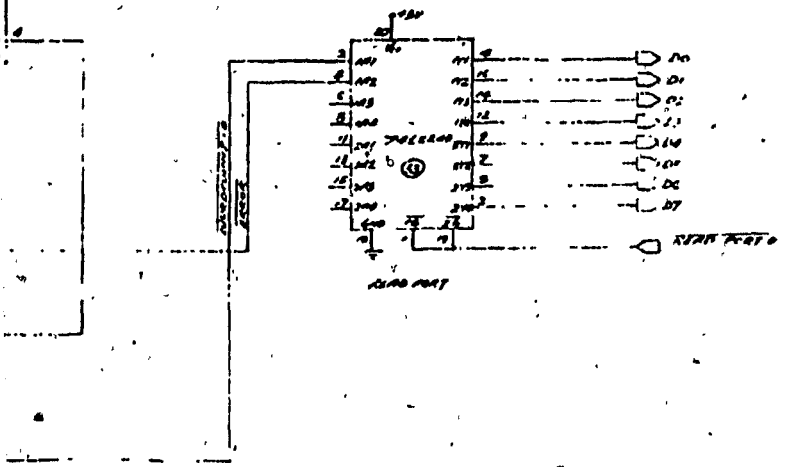

DATA BOGGLE
AUDICAY EXTENSION CONTROLLER
PAGE 2 OF 3

5 16 PIN DIPS
2 20 PIN DIPS

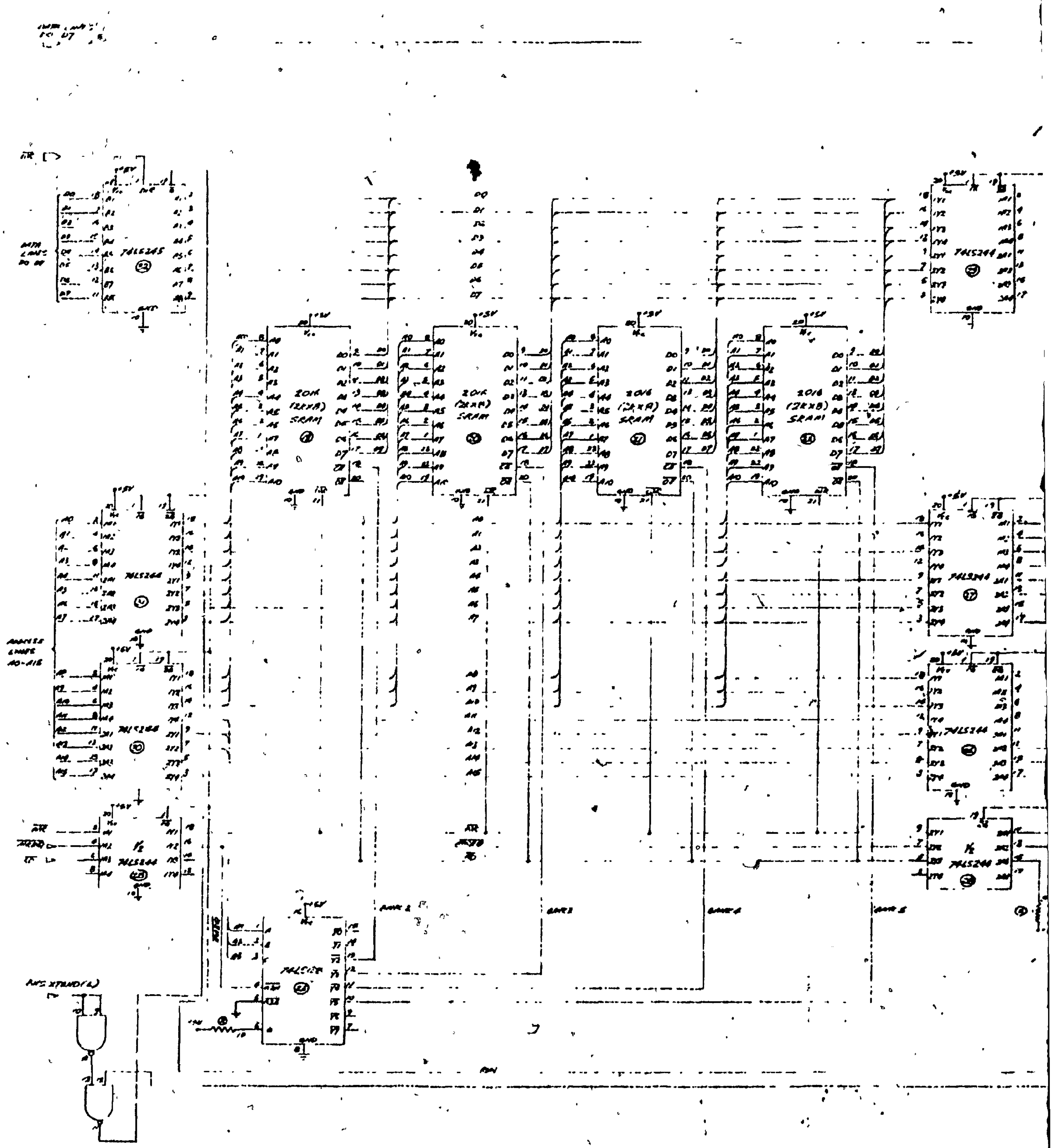
74LS245
74LS244
2016 (2KX8) SRAM
74LS138
+5V
GND

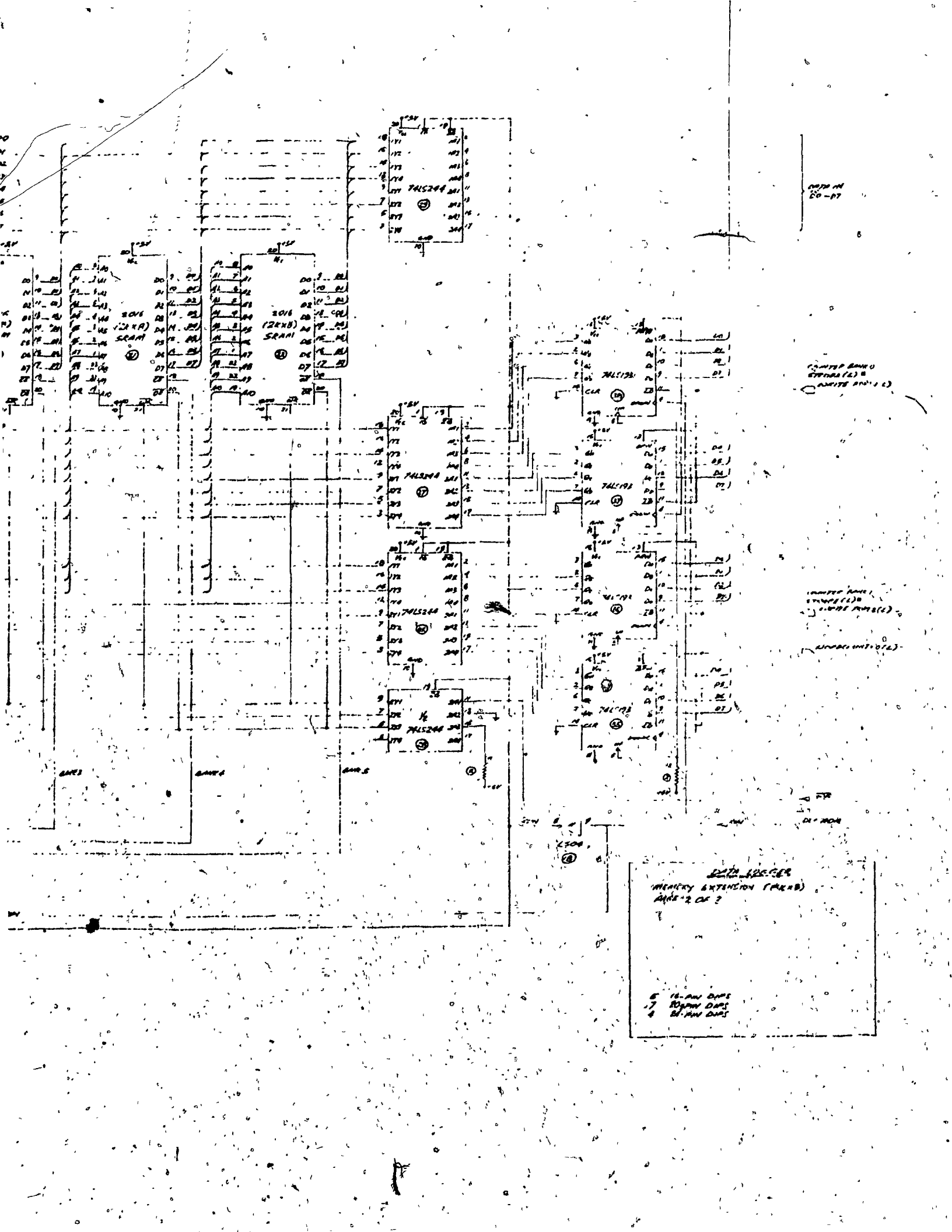
74LS244
2016 (2K x 8) SRAM
74LS193
DATA LOCATER
MEMORY EXTENSION (PAGE B)
PAGE 2 OF 3

APPENDIX D

LOG5 : A Program to Log Data into the Computer Through the Data Logger

```
dim limit(5),dur(5)
input "enter message that you wish to add to data of file",message$
rem get data file name, do not forget to include drive letter!
input "enter name of file to store data in ---> ",file$
if (file$ = "") or (file$="stop") then end
print " "
print " "

open "com1:9600,n,8,,rs,cs,ds,cd" as #1
open file$ as #2 len=512
field #2, 256 as blck1$, 256 as blck2$

rem print #1,chr$(0)          :rem tell logger to reset right away

rem  initialize total length

10 total = 0

rem  send out command byte (first get decimal value of command)
rem  34 seems to be a good number

15 k=loc(1)                                  :rem   to clear the com buffer
   if k>0 then a$=input$(k,#1):goto 15       :rem      "    "    "

17 input "enter the number of time ( < or = 5 ) intervals to log --> ",per
   if per = 99 then end  :rem abort input is 99
   if per > 5 then 17
   print " "
   print " "
   print "please input the number of scan lines to capture and the"
   print "interval between them for";per;" time periods."

   numtot% = 0

   for i = 1 to per
      print i;"-- ";
      input "( number,duration ) ",limit(i),dur(i)
      if (limit(i)=99) or (dur(i) = 99) then end :rem abort input is 99
```

```
    numtotl% = numtotl% + limit(i)
    dur(i) = dur(i)*2                          :rem '*2' because data is read
    limit(i) = limit(i)*dur(i)          :rem in 1/2 scan line blocks
  next i

rem the next block of code puts a header on the data file to tell the
rem decode program how many samples of dat to expect


   ini$=" "
   a$=string$(255,ini$)

rem at this point you can add a message to the stored file
rem do so by putting the message into the variable "message$"
rem i.e. message$ = "hi there or whatever"

   v$=mki$(numtotl%)

   mid$(a$,1)=v$

   mid$(a$,3)=message$
   lset blck1$=a$
   lset blck2$=a$

   put #2


rem  input "enter decimal value of command byte -->",cmd
rem  fix the command byte to 34

   cmd = 34

   print #1,chr$(cmd);chr$(cmd);     :rem send command out twice



rem  print out Thong's answer

22 k=loc(1)        :rem it should just print out an 'A' on the screen
   if k<1 then 22
   a$=input$(1,#1)
   print a$

rem  now start taking in the data in blocks of 255 length

   for i = 1 to per      :rem repeat the whole thing for 'per' time periods

     durcnt =0
```

```
    limit(i)=limit(i) + total

25  k=loc(1)                    :rem wait until 255 bytes in buffer
    if k<255 then 25

    total = total + 1           :rem increment total length block of 255 counter
    print "a block done  t=";total/2;"seconds"

50  a$=input$(256,#1)           :rem take 256 bytes of data out of com buffer

    durent = durent + 1
    if durent = dur(i)-1 then lset blck1$=a$
    if durent = dur(i) then lset blck2$=a$: durent = 0:put #2:print "sampled!"


    if total < limit(i) then 25     :rem the number of 255 byte segments to get

  next i

  print #1,chr$(0);             :rem stop the logger device


60 rem

rem  it is a very important thing to properly close the opened files

  close #1
  close #2
```

APPENDIX E

DECODE6 : A Program to Decode the Data & Compare to a Set Threshold

```
rem program to get data out of a file

dim ans(512)
dim cur(80)
dim eighty(80)
input "input filename which contains the data  ";file$
input "enter filename to output the numbers to ";file2$
input "enter threshold level";t

open file$ as #1 len=512
field #1, 256 as blck1$, 256 as blck2$

open file2$ for output as #2

get #1
numtotl$=mid$(blck1$,1,2)
loop = cvi(numtotl$)
print "there are";loop;"samples of data to decode"
message$ = mid$(blck1$,3,250)
for looper = 1 to loop


get #1
a$=blck1$
b$=blck2$

for i = 1 to 256
   x$ = mid$(a$,i,1)
   ans(i) = asc(x$)
next i

for i = 257 to 512
   ii = i-256
    x$ = mid$(b$,ii,1)
   ans(i) = asc(x$)
next i
```

```
rem put analaysis program here
for i=1 to 512
    if ans(i)<t then counter=counter+1
    if ans(i)>=t then counter=0
    if counter>10 then last=i
next i
counter=0
for i=512 to 1 step -1
    if ans(i)<t then counter=counter+1
    if ans(i)>=t then counter=0
    if COUNTER>10 then first=i
next i
print "first=" first,"last=" last
diam=(last-first+1)*12.5
PRINT "DIAMETER=" DIAM
print #2,diam
rem leave this here for now remove later ->if not eof(1) then 10

next looper

close #1

end
```

APPENDIX F

ACCURACY, REPRODUCIBILITY AND ERROR ANALYSIS

In this appendix we make some comments regarding the accuracy and reproducibility of the measurements made by the die swell apparatus and introduce a simplified error analysis of the technique involved.

F.1 Accuracy of Diameter Measurements

Table F.1 shows comparison between measurements made under a microscope and those made with the die swell optical system for 8 glass and metal standard rods. These results show that the deviation between the two measurements was below 15 microns. The maximum deviation observed was 1.7%.

F.2 Reproducibility

For each of the resins W1, W3 and W4, replicate measurements of extrudate equilibrium diameter and swell were made, while attempting to hold all variables constant. The results are shown in Table F.2. They show that the maximum measured spread in diameter was 37.5 μ (micron). The corresponding spread in the swell value would be 0.028 for the die used in the analysis (D = 1320 μ).

TABLE F.1

The Diameters of Eight Metal and Glass Standards Measured Under the Microscope (d1) and Using the Apparatus (d2)

No.	d1 (micron)	d2 (micron)	d1 - d2 (micron)	$\frac{d1 - d2}{d1} \times 100\%$
1	725	712.5	-12.5	-1.7%
2	980	987.5	+ 7.5	+0.7%
3	1115	1125	+10	+0.9%
4	1414	1400	-14	-0.7%
5	1962	1950	-12	-0.6%
6	2310	2312.5	+ 2.5	+0.1%
7	2574	2562.5	-11.5	-0.5%
8	2960	2975	15	+0.5%

TABLE F.2

The Results of Three Sets of Experiments Repeated Under the Same Conditions for Each Set. Melt Temperature in All Cases = 190°C

Resin	Shear Rate (s^{-1})	Diameter (μ)	Swell	Maximum Spread (μ)	Maximum Spread in Swell
W1	77	2650 2675 2662.5 2675 2637.5	2.008 2.027 2.017 2.027 1.998	37.5	0.028
W3	13.8	2087.5 2100 2100 2075 2087.5	1.581 1.591 1.591 1.572 1.581	25	0.019
W4	142	2312.5 2287.5 2287.5 2275 2312.5	1.752 1.733 1.733 1.724 1.752	37.5	0.028

F.3 Simplified Error Analysis

The following discussion attempts to evaluate the contribution of uncertainties in some of the system variables to the overall error in the measurement of die swell.

Systematic errors in the measurement of extrudate swell might result from the following factors.

F.3.1 The Error Due to Element-To-Element Spacing E_{sp}

a) ∓ 1 element uncertainty $\equiv \mp 25\ \mu$

$$B_{True} = \frac{D_e \mp 25}{D_c} = \frac{D_e}{D_c} \mp \frac{25}{D_c} \qquad (F.1)$$

where D_e is the measured diameter of the extrudate in microns

D_c is the diameter of the die in microns.

If the diameter of the used die is 1320 μ then

$$B_{True} = B_{measured} \mp 0.0189$$

For a measured diameter of 2000 μ (B = 1.52) the percentage error would be

$$E_{sp} = \frac{0.0189}{1.52} \times 100\% \approx 1.3\% \text{ of the measured value}$$

b) Magnification would increase the accuracy and reduce the uncertainty.

For a magnification of 2.0

$$B_{True} = B_{measured} \mp \frac{0.0189}{2} = B_{measured} \mp 0.0095$$

For the special case under consideration

$$E_{sp} = 0.65\%$$

F.3.2 Errors Due to Positioning Uncertainty E_p

The distances between the optical components could be controlled to a certain limit:

a) The distances between the lens and the photodiode array could be set within an accuracy of ∓0.5 mm. this accuracy reflects on the measured diameter (magnified) as indicated by Equation (3.2)

$$M = \frac{I}{O}$$

where I is the distance between the lens and the photodiode array (image distance) and O is the distance between the extrudate and the lens (object distance).

For a magnification of two (M = 2.0), using a lens with a focal length of 50 mm

$$I = 150 \text{ mm}$$

$$O = 75 \text{ mm}$$

therefore

$$M = \frac{150 \mp 0.5}{75} = 2 \mp 0.007$$

b) The extrudate may move in the oil in the direction of the optical path resulting in an inaccuracy in the measurement.

Assume that this movement is ∓1 mm (if the density of the oil is set correctly). Thus

$$M = \frac{150}{75 \mp 1} = 2 \mp 0.027$$

The maximum possible inaccuracy in magnification, therefore, is

$$M = 2 \mp 0.034$$

This will lead to a $\mp \frac{0.034}{2} \times 100\% = \mp 1.7\%$ error in the measured diameter

$$E_p = \mp 1.7\%$$

F.3.3 Error Resulting from Temperature Fluctuations (E_{TB}) in the Barrel

The temperature in the barrel can be maintained within ∓0.5°C. This will affect the accuracy of the measurement in proportion to the effect of temperature on extrudate swell.

$$E_{TB} = f\left(\frac{dB}{dT}\right) \qquad (F.2)$$

For resin W1, as Table 4.3 shows, an increase of 20°C in the melt temperature caused 0.10 increase in extrudate swell.

If $\frac{dB}{dT}$ is assumed linear (not necessarily true), then a ∓ 0.5°C change would correspond to ∓ 0.005 change in the swell value

$$E_T = \frac{\mp 0.005}{(1.85 + 1.75)/2} \times 100\% = \mp 0.3\%$$

where 1.85 and 1.75 are the swell values at 190°C and 210°C, respectively.

F.3.4 Error Resulting from Fluctuation of Temperature in the Thermostating Chamber E_{TC}

The uncertainty about this temperature could lead to an inaccuracy, which reflects on the calculated thermal expansion correction. The error resulting from this is, however, negligible ($\approx 0.01\%$).

F.3.5 Summary

The measurement errors are summarized in Table F.3. The total static error (TSE) of this measurement system can be estimated in terms of the root-mean-square of the component characteristic errors

$$TSE = \sqrt{E_{sp} + E_p + E_{TB} + E_{TC}} = 1.64 \approx 2\%$$

TABLE F.3

A Summary of the Important Measurement Errors

	Error	Magnitude
1	Spacing Error, E_{sp}	∓0.65%
2	Positioning Error, E_p	∓1.7%
3	Barrel Temperature Error, E_{TB}	∓0.3%
4	Chamber Temperature Error, E_{TC}	∓0.03%
	Total Static Error, TSE	∓2%

APPENDIX G

EXTRUDATE SWELL DATA

Extrudate Swell Data for Resin W1

Shear Rate (s^{-1})	14	39	77	144	366	732
Time (sec)						
16	1.56	1.60	1.65	1.72	1.76	1.84
32	1.58	1.64	1.70	1.77	1.82	1.89
48	1.61	1.65	1.71	1.80	1.83	1.92
64	1.63	1.70	1.76	1.85	1.88	1.99
80	1.64	1.70	1.78	1.87	1.90	2.01
96	1.66	1.74	1.80	1.88	1.93	2.04
112	1.68	1.75	1.82	1.90	1.94	2.05
128	1.69	1.76	1.84	1.91	1.97	2.07
144	1.71	1.76	1.83	1.91	1.98	2.08
160	1.69	1.77	1.85	1.93	2.00	2.10
176	1.71	1.79	1.86	1.95	2.02	2.11
192	1.75	1.80	1.87	1.96	2.02	2.11
208	1.72	1.81	1.87	1.96	2.03	2.13
224	1.75	1.81	1.89	1.98	2.04	2.14
240	1.74	1.83	1.89	1.98	2.05	2.15
256	1.77	1.82	1.88	1.99	2.05	2.15
272	1.79	1.84	1.90	2.02	2.07	2.17
288	1.78	1.84	1.90	2.01	2.06	2.16
304	1.81	1.85	1.91	2.02	2.08	2.17
320	1.82	1.84	1.91	2.01	2.08	2.18
336	1.83	1.86	1.91	2.02	2.09	2.19
352	1.81	1.85	1.91	2.02	2.09	2.18
368	1.83	1.85	1.91	2.03	2.09	2.18
384	1.83	1.87	1.94	2.04	2.11	2.19
400	1.83	1.87	1.94	2.06	2.12	2.19
416	1.83	1.87	1.93	2.05	2.12	2.19
432	1.82	1.87	1.93	2.04	2.11	2.18
448	1.83	1.88	1.95	2.06	2.12	2.19
464	1.84	1.87	1.95	2.06	2.12	2.18
480	1.85	1.88	1.95	2.07	2.12	2.20
496	1.86	1.88	1.96	2.06	2.13	2.18
512	1.87	1.90	1.97	2.08	2.15	2.21
528	1.83	1.88	1.96	2.06	2.13	2.21
544	1.84	1.88	1.96	2.07	2.13	2.20
560	1.86	1.91	1.98	2.08	2.14	2.21
576	1.83	1.88	1.95	2.06	2.13	2.18
592	1.85	1.90	1.98	2.09	2.15	2.21
608	1.86	1.90	1.98	2.09	2.17	2.21
624	1.87	1.91	1.99	2.09	2.16	2.23
640	1.86	1.90	1.98	2.09	2.17	2.21
656	1.86	1.91	1.98	2.11	2.16	2.23
672	1.87	1.91	1.99	2.12	2.16	2.22
688	1.87	1.91	1.99	2.09	2.16	2.23
704	1.87	1.91	1.99	2.09	2.16	2.23
720	1.87	1.94	2.02	2.10	2.18	2.25

Extrudate Swell Data for Resin W2

Time (sec)	Shear Rate (s^{-1}) 3.3	6.4	14.3	36
16	1.64	1.65	1.71	1.78
32	1.62	1.65	1.69	1.77
48	1.63	1.65	1.73	1.78
64	1.63	1.65	1.74	1.80
80	1.65	1.66	1.75	1.80
96	1.65	1.66	1.75	1.81
112	1.65	1.67	1.77	1.83
128	1.65	1.68	1.77	1.85
144	1.65	1.69	1.78	1.84
160	1.66	1.69	1.79	1.86
176	1.65	1.69	1.79	1.87
192	1.65	1.69	1.79	1.87
208	1.65	1.69	1.78	1.85
224	1.65	1.70	1.79	1.87
240	1.65	1.70	1.78	1.87
256	1.65	1.71	1.79	1.87
272	1.66	1.71	1.81	1.89
288	1.65	1.71	1.81	1.88
304	1.66	1.71	1.81	1.88
320	1.65	1.72	1.81	1.88
336	1.67	1.72	1.82	1.90
352	1.66	1.71	1.80	1.89
368	1.66	1.72	1.81	1.89
384	1.66	1.73	1.81	1.90
400	1.67	1.72	1.83	1.90
416	1.67	1.74	1.82	1.92
432	1.66	1.72	1.80	1.91
448	1.67	1.72	1.82	1.91
464	1.66	1.73	1.84	1.91
480	1.66	1.73	1.85	1.92
496	1.67	1.73	1.83	1.93
512	1.68	1.74	1.83	1.93
528	1.67	1.73	1.83	1.93
544	1.67	1.74	1.84	1.94
560	1.67	1.74	1.84	1.93
576	1.66	1.72	1.82	1.92
592	1.67	1.72	1.83	1.93
608	1.67	1.73	1.83	1.95
624	1.67	1.74	1.83	1.94
640	1.66	1.73	1.84	1.94
656	1.66	1.73	1.86	1.95
672	1.68	1.74	1.85	1.95
688	1.66	1.73	1.83	1.95
704	1.67	1.73	1.84	1.96
720	1.68	1.74	1.84	1.96

Extrudate Swell Data for Resin W3

Shear Rate (s^{-1}) / Time (sec)	3.2	6.4	14.3
16	1.50	1.50	1.48
32	1.47	1.46	1.46
48	1.48	1.47	1.47
64	1.49	1.49	1.48
80	1.50	1.50	1.50
96	1.51	1.50	1.50
112	1.51	1.51	1.51
128	1.53	1.52	1.52
144	1.52	1.53	1.54
160	1.54	1.54	1.55
176	1.54	1.54	1.54
192	1.54	1.54	1.54
208	1.53	1.53	1.53
224	1.54	1.54	1.53
240	1.54	1.55	1.54
256	1.55	1.55	1.55
272	1.56	1.55	1.56
288	1.54	1.55	1.56
304	1.55	1.55	1.55
320	1.56	1.55	1.55
336	1.56	1.56	1.57
352	1.56	1.56	1.56
368	1.56	1.56	1.57
384	1.56	1.56	1.57
400	1.57	1.57	1.57
416	1.57	1.57	1.57
432	1.57	1.56	1.57
448	1.57	1.56	1.57
464	1.58	1.58	1.60
480	1.58	1.57	1.60
496	1.58	1.59	1.59
512	1.59	1.58	1.58
528	1.58	1.58	1.59
544	1.58	1.58	1.59
560	1.59	1.59	1.60
576	1.56	1.57	1.57
592	1.57	1.57	1.57
608	1.57	1.58	1.59
624	1.59	1.57	1.57
640	1.59	1.57	1.59
656	1.59	1.58	1.59
672	1.59	1.58	1.58
688	1.58	1.58	1.58
704	1.59	1.58	1.59
720	1.59	1.59	1.59

Extrudate Swell Data for Resin W4

Time (sec) \ Shear Rate (s^{-1})	7	14	36	71	142	370	760
16	1.31	1.35	1.43	1.50	1.60	1.66	1.81
32	1.29	1.34	1.43	1.49	1.59	1.68	1.85
48	1.30	1.35	1.44	1.51	1.61	1.72	1.89
64	1.31	1.36	1.46	1.53	1.62	1.74	1.92
80	1.31	1.37	1.47	1.55	1.64	1.77	1.93
96	1.31	1.36	1.48	1.55	1.66	1.78	1.95
112	1.32	1.38	1.50	1.57	1.68	1.80	1.96
128	1.32	1.40	1.49	1.58	1.69	1.82	1.99
144	1.32	1.39	1.50	1.58	1.70	1.82	2.00
160	1.33	1.39	1.51	1.60	1.70	1.83	2.01
176	1.34	1.41	1.52	1.60	1.72	1.84	2.03
192	1.32	1.40	1.52	1.60	1.70	1.84	2.03
208	1.32	1.39	1.52	1.60	1.71	1.83	2.03
224	1.33	1.40	1.52	1.60	1.72	1.86	2.03
240	1.33	1.40	1.51	1.60	1.71	1.85	2.04
256	1.32	1.41	1.52	1.62	1.72	1.85	2.06
272	1.33	1.41	1.53	1.61	1.73	1.86	2.06
288	1.32	1.41	1.52	1.60	1.74	1.85	2.05
304	1.33	1.41	1.53	1.62	1.74	1.86	2.07
320	1.34	1.40	1.54	1.63	1.74	1.85	2.07
336	1.34	1.41	1.54	1.63	1.74	1.87	2.07
352	1.32	1.41	1.53	1.62	1.74	1.85	2.06
368	1.33	1.41	1.54	1.62	1.74	1.87	2.07
384	1.34	1.41	1.53	1.62	1.74	1.87	2.08
400	1.34	1.41	1.54	1.62	1.74	1.87	2.08
416	1.33	1.42	1.55	1.63	1.75	1.87	2.09
432	1.33	1.41	1.53	1.62	1.75	1.87	2.07
448	1.34	1.41	1.53	1.62	1.75	1.87	2.08
464	1.33	1.41	1.54	1.63	1.75	1.88	2.09
480	1.33	1.42	1.55	1.63	1.76	1.87	2.08
496	1.34	1.42	1.55	1.63	1.76	1.88	2.09
512	1.33	1.42	1.55	1.64	1.75	1.89	2.09
528	1.33	1.41	1.54	1.63	1.74	1.87	2.08
544	1.33	1.41	1.54	1.62	1.75	1.88	2.09
560	1.34	1.41	1.54	1.64	1.75	1.88	2.09
576	1.31	1.40	1.53	1.61	1.75	1.87	2.08
592	1.32	1.40	1.53	1.62	1.74	1.87	2.08
608	1.32	1.40	1.54	1.62	1.73	1.87	2.08
624	1.31	1.40	1.53	1.62	1.75	1.88	2.09
640	1.30	1.40	1.53	1.63	1.74	1.88	2.09
656	1.32	1.41	1.53	1.63	1.76	1.88	2.09
672	1.33	1.40	1.54	1.63	1.76	1.88	2.09
688	1.31	1.40	1.54	1.62	1.74	1.88	2.09
704	1.31	1.40	1.53	1.62	1.74	1.88	2.09
720	1.31	1.40	1.53	1.63	1.75	1.88	2.09

Extrudate Swell Data for Resin W5

Shear Rate (s^{-1}) / Time (sec)	64	128
16	1.60	1.64
32	1.59	1.64
48	1.62	1.67
64	1.63	1.68
80	1.65	1.71
96	1.62	1.71
112	1.65	1.71
128	1.65	1.73
144	1.67	1.72
160	1.66	1.73
176	1.70	1.75
192	1.70	1.74
208	1.68	1.75
224	1.69	1.73
240	1.68	1.76
256	1.69	1.76
272	1.71	1.76
288	1.69	1.74
304	1.69	1.76
320	1.71	1.76
336	1.70	1.75
352	1.68	1.74
368	1.69	1.75
384	1.70	1.75
400	1.67	1.75
416	1.70	1.75
432	1.71	1.75
448	1.70	1.77
464	1.71	1.77
480	1.69	1.77
496	1.67	[illegible]
512	[illegible]	[illegible]
528	1.69	[illegible]
544	[illegible]	1.75
560	1.70	1.75
576	1.68	1.75
592	1.70	1.75
608	1.68	1.75
624	1.69	1.75
640	1.67	1.75
656	1.67	1.76
672	1.68	1.75
688	1.66	1.77
704	1.67	1.76
720	1.67	1.76

Extrudate Swell Data for PP Resin

Shear Rate (s^{-1}) / Time (sec)	35	70	140
16	1.57	1.59	1.60
32	1.59	1.61	1.63
48	1.60	1.62	1.65
64	1.61	1.62	1.67
80	1.62	1.65	1.69
96	1.62	1.66	1.68
112	1.63	1.66	1.72
128	1.65	1.67	1.73
144	1.65	1.69	1.73
160	1.64	1.68	1.72
176	1.64	1.68	1.73
192	1.65	1.70	1.75
208	1.65	1.69	1.76
224	1.65	1.71	1.76
240	1.65	1.69	1.76
256	1.65	1.71	1.77
272	1.67	1.70	1.79
288	1.68	1.70	1.77
304	1.65	1.72	1.80
320	1.67	1.71	1.79
336	1.67	1.74	1.79
352	1.67	1.74	1.79
368	1.68	1.74	1.81
384	1.66	1.73	1.79
400	1.67	1.73	1.79
416	1.68	1.72	1.81
432	1.68	1.72	1.81
448	1.68	1.74	1.80
464	1.68	1.73	1.80
480	1.68	1.74	1.83
496	1.69	1.75	1.81
512	1.68	1.74	1.81
528	1.69	1.74	1.82
544	1.69	1.75	1.81
560	1.68	1.77	1.82
576	1.68	1.75	1.80
592	1.69	1.75	1.83
608	1.68	1.74	1.81
624	1.69	1.74	1.82
640	1.69	1.75	1.83
656	1.69	1.75	1.82
672	1.69	1.75	1.82
688	1.72	1.75	1.82
704	1.70	1.76	1.81
720	1.69	1.76	1.82

Extrudate Swell Data for Filled PP

Time (sec)	Shear Rate (s^{-1}) 26	104
16	1.01	1.01
32	1.01	1.05
48	0.99	1.02
64	1.02	0.99
80	1.01	0.99
96	0.98	0.99
112	0.98	0.99
128	0.99	0.99
144	0.99	0.99
160	1.01	1.02
176	0.98	1.04
192	0.98	1.04
208	0.98	1.04
224	0.97	1.04
240	0.97	1.04
256	0.97	1.02
272	0.98	1.03
288	0.99	1.04
304	1.00	1.02
320	0.99	1.03
336	1.00	1.04
352	0.99	1.04
368	1.01	1.04
384	1.01	1.04
400	1.00	1.04
416	1.00	1.04
432	1.00	1.04
448	1.01	1.03
464	1.02	1.03
480	1.01	1.04
496	1.01	1.01
512	1.02	1.02
528	1.02	1.04
544	1.01	1.03
560	1.01	1.03
576	1.00	1.03
592	1.01	1.03
608	1.01	1.02
624	1.01	1.02
640	1.00	1.02
656	1.00	1.02
672	0.99	1.01
688	1.00	1.01
704	1.01	1.01
720	1.01	1.01

Extrudate Swell Data for LCP Resin

Time (sec)	Shear Rate (s^{-1}) 26	104
16	0.99	1.02
32	0.99	1.01
48	0.99	1.01
64	0.99	1.00
80	0.99	1.01
96	0.99	1.01
112	0.99	1.01
128	0.99	1.01
144	0.99	1.00
160	0.99	1.01
176	0.99	1.01
192	0.99	1.01
208	0.99	1.02
224	0.99	0.99
240	0.99	1.01
256	0.99	1.01
272	0.99	1.01
288	0.99	1.01
304	0.99	1.01
320	0.99	1.01
336	0.99	1.00
352	1.00	1.00
368	0.99	1.00
384	0.99	1.02
400	0.99	1.00
416	0.99	1.01
432	0.99	1.01
448	0.99	1.01
464	0.99	1.01
480	0.99	1.01
496	0.99	1.01
512	0.99	1.01
528	1.00	1.01
544	0.99	1.01
560	0.99	1.00
576	0.99	1.00
592	0.99	1.01
608	0.99	1.03
624	0.99	1.01
640	1.00	1.00
656	0.99	1.01
672	0.99	1.01
688	0.99	1.00
704	0.99	1.01
720	0.99	1.00